

## Response to Reviewer #1

**[Reviewer Comment; RC1]** This manuscript presents measurements from a 5 month study of fluorescing biological aerosol particles (FBAP) at an elevated, moderately remote site in southern India. The data quality appears to be very good and the scientific significance is potentially high. The problem is that the paper is probably twice as long as it needs to be and the conclusions drawn are much too speculative with not enough concrete statistics to support the hypotheses put forth regarding either the source of the FBAPs or the physical mechanisms underlying the observed trends. When discussing the results, the objective is to highlight the main points without trying to describe each and every peak and wiggle. Let the Tables list all the statistical details and focus on the most important variations that will then be used to drive the discussion. At the moment there are probably twice as many pages of results and twice as many figures as needed.

**[Author Response; AR1]** We would like to thank Dr. Baumgartner for his positive evaluation of our results mentioning, “The data quality appears to be very good and the scientific significance is potentially high”. The comments provided by the reviewer and corrections suggested in the manuscript have greatly helped us to improve the quality of the manuscript. The suggestions have been meticulously implemented wherever appropriate and we believe changes will be acceptable. As suggested by the Reviewer manuscript is shortened by cutting short the description on of monthly plots and supplementary figures and also by rearranging the text wherever appropriate. We have also revised the figures by combining few of them and moving one to the supplement. The description on size distribution is also shortened and modified accordingly, to highlight the main points.

What is missing:

**[RC2]** A topographical map of the research site and surrounding area, preferably something like a Google Earth rendition that would show the surrounding vegetation as well as areas with no vegetation such as is referred to in the text. Given the very low wind speeds, it is likely that most of the trends that are seen can be linked to more local sources.

**[AR2]** We have now provided a land-use map of the southern India in the supplement clearly indicating the significance of the chosen site. As for the topography, note that Fig. 1 in the main text is scaled by the altitude. Relation between low wind speed and local source is explained in the manuscript (L726 – L730)

**[RC3]** A more in depth analysis of the periods with rain, taking a much closer look at the properties of the FBAP just before, during and after each event.

**[AR3]** We have performed the in-depth analysis exploring the relation between rainfall and FBAP number concentration just before, during, and after rainfall and the result indicated no significant effect on FBAP number concentration.

Hence, it was very difficult to make any sound and conclusive statement pertaining to effect of rainfall on FBAP number concentration. One reason, as pointed out by Reviewer#3, could be the persistent and heavy rainfall. However, during the second part of the campaign carried out during winter season, we did observe impact of rainfall on the FBAP number concentrations. These results will be discussed in detail in follow up study. In addition we have given a hypothesis explaining the absence of effect of rainfall on FBAP number concentration at this particular location (L850 – L863).

**[RC4]** A cross-correlational analysis between the FPAB properties and the meteorological conditions. One would not necessarily expect a one to one correlation between the meteorology and the FPAB concentrations, particularly if the spore production is local. Only for advected aerosols would they be linked one to one.

**[AR4]** We agree with Reviewer that one cannot expect one to one correlation between meteorology and FBAP concentration, however, it may not be true in all the cases and not necessary be always linked for advected bioaerosols. For example, FBAP concentration, depending up on the type of spore, is known to have varied response/relationship with relative humidity (RH). The emissions of few specific types of spores emitted locally are positively related with relative humidity whereas some have shown decrease in concentration with increasing RH (Oliveira et al., 2010; Herrero et al., 1996; Kurkela, 1997; Oh et al., 1998; Healy et al., 2014., Quintero et al., 2010; Hjelmroos, 1993; Ho et al., 2005., Sabariego et al., 2000., Calderon et al., 1995). This has been clearly mentioned in the manuscript (L764 – L774). The relation of wind speed and direction may be useful to further study the impact of advected bioaerosols, which has been detailed in the manuscript (L731 – L738; Hameed et al., 2012; Almaguer et al., 2013; Lyon et al., 1984; Quintero et al., 2010; Huffman et al., 2012; Jones and Harrison, 2004; Troutt and Levetin, 2001; Kurkela, 1997).

**[RC5]** It is impossible to compare the shapes of size distributions when they are on different figures. Since the concentrations are quite different, normalize them to a unit area then put only the means or medians on the same figure so that any differences in the shapes can be clearly seen. These differences can then be evaluated quantitatively and linked to the hypothesis.

**[AR5]** Based on Reviewer's suggestion we attempted to prepare a figure comparing the mean FBAP number and mass size distribution for each focus period in single panel. We have replaced Fig. 10 and 11 (original manuscript) with the new figure (Fig.8, revised manuscript). We have also added the prepared figure below for Reviewer's kind read-through.

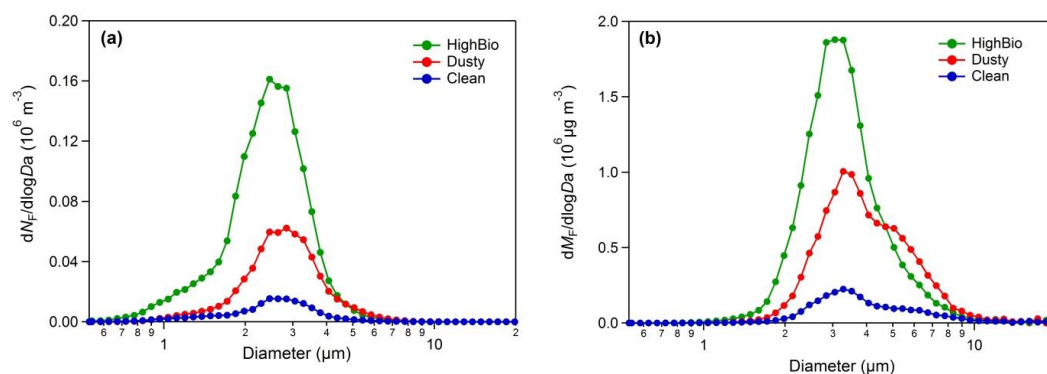


**Figure R1.1:** FBAP number size distributions ( $dN_F/d\log D_a$ ) and mass size distribution ( $dM_F/d\log D_a$ ) averaged over each distinct focus periods during the measurement campaign carried out at Munnar.

**[RC6]** The back trajectory analysis is useless as currently given. There needs to be an analysis of not only where the air came from horizontally, but vertically as well. Questions to be asked: a) How long had the air been close to the surface before reaching the site? b) What were the meteorological conditions along the trajectory, i.e. precipitation and humidity and c) How long had the air been close to the site? These all will impact the history of the particle as well as the air and whether particles had been removed after leaving their source.

**[AR6]** Indeed, the back trajectory plots shown in Figure 1 are color-scaled by pressure (altitude) to highlight the vertical component of the air motion. We chose not to discuss this in great detail in the paper, because it would make the already long manuscript even longer and we felt this analysis would be beyond the scope of the manuscript. We also felt that it would not be helpful in improving the primary scientific conclusion specifically that during the monsoon season over Indian region, and could lead to further confusion. Further, our sole aim with this figure is to show the back trajectory is only to provide an orientation to reader that this site experiences very contrasting winds during contrasting seasons (monsoon vs. winter), and a broader picture of air mass origin with rough estimates about air mass composition (Vinoj and Satheesh, 2003; Li and Ramanathan, 2002; Satheesh and Srinivasan, 2002; Vinoj et al., 2010, 2014; Prospero, 1979; Moorthy et al, 1991.). To investigate the relation of impact of wind direction and speed separate meteorological measurement in high time resolution were performed and were reported. In any case, we believe that Referee has overlooked the fact that back trajectories are already color scaled by pressure.

**[RC7]** An error analysis of the measurements. What is the expected error in size and concentration based on error propagation that no doubt has already be detailed in earlier publications. Nothing is said about FBAPs that are not complete particles but are fragments. There needs to be an estimate of the size dependent losses in the sampling system. Even with no bends, there will be diffusion and turbulence losses that can easily be calculated with Aerocalc (Baron and Willeke).

**[AR7]** Reviewer may be aware of the fact that UV-APS cannot differentiate the particle type; instead it only measures the aerodynamic diameter and spectrally integrated fluorescence. Under this scenario, a plant/animal fragment sampled will be treated as a complete particle where instrument will assign the equivalent aerodynamic diameter. We have calculated the equivalent aerodynamic diameter of a non-spherical particle. For example an ellipsoid particle with length of 4  $\mu\text{m}$  long and width of 2  $\mu\text{m}$  will be treated as particle with aerodynamic diameter of 3.6  $\mu\text{m}$ . As suggested by Reviewer a sentence (average penetration efficiency of 99.8% at 290K and 840 hPa ) discussing about the size dependent losses in the sampling system is now added based on Aerocalc/previous literature.

I have attached an annotaed version of the paper that includes many more questions and comments, The paper is relatively readable, given that the first author is not a native English; however, I am annoyed whenever I read a paper written by a non-English speaker but who has co-authors that are but who obviously have not read the paper, otherwise the numerous grammatical errors would have been corrected.

The suggestions provided in the annotated version of the manuscript have been implemented wherever appropriate and we thank Reviewer for his valuable edits.

## References:

Almaguer, M., Aira, M.-J., Rodríguez-Rajo, F. J., and Rojas, T. I.: Temporal dynamics of airborne fungi in Havana (Cuba) during dry and rainy seasons: influence of meteorological parameters, *International Journal of Biometeorology*, 58, 1459-1470, 10.1007/s00484-013-0748-6, 2013.

Calderon, C., Lacey, J., McCartney, H. A., and Rosas, I.: Seasonal and diurnal-variation of airborne basidiomycete spore concentrations in Mexico-city, *Grana*, 34, 260-268, 1995.

Hameed, A. A. A., Khoder, M. I., Ibrahim, Y. H., Saeed, Y., Osman, M. E., and Ghanem, S.: Study on some factors affecting survivability of airborne fungi, *Science of the Total Environment*, 414, 696-700, 10.1016/j.scitotenv.2011.10.042, 2012.

Healy, D. A., Huffman, J. A., O'Connor, D. J., Poehlker, C., Poeschl, U., and Sodeau, J. R.: Ambient measurements of biological aerosol particles near Killarney, Ireland: a comparison between real-time fluorescence and microscopy techniques, *Atmospheric Chemistry and Physics*, 14, 8055-8069, 10.5194/acp-14-8055-2014, 2014.

Herrero, B., FombellaBlanco, M. A., FernandezGonzalez, D., and ValenciaBarrera, R. M.: The role of meteorological factors in determining the annual variation of *Alternaria* and *Cladosporium* spores in the atmosphere of Palencia, 1990-1992, *International Journal of Biometeorology*, 39, 139-142, 10.1007/bf01211226, 1996.

Hjelmroos, M.: Relationship between airborne fungal spore presence and weather variables - *cladosporium* and *alternaria*, *Grana*, 32, 40-47, 1993.

Ho, H. M., Rao, C. Y., Hsu, H. H., Chiu, Y. H., Liu, C. M., and Chao, H. J.: Characteristics and determinants of ambient fungal spores in Hualien, Taiwan, *Atmospheric Environment*, 39, 5839-5850, 10.1016/j.atmosenv.2005.06.034, 2005.

Huffman, J. A., Sinha, B., Garland, R. M., Snee-Pollmann, A., Gunthe, S. S., Artaxo, P., Martin, S. T., Andreae, M. O., and Pöschl, U.: Size distributions and temporal variations of biological aerosol particles in the Amazon rainforest characterized by microscopy and real-time UV-APS fluorescence techniques during AMAZE-08, *Atmospheric Chemistry and Physics*, 12, 11997-12019, 10.5194/acp-12-11997-2012, 2012.

Jones, A. M., and Harrison, R. M.: The effects of meteorological factors on atmospheric bioaerosol concentrations - a review, *Science of the Total Environment*, 326, 151-180, 10.1016/j.scitotenv.2003.11.021, 2004.

Kurkela, T.: The number of *Cladosporium* conidia in the air in different weather conditions, *Grana*, 36, 54-61, 1997.

Li, F., and Ramanathan, V.: Winter to summer monsoon variation of aerosol optical depth over the tropical Indian Ocean, *Journal of Geophysical Research-Atmospheres*, 107, 10.1029/2001jd000949, 2002.

Lyon, F. L., Kramer, C. L., and Eversmeyer, M. G.: Variation of airspora in the atmosphere due to weather conditions, *Grana*, 23, 177-181, 1984.

Oh, J.-W., Lee, H.-B., Lee, H.-R., Pyun, B.-Y., Ahn, Y.-M., Kim, K.-E., Lee, S.-Y., and Lee, S.-I.: Aerobiological study of pollen and mold in Seoul, Korea, *Allergology International*, 47, 263-270, <http://dx.doi.org/10.2332/allergolint.47.263>, 1998.

Oliveira, M., Amorim, M. I., Ferreira, E., Delgado, L., and Abreu, I.: Main airborne Ascomycota spores: characterization by culture, spore morphology, ribosomal DNA sequences and enzymatic analysis, *Applied Microbiology and Biotechnology*, 86, 1171-1181, [10.1007/s00253-010-2448-z](https://doi.org/10.1007/s00253-010-2448-z), 2010.

Prospero, J. M.: Mineral and sea salt aerosol concentrations in various ocean regions, *Journal of Geophysical Research-Oceans and Atmospheres*, 84, 725-731, [10.1029/JC084iC02p00725](https://doi.org/10.1029/JC084iC02p00725), 1979.

Quintero, E., Rivera-Mariani, F., and Bolanos-Rosero, B.: Analysis of environmental factors and their effects on fungal spores in the atmosphere of a tropical urban area (San Juan, Puerto Rico), *Aerobiologia*, 26, 113-124, [10.1007/s10453-009-9148-0](https://doi.org/10.1007/s10453-009-9148-0), 2010.

Sabariego, S., de la Guardia, C. D., and Alba, F.: The effect of meteorological factors on the daily variation of airborne fungal spores in Granada (southern Spain), *International Journal of Biometeorology*, 44, 1-5, [10.1007/s004840050131](https://doi.org/10.1007/s004840050131), 2000.

Satheesh, S. K., and Srinivasan, J.: Enhanced aerosol loading over Arabian Sea during the pre-monsoon season: Natural or anthropogenic?, *Geophysical Research Letters*, 29, [10.1029/2002gl015687](https://doi.org/10.1029/2002gl015687), 2002.

Troutt, C., and Levetin, E.: Correlation of spring spore concentrations and meteorological conditions in Tulsa, Oklahoma, *International Journal of Biometeorology*, 45, 64-74, [10.1007/s004840100087](https://doi.org/10.1007/s004840100087), 2001.

Vinoj, V., and Satheesh, S. K.: Measurements of aerosol optical depth over Arabian Sea during summer monsoon season, *Geophysical Research Letters*, 30, [10.1029/2002gl016664](https://doi.org/10.1029/2002gl016664), 2003.

Vinoj, V., Rasch, P. J., Wang, H., Yoon, J.-H., Ma, P.-L., Landu, K., and Singh, B.: Short-term modulation of Indian summer monsoon rainfall by West Asian dust, *Nature Geoscience*, 7, 308-313, [10.1038/ngeo2107](https://doi.org/10.1038/ngeo2107), 2014.

Vinoj, V., Satheesh, S. K., and Moorthy, K. K.: Optical, radiative, and source characteristics of aerosols at Minicoy, a remote island in the southern Arabian Sea, *Journal of Geophysical Research-Atmospheres*, 115, [10.1029/2009jd011810](https://doi.org/10.1029/2009jd011810), 2010.

Moorthy, K. K., Nair, P. R., and Murthy, B. V. K.: Size distribution of coastal aerosols - effects of local-sources and sinks, *Journal of Applied Meteorology*, 30, 844-852, [10.1175/1520-0450\(1991\)030<0844:sdocae>2.0.co;2](https://doi.org/10.1175/1520-0450(1991)030<0844:sdocae>2.0.co;2), 1991.

## Response to Reviewer #2

**[Reviewer Comment; RC1]** The manuscript presents measurements of Fluorescent Biological Aerosol Particles (FBAP) made using an Ultraviolet Aerodynamic Particle Sizer (UV-APS) at a high-altitude tropical site in southern India over a period covering the southwest monsoon season. A thorough background research, set of measurements and description of these has been presented and is potentially worthy of publication. However, I do feel some improvements could be made to the current manuscript as detailed below. Although I'm sure any new field measurements using a UVAPS or similar qualify as valid research, it is difficult to see the real contribution of this work to the field, other than to validate previous similar measurements at a new location. I believe the information is there, but is swamped in meticulous depiction and description of all measurements. Perhaps the manuscript could be streamlined and given more structure to emphasize this. The properties of the new site and results specific to this should be highlighted, with an eye on how it will be useful for future research and how the presented measurements will support that research. The technical content of the paper appears good and accurate. Figures have been chosen well to depict and compare the measurements (haven't seen the supplementary figures, which do not appear to be with the manuscript). Work in the field I was aware of, and much more besides has been appropriately cited.

**[AR1]** We would like to thank Reviewer for positively evaluating our manuscript stating following important points:

- "A thorough background research, set of measurements and description of these has been presented and is potentially worthy of publication"
- "The technical content of the paper appears good and accurate"
- "Figures have been chosen well to depict and compare the measurements"
- "Work in the field I was aware of, and much more besides has been appropriately cited"

The reviews provided here have been very helpful for us in improving the overall quality of the manuscript. We have also tried to fine-tune the key messages highlighting the findings of this study and how it would be useful in future in conclusion section. In addition to reduce the length of the manuscript we have now moved few figures to supplementary material and merged Fig. 3 and Fig. 5.

Some suggested alterations below.

**[RC2]** Pg 10: The inlet system is described here. Could the effects of the inlet system be assessed by a comparison of measurements of a range of particle sizes under controlled conditions both with and without the inlet tubing in place?

**[AR2]** Following the experiment, we performed a test with room air to estimate particle losses in the inlet tube. Observing particle distributions with and without tubing showed that no noticeable difference in the particle number

concentration or size distribution. We also performed theoretical calculations to calculate the diffusion losses during the entire sampling for all the size-ranges sampled and found that average penetration was 99.8% at 290K and 849 hPa.

**[RC3]** Line 445: Should read "Basically the UV-APS measures the particle number and aerodynamic size; the average mass of size-resolved particles can"  
Lines 445-447: Can this statement be backed-up by a reference?

**[AR2]** We have now added an appropriate reference for this statement.

**[RC3]** Line 457 and few lines preceding: Were all the compared measurements made using the same density value?

**[AR3]** As far as we could found out from the literature all the measurements were carried out using same density values ( $1 \text{ g cm}^{-3}$ ).

**[RC4]** Lines 709-716: Description is confusing; maybe a mistake in the period references in the figure has been made? Here and everywhere else the three named focus periods are mentioned, the period names should perhaps be written within inverted commas or in italics to make reading easier.

**[AR4]** We thank Reviewer for pointing this out. The *focus* periods are now written in italics throughout manuscript.

**[RC5]** Figure 2: The shadowed blocks representing the focus periods don't seem to be visible on my copy of the manuscript.

**[AR5]** This mistake has been corrected. We have now added the shadowed blocks in Fig. 2.

**[RC6]** Finally grammar details. While the document is largely well written, there are numerous grammar mistakes that, at times, make it quite difficult to read. These often consist of a missing 'a' or 'the'. Although too numerous for individual attention, I have indicated some instances below and suggest that one of the authors go through the whole manuscript again and tidy this up.

**[AR6]** We thank Reviewer for pointing this out. Once we receive the final acceptance from The Editor before the final publication we intend to get our manuscript English edited from a professional service.

**[RC6.1]** Line 27: Missing 'a' between 'constitute' and 'large'.

**[AR6.1]** Done

**[RC6.2]** Line 55: Should read "selected areas. These measurement results confirm the fact that the fraction of PBAP to TAP is".

**[AR6.2]** Done



**[RC6.3]** Line 56: Missing 'a' between 'constitute' and 'significant'.

[\[AR6.3\] Done](#)

**[RC 6.4]** Line 172: Missing 'the' between 'including' and 'Arabian'.

[\[AR6.4\] Done](#)

**[RC6.5]** Line 173: Should read, "movement of the ITCZ reaching up to the equator is associated with the NE monsoon, which is also marked".

[\[AR6.5\] Done](#)

## Response to Reviewer #3

### General

**[Reviewer Comment; RC1]** This paper reports results of a three month measurement campaign of fluorescent biological aerosol particles (FBAP) at a high altitude tropical site in southern India. There are some unique aspects on the data. First, the marine air masses can be compared to local FBAP sources. Secondly, the campaign included long periods of heavy and persistent rain. Consequently, the authors observed a lack of correlation of FBAP with precipitation, contrary to several recent studies from other areas. The data has been presented in diverse ways that are also comparable to earlier studies. The material seems to merit publication. However, there are several issues that should be treated.

**[Authors Response; AR1]** We would like to thank reviewer for his thoughtful and detailed comments, which have helped us in improving the quality of the manuscript. We also thank reviewer for making following positive observations about our work.

- “There are some unique aspects on the data”
- “First, the marine air masses can be compared to local FBAP sources. Secondly, the campaign included long periods of heavy and persistent rain”
- “The data has been presented in diverse ways that are also comparable to earlier studies”

**[RC2]** Most importantly, the paper is unnecessarily long. The authors should concentrate on the findings that are unique to this study. Although it is good to treat many facets of the data, I think the paper would benefit of focusing also in this respect. The authors have divided the three month period first into months and later to three focus periods that they call dusty, clean, and high bio. I find the latter division much more useful. I recommend keeping it and getting rid of the monthly results. Because the data is treated from many angles, many of the explaining factors and arguments are presented several times. An example is the effect of the clean SW winds. It would be good to try to collect the findings first and then treat them at once.

**[AR2]** We thank Reviewer for pointing this out and we have now implemented Reviewer's suggestions. Accordingly, we have reduced the length of manuscript by moving figures related to monthly division of the observed data to the supplement and corresponding description has also been reduced substantially.

### Specific

**[RC3]** In subsection 3.5 on SEM images the authors state that “these images are not being presented here for any quantitative purpose and to draw any specific scientific conclusions”. Indeed, there are only a few particles shown. However, the authors use the images to support their hypotheses on the particle species. I

propose either analyzing a large number of samples and particles to corroborate the hypotheses or moving the subsection to the supplement and being cautious on using them as evidence.

**[AR3]** We understand the reviewer's concern. What we meant was not to draw any scientific conclusions using the SEM images regarding neither the variabilities in bioaerosol number/mass concentration nor the type of bioaerosols. Our sole intention was to orient the reader to the dominant particle types in an air mass during three distinct focus periods. Note that we have investigated more than 100 individual particles randomly collected on five occasions and have shown few as exemplary images. This has now been clarified in the revised manuscript text (L637 – L639).

**[RC4]** The measurements have been done with the UV-APS. Regarding the data interpretation, it would be good to acknowledge and point out that the detection efficiency for fluorescent particles of the UV-APS is low especially below approximately 2 microns (e.g. Healy, et al., ACP2014, Saari et al., AST 2014). This mostly affects the reported fluorescent particle size distributions. Further, it would be good to state whether a zero check cycle for the instrument was used.

**[AR4]** As pointed out by the Reviewer few studies have reported that counting efficiency of UV-APS decreases below 2 $\mu$ m. Considering this limitation associated with the instrument we report the number concentrations of FBAPs measured using UV-APS as the lower limit proxy for bioaerosols present in the atmosphere. A line (L200) is now added in the manuscript to point out this limitation in the detection efficiency. We have performed the zero tests using HEPA filter and found no particle was detected during zero test.

**[RC5]** Line 250 to 273: The authors find that the fluorescent and total particle concentrations do not correlate much, independent of whether the particles are coarse or fine. They then argue that the fluorescent concentration is not affected by non-biological particles. They later hypothesize that particles from combustion or similar activities do not get transported to the measurement site. This might well be the case, but what are the high concentrations of fine non-fluorescent particles (figure S2) then? Maybe a scatter plot of NF (<1 $\mu$ m) VS NF(>1  $\mu$ m) would be useful. I would expect the submicron biological particles to correlate with the supermicron biological ones somewhat. Maybe use this point for shortening the paper and just state that there seldom are major sources of fluorescent non-biological coarse particles and therefore the numbers reported are relevant. I hypothesize that the lack of correlation for fine particles is at least partly caused by the low fluorescent particle detection efficiency of the UV-APS unit.

**[AR5]** We understand Reviewers concern. Our intention of carrying out the correlation analysis was to indicate that under certain conditions (mainly clean conditions persisting during monsoon at this site) UV-APS may be used to detect and segregate the particles of biological origin in sub-micron range from non-biological aerosol particles. However, interference from non-biological but fluorescent particles needs to be carefully analyzed. Further, as pointed out by

Reviewer there may be a high number concentration of the particles in sub-micron range, which are non-biological and non-fluorescent (as in our case); these particle do not likely affect the number concentration of fluorescent aerosol particles. In our case we believe, as supported by TAP number size distribution and SEM images, the non-biological and non-fluorescent particles in submicron range were mostly dominated by sea-salt and mineral dust. As suggested by Reviewer we have prepared the scatter plot of  $N_F$  for particle size range of  $<1\ \mu\text{m}$  and  $>1\ \mu\text{m}$  and is shown below. We infer that the particles in submicron size range, which are of not likely of biological origin are not introducing any interference in the fluorescence.

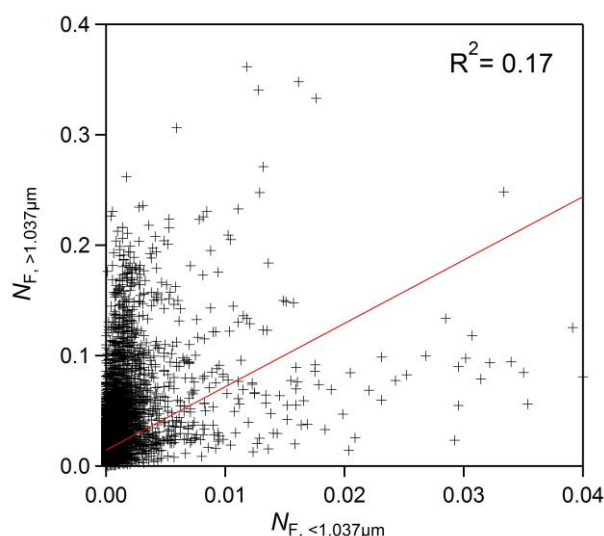


**Figure R3.1:** Scatter plot between  $N_F$  concentration integrated for particle size range of  $<1\ \mu\text{m}$  and  $>1\ \mu\text{m}$ .

[RC6] Line 357-360: The high extreme values of  $N_F/N_T$  actually do result from high variations of  $N_F$ , as evident from fig S2. The presented figures do not support the argued inverse correlation between  $N_T$  and  $N_F/N_T$ . The argument should be backed with a figure or a calculation or removed.

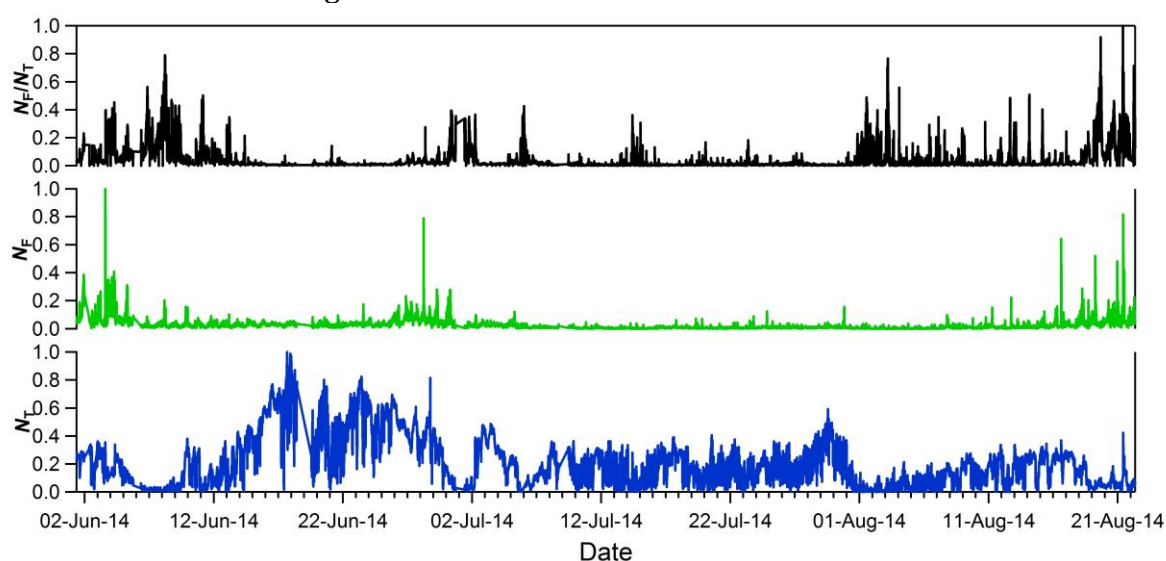


**Figure R3.2:** Variability in  $N_T$ ,  $N_F$  and  $N_F/N_T$  averaged over the course of entire campaign.

**[AR6]** We are unable to understand what Reviewer means to point out. Note that we have mentioned that “The time series of relative contribution of FBAP to TAP number during the campaign overall exhibited the similar temporal variability to  $N_F$ . However, pronounced extreme values of  $N_F / N_T$ , on the other hand, resulted from strong variability in the concentration of  $N_T$ . Please refer to Figure R3.2 above, where it clearly shows the high variability in  $N_T$  (lowest panel) is much pronounced and higher during the entire measurement period. However, the corresponding variability in  $N_F$  much less pronounced and episodic. Hence, resulting variability in  $N_F / N_T$  is to an extent shows similar temporal variability as like  $N_F$  but clearly shows the inverse relation with  $N_T$ . We have mentioned the equation to derive the variability in the manuscript [L768 - L770]

**[RC7]** Line 703-729: The  $N_F$  axis in fig 13 is such that it is very difficult to spot small changes in concentration. However, the slightly higher concentration starts at 17.00, not at 20.00. Apparently this data does not support the nocturnal sporulation argument. The argument on humidity is later supported by the scatter plot, but it might be good to show the diurnal pattern of RH here also.

**[AR7]** We thank Reviewer for pointing this out, which resulted from wrong choice of scaling. This error has now been corrected in the revised version. We have also removed the sentence mentioning the nocturnal sporulation of spores to avoid confusions. As suggested by Reviewer we have now added the diurnal variations in RH, temperature, and wind speed in the revised figures. We hope that changes will be acceptable to the Reviewer.

Technical

**[RC8]** Line 75: The first paragraph of introduction is rather long. It would be good to separate the latter part into a new paragraph, starting on line 75 from “It is likely that the surface”. This latter part should also reformulated, as it is very difficult to follow the line of thought now:

**[AR8]** Done.

**[RC9]** “surface structure, ice nucleating proteins, and other characteristics” – characteristics of what? Of PBAP, bacteria, bacterial spores?

**[AR9]** We meant to mention that surface structure, ice nucleating proteins, and other characteristics of bioaerosols can influence heterogeneous ice formation. The sentence has been modified accordingly.

**[RC10]** “Other bioaerosols like pollen” Other than what?  
 “..Other bioaerosols like pollen and fungal spores are often using air as the transportmedium.”. By definition, all atmospheric aerosol particles use air as the transport medium. Maybe: Plants and fungi use the air as a transport medium for their pollenand spores

**[AR10]** We agree to the Reviewer and have modified the sentence as per his/her suggestion.

**[RC11]** “Play an important role in public health..” It would be good to convey the idea that the role is negative.

**[AR11]** As per Reviewers suggestion the sentence has been modified accordingly.

**[RC12]** Line 123: The authors should either explain the relevance of the present study to Indian agriculture (or vice versa) or remove the sentence.

**[AR12]** The sentence has been modified to emphasis the importance of present study to Indian agriculture.

**[RC13]** Lines 192: The description of the drop of the detection efficiency is tautological with the text starting on line222.

**[AR13]** We thank Reviewer for indicating this. To avoid repeatability we have removed this statement from line L192.

**[RC14]** Line 195 on: For particles in the size range of 15-20 microns, the aspiration and transport efficiency of the sampling system probably is a more important issue than the calibration of the APS.

**[AR14]** This has been removed to avoid further confusion.

**[RC15]** Line 225: It would be good to state that the 1 micron as the fine particle size limit is adhoc.

**[AR15]** The sentence has been modified accordingly.

**[RC16]** Line 316-318: This is plausible, but should be written so that it is clear that there is no direct evidence within the present study.

**[AR16]** The sentence has been modified accordingly.

**[RC17]** Line 476-478: This is not due to the calculation. The mode mass will peak at higher diameter than number for any atmospheric particles one could find.

**[AR17]** To avoid any confusion, we have now removed this sentence.

**[RC18]** Line 484-486: Although the size limit is the same, the authors should warn the readers that the mode largely absent in NT as submicron is present in MT as supermicron.

**[AR18]** The reason behind such a shift from a mode in  $N_T$  in submicron range to a mode in  $M_T$  in supermicron range is clearly explained in revised manuscript (L422 – L423).

**[RC19]** Lines 496, 659: Note that the downwards slope of the APS detection efficiency might cause a peak to appear at around 0.9  $\mu\text{m}$  even when the mode would actually peak at much lower particle diameter.

**[AR19]** The actual peak in the size distribution of TAP would generally occur at lower diameters ( $<0.5 \mu\text{m}$ ). However in case of marine aerosols a secondary peak at diameter  $<1 \mu\text{m}$  was also reported which was mostly contributed by the sea salt particles. In the present study since the air masses were of marine origin we believe it's important to report this peak.

**[RC20]** Line 536: Should this be figure 14?

**[AR20]** This description was with reference to the figures reported in the paper Valsan et al., 2015.

**[RC21]** Line 591 and elsewhere: The date format should be homogenized between the text and figures

**[AR21]** The date format has been homogenized.

**[RC22]** Line 625: "As expected, the NF was highest during the high bio period.."! This should be reformulated as the period was specifically chosen to be high bio.

**[AR22]** The sentence has been modified accordingly.

**[RC23]** Line 669 on: The medians in distributions do not make much sense for channels that exhibit a high number of zero values.

**[AR23]** For the completeness and consistency of the proper representation of figures we Request reviewer to retain us the same format of the figure.

**[RC24]** Line 770 on: The pollution/concentration rose figures are hard to read and difficult to use in backing up quantitative arguments. The interpretation instruction text in the caption of fig 15 is not helpful and the numbers seem to be wrong. Overall, it would be helpful if someone came up with a better way of displaying the correlation of measured quantities and wind. Why not start with this MS?

**[AR24]** We thank Reviewer for pointing this out. The caption of Fig. 15 (now Fig. 12) has been corrected accordingly and the scales shown in the wind rose diagrams were also revised for better understanding.

**[RC25]** Figures 10-12: If the median values are shown, it would be good to continue to show the mean/median legends on the figures.

**[AR25]** As indicated by the Reviewer, the mean/median legends were added on the appropriate figures.

## References:

Healy, D. A., Huffman, J. A., O'Connor, D. J., Poehlker, C., Poeschl, U., and Sodeau, J. R.: Ambient measurements of biological aerosol particles near Killarney, Ireland: a comparison between real-time fluorescence and microscopy techniques, *Atmospheric Chemistry and Physics*, 14, 8055-8069, 10.5194/acp-14-8055-2014, 2014.

Saari, S., Reponen, T., and Keskinen, J.: Performance of two fluorescence-based real-time bioaerosol detectors: BioScout vs. UVAPS, *Aerosol Science and Technology*, 48, 371-378, 10.1080/02786826.2013.877579, 2014.

Valsan, A. E., Priyamvada, H., Ravikrishna, R., Després, V. R., Biju, C. V., Sahu, L. K., Kumar, A., Verma, R. S., Philip, L., and Gunthe, S. S.: Morphological characteristics of bioaerosols from contrasting locations in southern tropical India – A case study, *Atmospheric Environment*, 122, 321-331, <http://dx.doi.org/10.1016/j.atmosenv.2015.09.071>, 2015.



1 **Fluorescent Biological Aerosol Particle Measurements at a Tropical High Altitude Site in**  
2 **Southern India during Southwest Monsoon Season**

3 A. E. Valsan<sup>1,\*</sup>, R. Ravikrishna<sup>2</sup>, C. V. Biju<sup>3</sup>, C. Pöhlker<sup>4</sup>, V. R. Després<sup>5</sup>, J. A. Huffman<sup>6</sup>, U.  
4 Pöschl<sup>7</sup>, and S. S. Gunthe<sup>1,\*\*</sup>

5  
6 <sup>1</sup>EWRE Division, Department of Civil Engineering, Indian Institute of Technology Madras,  
7 Chennai – 600 036, India.

8 <sup>2</sup>Department of Chemical Engineering, Indian Institute of Technology Madras, Chennai – 600  
9 036, India.

10 <sup>3</sup>Department of Civil Engineering, College of Engineering Munnar, PB.No:45, County Hills,  
11 Munnar – 685612, India.

12 <sup>4</sup>Biogeochemistry Department, Max Planck Institute for Chemistry, P. O. Box Number 3060,  
13 Mainz, Germany.

14 <sup>5</sup>Institute of General Botany, Johannes Gutenberg University, Mainz, Germany.

15 <sup>6</sup>Department of Chemistry and Biochemistry, University of Denver, 2190 E. Iliff Ave., Denver,  
16 CO, 80208, USA.

17 <sup>7</sup>Multiphase Chemistry Department, Max Planck Institute for Chemistry, P. O. Box 3060, Mainz,  
18 Germany

19

20

21 To whom correspondence should be addressed:

22 \* Aswathy E. Valsan (aswathyerat@gmail.com)

23 \*\* Sachin S. Gunthe ([s.gunthe@iitm.ac.in](mailto:s.gunthe@iitm.ac.in))

24

## 25 Abstract

26 ~~Primary Biological Aerosol Particles (PBAPs) like fungal spores, bacteria, pollen, etc. are~~  
27 ~~reported to constitute large fraction of the atmospheric aerosols. They are responsible~~ An  
28 ultraviolet aerodynamic particle sizer (UV-APS) was continuously operated for the ~~spread of~~  
29 ~~organisms~~ first time during two seasons to sample the contrasting winds during monsoon and  
30 ~~diseases throughout~~ winter to characterize the ~~biosphere and may impact atmospheric processes~~  
31 ~~and the hydrological cycle by acting as ice nuclei (IN) and giant cloud condensation nuclei~~  
32 ~~(CCN). Despite their importance in the biosphere and climate, continuous measurements of~~  
33 ~~PBAPs in high time and size resolutions are not available for the Indian subcontinent. Here we~~  
34 ~~report the first measurements~~ properties of fluorescent biological aerosol particles (FBAPs) ~~in~~  
35 ~~India. The measurements were carried out using an ultraviolet aerodynamic particle sizer (UV-~~  
36 ~~APS) in Munnar, ), at a high altitude tropical site in southern India. The study was conducted for~~  
37 ~~three consecutive months during the Southwest monsoon season (1 June 2014–~~  
38 ~~21 August 2014), which is marked by heavy and persistent rainfall and strong~~  
39 ~~Westerly/Southwesterly clean winds.~~

40 India. Averaged over the entire monsoon campaign (June 1, 2014 – August 21, 2014) the  
41 arithmetic mean number and mass concentrations of coarse-mode ~~FBAP ( $\geq 1 \mu\text{m}$ )~~ FBAP were  
42  $0.02 \text{ cm}^{-3}$  and  $0.24 \mu\text{g m}^{-3}$ , respectively, which corresponded to ~2 and 6 % of total aerosol  
43 loading, respectively. Average FBAP number size distribution exhibited a peak at  $\sim 3 \mu\text{m}$ , which  
44 ~~was most likely contributed by~~ is attributed to the fungal spores, as supported by scanning  
45 electron microscope (SEM) images, and ~~the~~ these results are consistent with previous studies  
46 made for FBAP. During eleven weeks of measurements the ~~corresponding variability of the~~ total  
47 ~~(TAP) coarse mode particle number~~ (TAP) concentration was ~~highly variable in contrast~~ high

48 | compared to ~~the variability that~~ observed in FBAP number concentration. ~~Averaged over the~~  
49 | ~~entire campaign the TAP number and mass concentrations were  $1.8 \text{ cm}^{-3}$  and  $7.0 \mu\text{g m}^{-3}$ .~~ The  
50 | TAP and FBAP number concentrations measured at this site were strongly dependent on changes  
51 | in wind direction and rainfall. During ~~the period~~ periods of ~~continuous and~~ westerly/southwesterly  
52 | winds with heavy persistent ~~rainfalls~~ rainfall, the TAP and FBAP concentration exhibited very  
53 | low ~~concentration levels~~ values ( $1.3 \text{ cm}^{-3}$  and  $0.005 \text{ cm}^{-3}$ , respectively) with no  
54 | ~~observed~~ significant diurnal variations. ~~Averaged over the entire campaign~~ Whereas during  
55 | periods of Northerly winds with scattered rainfall FBAP exhibited ~~a moderately~~ relatively high  
56 | concentration values ( $0.05 \text{ cm}^{-3}$ ) with pronounced diurnal ~~variation with highest concentration~~  
57 | ~~during early morning hours (-06:00—08:00 hrs).~~ variations, which were strongly coupled with  
58 | diurnal variations in meteorological parameters. The campaign averaged FBAP number  
59 | concentrations were shown to correlate with daily patterns of meteorological parameters and  
60 | were positively correlated with relative humidity (RH;  $R^2=0.58$ ), and negatively with  
61 | temperature ( $R^2=0.60$ ) and wind speed ( $R^2=0.60$ ). We did not observe any significant positive  
62 | correlation with precipitation as reported by previous researchers from selected areas. These  
63 | measurement results ~~confirms~~ confirm the fact that ~~fraction~~ the ratio of PBAPs to TAP is strongly  
64 | dependent on particle size and location and thus may constitute a significant proportion of total  
65 | aerosol particles.

## 1 Introduction

Aerosols are generally defined as a colloidal system of solid or liquid particles suspended in a gaseous medium (Fuzzi et al., 1997; Pöschl, 2005) and are ubiquitous in the Earth's atmosphere. The term "Primary Biological Aerosol Particles" (PBAPs; sometimes also referred as bioaerosols or biological aerosols), describes a subset of ~~aerosol particles, i.e. the~~ solid airborne particles originating from biological organisms, including viruses, pollen, microorganisms (bacteria, fungal spores, etc.) and, protozoa or algae, etc., together with fragments of biological materials such as animal dander, plant debris etc. (Artaxo and Hansson, 1995; Coz et al., 2010; Després et al., 2007, 2012; Elbert et al., 2007). Bioaerosols can range in size from a few nanometers to few hundred micrometers in aerodynamic diameter,  $D_a$ , (Coz et al., 2010; Després et al., 2012; Jones and Harrison, 2004; Matthias-Maser and Jaenicke, 1994) ~~with viruses being the smallest in size amongst the PBAPs followed by bacterial and fungal spores, while pollen, and plant and animal fragments represent the largest in size. Depending upon size and ecosystem PBAPs can~~ PBAPs have been shown to constitute 14 – 70% of total number of coarse mode particles and around 20 – 24 % of total mass of  $PM_{10}$  (particulate matter with size  $\leq 10 \mu m$ ; Elbert et al., 2007; Després et al., 2012; Pöschl et al., 2010; Huffman et al., 2012). ~~Bioaerosols are present in the ambient atmosphere either as a single particle, or as agglomerates (Valsan et al., 2015) and exhibit a variety of shapes and morphological characteristics.~~ Further, it is likely that the surface structure, ice nucleating proteins, and other characteristics of bioaerosols can influence ~~substantially the~~ heterogeneous ice nuclei formation at ~~various~~ relatively high temperature levels (Morris et al., 2004, 2014) ~~and they~~ Bioaerosols can also thus act as giant cloud condensation nuclei (GCCN) ~~),~~ thus affecting the hydrological cycle (Andreae and Rosenfeld, 2008; Möhler et al., 2007). ~~Other bioaerosols like~~ It is also known that pollen ~~or fungal~~ and spores associated with various plants

89 ~~and fungi~~ are ~~often using~~dispersed in air ~~as~~resulting in the ~~transport medium for~~distribution and  
90 transfer of genetic material ~~and thus can travel and get transported~~ over large distances (Huffman  
91 et al., 2010; Elbert et al., 2007; Hallar et al., 2011; Burrows et al., 2009). A side effect of such a  
92 transport and distribution, ~~however,~~ is that they ~~are produced and spread in large quantities and~~  
93 ~~can~~ play ~~an important~~a negative role in public health ~~as they can cause allergies.~~ Pathogenic  
94 fungi have long been recognized as major threats to animal health and plants including crops  
95 severely jeopardizing the food security (Fisher et al., 2012 and references therein).

96 ~~Since the last century numerous studies have been conducted in different parts of the world to~~  
97 ~~understand the abundance and diversity of bioaerosols using various sampling and measurement~~  
98 ~~techniques, however confining to traditional methods.~~ The last decade has experienced a  
99 substantial development and application of advanced online and offline techniques for studying  
100 ~~the~~ characteristic properties of bioaerosols in ~~the both~~ field and laboratory (Fröhlich-Nowoisky, et  
101 al., 2009; DeLeon-Rodriguez et al., 2013; Prenni et al., 2009; Huffman et al., 2010, 2012, 2013;  
102 Schumacher et al., 2013; Pöhlker et al., 2012, 2013).

103 Instruments utilizing laser-induced fluorescence (LIF) have been frequently deployed ~~to~~in the  
104 field, enabling real-time characterization of the number size distribution of PBAPs ~~in~~with high  
105 time and size resolution. However, instruments based on LIF do not provide detailed information  
106 ~~directly~~ about PBAPs ~~or the origin of particles,~~ but ~~rather~~ provide broadly categorized  
107 information due to a mixture of biological fluorophores, each detected with varying efficiency  
108 (Pöhlker et al., 2012, 2013). Most FBAP- measurements have shown that the dominant size  
109 range for PBAPs number size distribution is 1 – 4 µm with concentration varying within the  
110 factor of 10 (Gabey et al., 2011, 2013; Healy et al., 2014; Huffman et al., 2010, 2012, 2013;  
111 Saari et al., 2015; Schumacher et al., 2013; Toprak and Schnaiter, 2013; Yu et al., 2016). As

Formatted: Justified

112 | studied and described by Huffman et al., (2010)), based on ~~long-term PBAP~~four months of  
113 | measurements in central Europe, the signal detected by UV-APS (Ultraviolet Aerodynamic  
114 | Particle Sizer) ~~in ambient settings~~ was defined as Fluorescent Biological Aerosol Particles  
115 | (FBAP), ~~and the resulting quantification of FBAP was further discussed and it was concluded~~  
116 | ~~that FBAP represents an approximate lower limit of actual abundance of PBAPs present in the~~  
117 | ~~ambient air sampled by the UV APS. Thus, for the consistency and simplicity we use the similar~~  
118 | ~~terminology as suggested by Huffman et al., (2010)).~~ Hence, the term FBAP is used as a lower  
119 | limit proxy for primary biological aerosol particles (PBAPs), biological aerosols, biological  
120 | aerosol particles, bioaerosols and similar terms mentioned in this study.

121 | Despite such instrumental advancements described above, ~~the~~ studies related to the  
122 | quantification of bioaerosols and their role in climate and human health have been extremely  
123 | limited in space and time. ~~Particularly,~~This is particularly true for the Indian subcontinent, which  
124 | constitute ~~around~~ ~18% of the world's total population, where studies related to the bioaerosols  
125 | are relatively few and with ~~spotty~~ analysis performed only by traditional techniques (Bhati and  
126 | Gaur, 1979; Chakraborty et al., 1998; Gangamma, 2014; Srivastava et al., 2012; Sharma and Rai,  
127 | 2008; Pachauri et al., 2013; Valsan et al., 2015; Ansari et al., 2015; Adhikari et al., 2004). ~~Thus,~~  
128 | ~~sources,~~The abundance, ~~and properties~~ of bioaerosols, which ~~are~~is strongly dependent on  
129 | location and season, remains poorly characterized over the Indian subcontinent and need to be  
130 | addressed systematically.

131 | ~~Investigating~~Additionally, investigating and quantifying the role of bioaerosols over the Indian  
132 | continent is ~~not only~~ important ~~because of the scarcity in the literature but also~~ due to its diverse  
133 | land-use pattern and the unique climatic condition experienced ~~by the~~ in terms of two ~~Monsoon~~  
134 | monsoon seasons associated with two distinct synoptic scale wind patterns. ~~Indian agriculture is~~

135 ~~strongly dependent on the Southwest Monsoon, and is the largest livelihood provider in India~~  
136 ~~and contributes a significant figure to the Gross Domestic Product (GDP). Therefore, it is very~~  
137 ~~important to better understand and quantify the role of bioaerosols in cloud and precipitation~~  
138 ~~formation during Monsoon and convective rainfall. The concentrations~~ The concentration of  
139 fluorescent aerosol particles in a semi-arid forest in the Western US was shown to increase  
140 during and after rainfall ~~in a semi-arid forest in the Western US~~ (Huffman et al., 2013), ~~but the~~  
141 ~~same pattern was not observed in a similar study in the Amazon basin (-).~~ Rainfall-triggered  
142 increase in bioaerosol concentration can potentially enhance further precipitation by convective  
143 upward movement of bioaerosols into clouds where they can serve either as IN or giant CCN  
144 (Shcumacher et al., 2013; Huffman et al., 2012)., 2013). Thus, the bioaerosols emitted during  
145 monsoon ~~season-rainfall~~ could potentially play an important role in cloud and precipitation  
146 formation ~~as shown by over India~~ (Ansari et al., 2015).  
147 Therefore, it is very important to understand and quantify the role of bioaerosols in cloud and  
148 precipitation formation during monsoon and convective rainfall. Additionally, bioaerosols over  
149 the Indian sub-continent can ~~have a direct societal impact where huge set of population may~~  
150 directly ~~get affected by~~ impact society through the spread of diseases and ~~covertly~~ indirectly due  
151 to ~~the~~ increased risk of loss ~~in~~ of agricultural output.  
152 ~~Thus, studies~~ due to emerging diseases caused by the fungi (Fisher et al., 2012).  
153 Studies involving characterization of bioaerosols using advanced techniques over this region are  
154 important to understand and quantify the impact of bioaerosols on regional biodiversity with  
155 larger implication towards human and ecosystem health. With this motivation we have deployed  
156 ~~an~~ a UV-APS for the detection and measurement of number size distribution of PBAPs at a high-  
157 altitude site of Munnar in Western Ghats of southern tropical India during Southwest monsoon

158 | season for ~3 months. To our knowledge this study presents the first ~~multi-month~~ ambient  
159 | measurement ~~investigations~~investigation involving UV-APS for multiple months over the Indian  
160 | subcontinent.

161 |

## 162 | 2 Methods

### 163 | 2.1 Site Description

164 | Measurements were performed to sample the air masses (see section 2.2) from a high-altitude  
165 | site (Munnar; 10.09°N, 77.06°E; 1605 m amsl – above mean sea level – Fig. 1) located in the  
166 | Western Ghats region of Southern, tropical India, just 90 km away ~~as the crow flies~~ from the  
167 | Arabian Sea ~~in the Southern part of tropical India~~. The observational site is located on a hill with  
168 | a valley towards the South and a small mountain towards the North surrounded by dense  
169 | vegetation including tea gardens and Eucalyptus trees. Climatologically this region is classified  
170 | as subtropical highland with dry winters and is listed as the Shola forest-grass ecosystem as  
171 | defined in the land-use type terminology ~~–~~ (Fig. S1). The Western Ghats, one of the eight  
172 | mountain ranges in India and identified as one of the ~~hottest~~most significant hot spots of  
173 | biodiversity (Myers et al., 2000) in the world, originates near the border of Maharashtra and  
174 | Gujarat running ~1600 km towards South, parallel to the Western coast through the states of  
175 | Gujarat, Maharashtra, Karnataka, Kerala, and Tamilnadu ending at the Southern tip of India near  
176 | ~~Kaniyakumari~~Kanyakumari. This mountain range separates the coastal plain from the Deccan  
177 | plateau making Western coastal plain a narrow land strip with a maximum width of ~ 110 – 120  
178 | km, sandwiched between the Western Ghats and the Arabian Sea. During the SW Monsoon  
179 | season (June – September) the Southwesterly, moisture laden winds are intercepted by the  
180 | Western Ghats causing persistent and heavy rainfall on the windward side of these mountains.

Formatted: Font: Bold

Formatted: Space After: 0 pt

Formatted: Justified



181 This causes the wash out and wet deposition of the pollutants in the coastal strip (Kerala) emitted  
182 due to anthropogenic activities, thus bringing clean marine influx with minimum impact of  
183 anthropogenic emissions (Satheesh and Srinivasan, 2002). Therefore, during this particular  
184 season this observational site can be regarded as relatively pristine, as compared to any other  
185 operational high-altitude observatory/site in Indian tropical region (Shika et al., 2016).

186

## 187 2.2 General Meteorology

188 Southern India nominally experiences two Monsoon seasons, the ~~Southwest~~SW monsoon (~~SW;~~  
189 ~~June – September~~) and the Northeast monsoon (NE; November – January), which are strongly  
190 associated with the movement of Inter-Tropical Convergence Zone, the ITCZ (Kanawade et al.,  
191 2014). The SW monsoon winds ~~are dominant during June to September bringing almost~~  
192 ~~anthropogenically “bring relatively clean” (not affected by human activities)~~ marine influx over  
193 the continent from Arabian Sea when the ITCZ moves Northwards reaching 30°N during July  
194 (Naja and Lal, 2002). These air masses originate over the Indian Ocean and travel thousands of  
195 kilometers over ~~oceanic water~~the ocean, including the Arabian Sea, before reaching the  
196 observational site. The Southward movement of ITCZ reaching up to the equator is associated  
197 with the NE monsoon, which is also marked as winter season in India occurring during October  
198 to January, when the prevailing winds are predominantly blowing in the NE direction. The  
199 measurement site of Munnar receives more than 85% of its annual rainfall during SW monsoon  
200 season and experiences scattered rainfall events during NE monsoon~~-season~~. The detailed  
201 meteorological parameters measured during the field measurement campaign carried out during  
202 SW Monsoon season at Munnar are discussed below.

203

Formatted: Justified

204 **2.23 Real-time fluorescence measurement**

205 ~~The biological~~Biological aerosol particles ~~from a high-altitude relatively pristine site at Munnar~~  
206 were measured using ~~an a~~ UV-APS (TSI Inc. Model 3314; ~~Serial Number: 71331023~~) as per the  
207 standard instructions given in the technical manual. The detailed description about the instrument  
208 including operating principles, field operation, data analysis protocol, and critical operational  
209 parameters are discussed elsewhere (Kanaani, et al., 2007, 2008; Agranovski et al., 2003, 2004,  
210 2005; Brosseau et al., 2000; Huffman et al., 2010, 2012; Hairston et al., 1997).

211 Briefly, the instrument is capable of measuring ~~the~~ aerosol particles in the aerodynamic diameter  
212 ( $D_a$ ) range of ~~0.54 – 19.815 – 20~~ 0.54 – 20  $\mu\text{m}$  over 52 channels by ~~means of~~ measuring the time-of-flight  
213 of particles between two He-Ne red lasers ( $\lambda=633$  nm). Once the particle size is determined, ~~the~~  
214 ~~same each~~ particle is ~~further~~ excited using ~~a third~~an ultraviolet Nd:YAG laser ( $\lambda=355$  nm) and  
215 ~~emissions are~~ fluorescent emission is measured in the range of 420 – 575 nm. The spectrally  
216 unresolved total fluorescence is recorded for each individual particle in to one of ~~the~~ 64 channels  
217 ~~with increasing order of fluorescence intensity. Huffman et al., (2010) described that the~~  
218 ~~counting efficiency of the instrument drops below 100% at  $D_a < 0.7 \mu\text{m}$  (counting efficiency~~  
219 ~~–50% at  $0.54 \mu\text{m}$ ), hence, the particle number concentration values reported for particle sizes of~~  
220  ~~$< 0.7 \mu\text{m}$  are lower limit of the actual concentration of the air sample. During analysis presented~~  
221 ~~in this paper the particles detected in the size range of  $15 – 20 \mu\text{m}$  were included and the reported~~  
222 ~~number concentration values should be considered as the lower limit of the actual values present~~  
223 ~~in the air sample, due to limitations in the size calibration for particles of this size.~~ The UV-APS  
224 ~~measurement cycle was initiated with~~ measurements were obtained at 5 minutes interval  
225 ~~(including the full diameter range scan for 285 seconds and 15 seconds of back scanning~~  
226 recording a total of 22280 sampling points during entire measurement campaign) ~~where air~~

Formatted: Justified

227 ~~sample was drawn~~ with a volumetric flow rate of 5 ~~L min<sup>-1</sup> (lpm)~~ Lpm at ambient temperature  
 228 and pressure. All ~~the~~ times reported in this study ~~are local time pertaining to~~ were Indian  
 229 Standard Time (IST; ~~GMT+5:30~~).  
 230 ~~The UV-APS~~ Sampling was ~~placed next to the window inside~~ performed at a ~~room in building of~~  
 231 the College of Engineering, Munnar, Kerala ~~located on a hill. A stain-less steel tubing with 3/4"~~  
 232 ~~OD (outer diameter) and TSP. The sampling~~ inlet was ~~used to construct the inlet unit for air~~  
 233 ~~sampling, which was 9 m and~~ approximately 2 m above the rooftop of the building and 8 m  
 234 above the ground ~~and rooftop, respectively. Thus the sampled air masses were expected to have~~  
 235 ~~minimal influence caused by the dynamics associated with the building structure.~~ level. The  
 236 sampling inlet was connected to the UV-APS, which was placed next to the window inside a  
 237 room using 3m of 3/4" OD stainless steel tubing. To minimize the particle losses, due to  
 238 impaction resulting from sharp bends, ~~the~~ electrically conductive silicon rubber tubing (~1.5 m;  
 239 12 mm inner diameter) was attached to the ~~stain-less~~ stainless steel tube just outside the window  
 240 (Fig. S1) ~~avoiding the sharp bends. Before the sampled air~~ The air sample was passed ~~to the~~  
 241 ~~instrument, through a~~ diffusion dryer (~1 m length) with silica gel (~~orange color indicating~~) ~~was~~  
 242 ~~used to dry and maintain~~ before entering the UV-APS, thus maintaining the relative humidity of  
 243 inlet air to <40%. ~~Thus combining all the tubing involved in the air sampling the sample flow~~  
 244 The residence time of sampled air in the inlet tube was calculated to be ~ 20 seconds. ~~The sample~~  
 245 , and the flow ~~through all the tubing was expected~~ calculated to be laminar ~~during in the~~ entire  
 246 sampling ~~period and hence~~ line. Hence, diffusion losses ~~are~~ were expected to be negligible for all  
 247 the size-ranges of the sampled particles. (average penetration efficiency of 99.8% at 290K and  
 248 840 hPa; Baron and Willeke, 2005).

249 For the present study ~~we derived~~the number size distribution of fluorescence biological aerosol  
 250 particles,  ~~$(dN_F/d\log D_a)$~~ , for each size bin was derived by summing up the particle number  
 251 concentration from the fluorescence channel numbers 3 – 64 and similarly the total particle  
 252 number size distribution,  ~~$(dN_T/d\log D_a)$~~ , was derived from channel numbers 1 – 64. In the  
 253 present study we have used 1.0  $\mu\text{m}$  as a cut-off diameter for given  $dN_F/d\log D_a$  and  $dN_T/d\log D_a$   
 254 to calculate the fluorescence biological aerosol number and total aerosol number concentrations,  
 255  $N_F$  and  $N_T$ , respectively. This is mainly due to the fact that particle counting efficiency of the  
 256 UV-APS drops below unity at 0.7  $\mu\text{m}$  (counting efficiency ~50% at 0.54  $\mu\text{m}$ ) and the  
 257 interferences ~~due to fluorescence~~ from non-biological aerosol particles below 1.0  $\mu\text{m}$  can at  
 258 times be very high (Huffman et al., 2010). ~~Also note that the cutoff at 1  $\mu\text{m}$  moreover represents~~  
 259 ~~the border between fine ( $<1\mu\text{m}$ ) and coarse ( $>1\mu\text{m}$ )~~ (2010). Few other studies have reported a decrease  
 260 in UV-APS counting efficiency for FBAPs  $< 2\mu\text{m}$  based on comparison of ambient FBAPs with  
 261 another LIF instrument (WIBS and BioScout) using different fluorescence wavelengths (Healy et  
 262 al. 2014, Saari et al., 2014). In the present study we define 1  $\mu\text{m}$  as the cutoff diameter to  
 263 distinguish between the submicron ( $<1\mu\text{m}$ ) and the super-micron ( $>1\mu\text{m}$ ) modes of the particle  
 264 number size distribution. The subscripts throughout this manuscript text “F” and “T” refer to  
 265 fluorescent and total coarse mode particles, respectively. ~~Please refer to~~See Table 1 for ~~the~~  
 266 abbreviations, notations, and symbols used in this manuscript. The particle mass size  
 267 distributions ( $dM/d\log D_a$ ) for total as well as fluorescent biological aerosol particles were  
 268 calculated for each size bin by multiplying  $dN/d\log D_a$  with volume of an aerodynamically  
 269 equivalent sphere with the geometric midpoint diameter ( $D_{a,g}$ ) and assuming the unit density (1 g  
 270  $\text{cm}^{-3}$ ) and unit shape factor. The integral mass concentrations of coarse fluorescent biological  
 271 aerosol particles and total coarse particles,  $M_F$  and  $M_T$ , respectively were calculated by

272 | integrating the particle mass distribution for  $D_a > 1\mu\text{m}$ ; ~~but,~~ thus particle mass reported here  
273 | should be viewed as first approximation as a result of uncertainty associated with the density and  
274 | shape of the particles (Huffman et al., ~~2010~~); 2010). To be consistent with previous UV-APS  
275 | results no standard temperature and pressure (STP) corrections were applied to the  
276 | concentrations reported in this study. These number concentrations can be normalized to the  
277 | volume that the sampled air would occupy under dry standard condition (STP: 273K, 1000 hPa,  
278 | and 0% RH) by multiplying the concentration values reported here with a factor of 1.29 derived  
279 | using ideal gas law.

280 | *Fluorescence of ~~submicron~~sub-micron particles*

281 | It has been reported by previous researchers that UV-APS is known to exhibit fluorescence for  
282 | some fraction of non-biological aerosol particles including soot, PAHs, and ~~cigarettes~~cigarette  
283 | smoke, which could be erroneously counted as FBAP (Huffman et al., 2010; Pan et al., 1999a,  
284 | 1999b). ~~It has also been emphasized that such interference can mostly occur for particles less~~  
285 | ~~than 1  $\mu\text{m}$  as the contribution from combustion sources at this size range is expected to be~~  
286 | ~~dominant.~~ To investigate the contribution of non-biological aerosol particles that are counted as  
287 | fluorescence biological aerosol particles, Huffman et al., (2010) ~~performed~~showed the  
288 | correlation between the integrated number concentrations of fluorescent particles ( $N_F$ ) and total  
289 | particles ( $N_T$ ) for different diameter ranges (only for the fluorescence channels  $>3$ ). ~~They found~~  
290 | ~~that the correlation for the submicron particles was systematically linear, whereas the correlation~~  
291 | ~~for supermicron particles was more random, indicating that a large fraction of submicron~~  
292 | ~~particles showing fluorescence might have been originated from anthropogenic sources, which~~  
293 | ~~may not be the case for the supermicron particles.~~ To ~~investigate~~examine the influence of  
294 | anthropogenic emissions on ~~submicron~~sub-micron fluorescent particles, we performed ~~the~~a

Formatted: Justified

295 similar correlation analysis for the entire campaign ~~and, however, found the different results.~~  
 296 The correlation between integrated number concentrations of fluorescent particles ( $N_F$ ) and total  
 297 particles ( $N_T$ ) for ~~supermicron~~super-micron ( $D_a > 1 \mu m$ ) and submicron ( $D_a < 1 \mu m$ ) diameter range  
 298 exhibited a very poor scatter ( $R^2 = 0.03$  and  $R^2 = 0.002$  respectively;  $N = 22280$ ; Figs. S2) indicating  
 299 extremely small percentage of fluorescence ~~was~~ contributed by non-biological aerosol particles  
 300 in ~~supermicron~~both super-micron and submicron particle ranges. This was in contrast with the  
 301 observations in Huffman et al (2010).  
 302 Since certain component of the mineral dust may exhibit a weak fluorescence (Huffman et al.,  
 303 2010; Sivaprakasam et al., 2004; Toprak and Schnaiter, 2013), we performed the separate  
 304 correlation analysis for ~~a focus~~the *dusty* period, which was dominated by the transport of mineral  
 305 dust from West Asia, North Africa, and Arabian region (discussed below). The correlation  
 306 between integrated number concentrations of  $N_F$  and  $N_T$  for  $D_a > 1 \mu m$  was moderately linear  
 307 ( $R^2 = 0.26$ ;  $N = 3138$ ; Fig. S3a) compared to ~~submicron~~the sub-micron size range during the *dusty*  
 308 period ( $R^2 = 0.007$ ;  $N = 3138$ ; Fig. S3b). ~~As a result, correlation between  $N_F$  and  $N_T$  indicates~~S3b).  
 309 indicating that the fraction of ~~supermicron~~super-micron particles exhibiting fluorescence may  
 310 have been contributed by mineral dust, but ~~this being not the case~~ for ~~submicron~~sub-micron  
 311 particles.  
 312 From these analyses we infer that the contribution of non-biological aerosol particles exhibiting  
 313 fluorescence was negligible in both ~~submicron~~sub-micron and ~~supermicron~~super-micron (except  
 314 during “*dusty* period”; discussed below) size ranges. Thus we hypothesize that due to persistent  
 315 rainfall the ~~submicron~~sub-micron and ~~supermicron~~super-micron particles ~~resulted~~resulting from  
 316 combustion ~~and other similar~~related activities, were either efficiently removed or were not  
 317 transported to the ~~observational~~observation site, ~~indicating that substantial fraction of the~~

Formatted: Font: Italic

Formatted: Font: Italic

318 ~~particles in both the size ranges were of biological origin.~~ Thus this ~~observational~~observation  
319 site could be ~~potentially~~ termed as relatively pristine and free from anthropogenic emissions  
320 during the monsoon season making this site scientifically interesting for investigating the  
321 characteristic properties of bioaerosols on long-term basis using advanced online and offline  
322 techniques.  
323 ~~Please note, however, that~~However, to ~~have~~maintain the consistency and uniformity in the  
324 comparison of  $N_F$ ,  $N_T$ , and other similar parameters reported ~~by the~~in previous studies ~~we~~  
325 ~~derived,~~ all the statistics associated with  $dN_F/d\log D_a$  and  $dN_T/d\log D_a$  with a cutoff diameter of  
326  $\sim 1 \mu\text{m}$  were derived.

327

## 328 **2.3.4 Meteorological parameter measurement**

329 ~~The meteorological~~Meteorological parameters ~~in parallel with the UV-APS measurements were~~  
330 were recorded during the entire campaign using ~~an ultrasonic~~ weather sensor (Lufft WS600-  
331 UMB) installed on ~~a~~the rooftop at the same height and a few meters away from the UV-APS  
332 inlet (Fig. 1b). These measurements were made concurrently with the UV-APS  
333 measurements.~~51~~ The weather station was capable of recording temperature, dew point  
334 temperature, relative humidity, precipitation intensity, wind speed, wind direction, and air  
335 pressure and was set to record these ~~meteorological~~ parameters ~~with every~~at 5 minutes interval  
336 with time synchronized to UV-APS measurement clock. The meteorological data ~~from the~~  
337 ~~weather sensor was stored by using an in-house developed external data logger. The~~ obtained  
338 ~~meteorological data~~at this site was compared with data obtained from another ~~ultrasonic~~ weather  
339 station (Vaisala WXT520) installed within the close vicinity ~~(Vaisala make).~~ The scatter plots  
340 between the data (10 ~~min averaged~~minute averages) obtained from ~~our~~both these weather ~~station~~

Formatted: Justified

341 | ~~and the one installed in the close vicinity~~stations exhibited very strong agreement for all the  
342 | meteorological parameters measured/recorded (average  $R^2 \geq 0.95$ ).

343 |

## 344 | **2.4.5 SEM Analysis**

345 | The samples for Scanning Electron Microscopy (SEM) analysis were collected on a 25 mm  
346 | diameter Nucleopore® Polycarbonate filter paper with pore sizes of 5  $\mu\text{m}$  and 0.2  $\mu\text{m}$  using a  
347 | two stage filtering method as described by Valsan et al., (2015). All samples were collected for  
348 | ~~approximately a~~approximate duration of 60 min at an average flow rate of 5 ~~lpm~~Lpm and were  
349 | stored in an air-tight container at 4°C until the SEM analysis. ~~The five~~ was carried out. More  
350 | than 100 individual particles analyzed from samples collected on five occasions during the entire  
351 | campaign, were ~~analyzed~~investigated using two different scanning electron microscopes. ~~1. a)~~  
352 | Quanta FEG 200 located at the Sophisticated Analytical Instrument Facility (SAIF) and ~~2. b)~~  
353 | Hitachi S 4A00 located at the Chemical Engineering Department of Indian Institute of  
354 | Technology Madras. Before loading the filter paper on to the ~~studs~~sample holders, they were cut  
355 | into small squares of  $\sim 1 \text{ cm}^2$  and sputter coated with gold particles. The biological aerosol  
356 | particles were identified purely based on their morphological features adopting the method  
357 | suggested by Matthias-Maser and Jaenicke (1991,1994). Detailed description on sample  
358 | collection and analysis was discussed elsewhere (Valsan et al., 2015).

359 |

## 360 | **3 Results and discussions**

### 361 | **3.1 Campaign overview**

Formatted: Justified



Figure 2 shows the temporal evolution and variability of the several ~~parameters characteristic for~~  
~~the meteorological conditions~~parameters, FBAP, and TAP properties observed throughout the  
measurement campaign during SW monsoon season at ~~a high altitude site of~~ Munnar.

~~Overall~~Several observations regarding the meteorological conditions during the campaign at  
Munnar can be ~~summarized as follows:~~made. The predominant wind direction was observed to  
be Westerly/Southwesterly (Fig. 1), which ~~characterizes~~is characteristic of the monsoon season  
and bringing ~~almost anthropogenically~~nearly clean marine influx (laden with dust and sea salt  
particles; Vinoj and Satheesh, 2003; Vinoj and Satheesh, 2003; Satheesh and Srinivasan, 2002;  
Vinoj et al., 2014; Prospero, 1979) over the continent marked by presence of persistent rainfall,  
high relative humidity (RH), higher wind speeds, and lower temperatures. ~~During this period the~~  
~~diurnal variations in temperature and relative humidity were totally absent and temperatures~~  
~~almost approached the dew point temperature. Further, the Westerly/Southwesterly air masses~~  
~~arriving at the observational site were free from any anthropogenic influence and were laden~~  
~~with dust and sea salt particles (Satheesh and Srinivasan, 2002; Vinoj et al., 2014; Prospero,~~  
~~1979). On few occasions, however, Northerly winds were also observed, which was associated~~  
~~with calm winds~~During this period diurnal variations in temperature and relative humidity were  
very small and temperatures approached the dew point. On a few occasions, however, Northerly  
winds were recorded, marked by relatively lower wind speeds, lower RH levels, higher  
temperatures, and reduced rainfall. During Northerly winds the temperature exhibited ~~relatively~~  
more pronounced diurnal variations compared to the relative humidity. The average  
meteorological parameters (arithmetic mean $\pm$ standard deviation) recorded during entire  
measurement period were: (840 $\pm$ 1.3) hPa absolute pressure, (17.2 $\pm$ 1.4) $^{\circ}$ C ambient temperature,

Formatted: Justified

(96.4±5.7) % relative humidity, (2.8±1.3) m s<sup>-1</sup> local wind speed, (270)° local wind direction (vector mean weighted by wind speed), and (4188) mm of accumulated rainfall.

The total of more than five months of bioaerosol measurements ~~in~~with high time and size resolution were performed at this site ~~comprising~~for two contrasting seasons: ~~the~~ monsoon (dominated by Southwesterly winds) and winter (dominated by Northeasterly winds). In this study, we present the results from ~~the~~this field campaign carried out during the SW monsoon season whereas the detailed results from the winter campaign from the same measurement site will be presented in ~~the~~a follow up study. We first discuss the characteristic features of the time series as a broad overview of the observed concentration levels, variability, and trends in  $N_T$  and  $N_F$ . Figure 2 (f,g,h,i,j) shows ~~the~~ time series of geometric mean diameter ( $D_g$ ),  $N_F$ ,  $N_F/N_T$ ,  $N_T$ , FBAP and TAP 3-D ~~and the~~ size distribution measured with the UV-APS for the entire campaign.

Throughout the measurement period the hourly averaged  $D_g$  time series consistently remained in the range of ~2 – 4 µm with almost no diurnal ~~variations~~variation. During the second half of the campaign, the  $D_g$ , however, exhibited relatively high variability with ~~an~~ average mean diameter of 2.6±0.7 µm. Unlike the  $N_T$  and  $N_F$  the variability in  $D_g$  ~~was observed~~did not seem to be ~~not~~ affected by ~~the~~ meteorological parameters except for wind direction (see section 3.64.1) on few occasions. The total coarse particle number concentration,  $N_T$ , exhibited high and consistent variability during entire measurement period, however, with no distinct diurnal cycle. ~~Averaged~~ (arithmetic mean±standard deviation) over the entire measurement period ~~was~~  $N_T$  was observed to be 1.8~~±~~ ~~±~~ 1.5 cm<sup>-3</sup> with lowest and highest concentrations of 0.01 cm<sup>-3</sup> and 8.6 cm<sup>-3</sup>, respectively. ~~The average  $N_T$  concentration during the months of June, July, and August was 2.7±1.9 cm<sup>-3</sup>, 1.5±0.96 cm<sup>-3</sup>, and 0.96±0.77 cm<sup>-3</sup>, respectively, with highest and lowest values for~~

individual months respectively as follows: June:  $8.6 \pm 0.04 \text{ cm}^{-3}$ ; July:  $5.1 \pm 0.02 \text{ cm}^{-3}$ ; and  
 August:  $3.6 \pm 0.01 \text{ cm}^{-3}$  (Fig. S4). The monthly averaged  $N_T$  concentration (Fig. S4) exhibited  
 a decreasing trend from June to August as the monsoon progressed (Tab. 2). In contrast to the  
 total aerosol particle number concentration,  $N_F$ , exhibited less pronounced but episodic peaks in  
 the time series during the majority of the measurement period, resulting in modest variability  
 and a campaign arithmetic mean value of  $0.02 \pm 0.02 \text{ cm}^{-3}$ . The highest  $N_F$   
 concentration of  $\sim 0.52 \text{ cm}^{-3}$  was observed on 3<sup>rd</sup> in June, prior to the onset of June (and few more  
 occasions) monsoon rainfall, whereas the lowest  $N_F$  concentration ( $< 0.0002 \text{ cm}^{-3}$ ) was  
 consistently observed on more than one occasion during the months of July and August. The  
 average monthly averaged  $N_F$  concentration during June and August was  $0.03 \pm 0.03 \text{ cm}^{-3}$  and  
 $0.015 \pm 0.02 \text{ cm}^{-3}$ , respectively with lowest  $N_F$  concentration of  $0.007 \pm 0.006 \text{ cm}^{-3}$  in July  
 (concentrations are listed in Tab. 2).  
 The time series of relative contribution of FBAP to TAP number,  $N_F/N_T$ , most of the time during  
 campaign exhibited the similar trend in temporal variability to  $N_T$  as displayed by  $N_F$  for most  
 during the campaign. The pronounced extreme values of  $N_F/N_T$  observed on a few occasions  
 resulted from strong variability in the concentrations of  $N_T$  rather than resulting from the  
 variations in the concentrations of  $N_F$ , indicating the inverse corresponded to low values of  $N_T$   
 implying a negative correlation between  $N_T$  and  $N_F/N_T$  during these measurements. Huffman et  
 al., (2010) have also reported the a similar inverse negative correlation between  $N_T$  and  $N_F/N_T$   
 from the measurements carried out at a semi-urban site from in central Europe. Temporal  
 evolution of  $N_F$ ,  $N_F/N_T$ , and 3-D number size distribution for individual campaign months is  
 shown in Fig. S5. A indicating that the variability in  $N_F/N_T$  was associated with changes in  $N_T$   
 concentrations. The campaign overview (including individual months) of FBAP mass

concentrations and 3-D size distribution for each five minutes of UV-APS ~~sample averaged over the entire measurement period and individual months~~ are shown in Figure S6. During the first month of measurement campaign  $M_F$  exhibited high concentration with sporadic spikes at irregular intervals with broader size distribution ( $\sim 2 - 8 \mu\text{m}$ ) towards the end of the month (with highest concentration  $\sim 6.0 \mu\text{g m}^{-3}$ ). As the measurement campaign progressed, with arrival of persistent and heavy rainfall (whole of July and first half of August)  $M_F$  exhibited a gradual decrease with minimum value reaching as low as  $6 \times 10^{-4} \mu\text{g m}^{-3}$ . After a period of consistent low mass concentration, during the last week of measurement campaign,  $M_F$  exhibited an increase with highest mass concentration of  $\sim 5.8 \mu\text{g m}^{-3}$ , which coincided with reduced and scattered rainfall [S5](#).

### 3.2.1.1 Particle number and mass concentrations

#### ~~3.2.1 Statistical distribution of~~ [The](#) number concentrations

~~Statistical distribution of five minute number and mass~~ concentration measurements carried out at Munnar over the course of the campaign are shown in Fig. 3 and tabulated in Tab. 2. [The box plots show statistical representation of five minute averaged data of the time series.](#) Over the entire measurement period the monthly mean of  $N_T$  varied by a factor  $\sim 3$  from [a](#) minimum in August ( $0.96 \text{ cm}^{-3}$ ) to a maximum in June ( $2.7 \text{ cm}^{-3}$ ). ~~In addition to the highest concentration, the Fig. 3a). The~~ variability of  $N_T$  was also found to be highest in the month of June as can be seen from the size of the 5 – 95<sup>th</sup> percentile ~~bars, which also reflected in Fig. 3a. The relative the~~ high variability ~~in~~ [of](#)  $N_T$  for entire measurement period ~~was largely contributed by the variability in  $N_T$  observed in the month of June.~~ During the initial phase of Southwest monsoon season, the predominant Westerly/Southwesterly winds are known to transport the mineral dust, which constitute large fraction of coarse mode (also in larger diameter size of fine mode fraction) TAP

Formatted: Font: Not Bold

Formatted: Justified, Space After: 0 pt

453 concentration, over the [Indian](#) continental region (Vinoj et al., 2010, 2014; Li and Ramanathan,  
 454 2002; Satheesh and Srinivasan, 2002; Vinoj and Satheesh, 2003). As the monsoon progresses the  
 455 persistent rainfall can cause the washout of these dust particles along the path of monsoonal rain,  
 456 thus reducing the coarse mode TAP concentration (Pranesha and Kamra, 1997a,b; Radke et al.,  
 457 1980; Moorthy et al., 1991). The monthly arithmetic mean and median average of  $N_T$  did not  
 458 exhibit significant differences. The monthly mean values of  $N_F$  varied by the factor of  $\sim 4$  with  
 459 ~~consistently high~~[moderate](#) variability during ~~all the observational months~~[entire campaign](#) (Fig.  
 460 [3b](#)). Similar to  $N_T$ , the monthly mean average value and variability in  $N_F$  was highest in the  
 461 month of June, with mean of  $0.03 \pm 0.03 \text{ cm}^{-3}$  and ~~high size of a~~ [95<sup>th</sup> percentile](#) (~~with~~ value of  
 462  $0.086 \text{ cm}^{-3}$ ), ~~respectively.~~ The lowest average concentration in  $N_F$  ( $0.007 \pm 0.006 \text{ cm}^{-3}$ ) [was](#)  
 463 observed in the month of July ~~was associated~~ with relatively lower variability as compared to  
 464 other months of field measurement campaign. Unlike  $N_T$ , the arithmetic mean and median  
 465 average of  $N_F$  for individual months exhibited a significant difference as can be seen from the  
 466 box plot shown in Fig. 3b. The variability of  $N_F/N_T$  showed ~~the~~[a](#) similar temporal pattern ~~as to~~  
 467 that ~~of~~[displayed by](#)  $N_F$ , except that [the](#) campaign average mean  $N_F$  concentration was higher than  
 468 that of the August, whereas the campaign averaged mean  $N_F/N_T$  was observed to be lower than  
 469 the mean calculated for August. ~~As can be seen from Fig. 3c, the mean relative contribution of~~  
 470  ~~$N_F$  to  $N_T$  was lowest in the month of July ( $\sim 1\%$ ) and highest in the month of June and August~~  
 471 ~~( $\sim 3\%$ ).~~ The median and mean for  $N_F/N_T$ , over the course of campaign were  $\sim 1$  and  $2\%$ ,  
 472 respectively. [\(Fig. 3c\)](#). The average values of  $N_F/N_T$  over this part of the globe were ~~found to be~~  
 473 lower ~~as compared to~~[than](#) previously investigated sites (Huffman et al., 2010, 2012; Bowers et  
 474 al., 2009; Schumacher et al., 2013; Matthias-Maser and Jaenicke, 1995; Matthias-Maser et al.,  
 475 2000; Gabey et al., 2010).

Formatted: English (U.S.)

476 *Diurnal patterns of ~~Though,~~ the number concentration*  
 477 ~~The average diurnal trends for three individual months and the entire measurement campaign~~  
 478 ~~were analyzed. Figure 4 shows the median FBAP values for each hour of the day for three~~  
 479 ~~individual months and entire campaign, and Fig. S7 shows the corresponding TAP plots. Overall~~  
 480  ~~$N_T$  exhibited a moderately diurnal pattern with consistent early morning (06:00 hr) peak at  $\sim 3$~~   
 481  ~~$\mu\text{m}$  (Fig. 4a) where in the month of July this early morning peak was absent. A relatively weak~~  
 482 ~~peak during late evening (20:00 hr) in FBAP concentration at  $\sim 3 \mu\text{m}$  was consistently observed~~  
 483 ~~in the month of July. In the month of June the average diurnal  $N_T$  concentration started increasing~~  
 484 ~~early in the evening ( $\sim 18:00$  hr), which gradually increased through the night and reaching~~  
 485 ~~maximum at  $\sim 06:00$  hr and started decreasing thereafter as day progressed. The average diurnal~~  
 486  ~~$N_T$  pattern in August exhibited more or less qualitatively similar features to that of diurnal pattern~~  
 487 ~~observed in June. In general the weak diurnal pattern observed in  $N_T$  during the month of July~~  
 488 ~~was consistent with weak RH and temperature diurnal patterns, and persistent rainfall observed~~  
 489 ~~during July. The early morning peak at  $\sim 3 \mu\text{m}$  on the diurnal scale was also reported from~~  
 490 ~~pristine Amazonian rainforest environment (Huffman et al., 2012). Corresponding average size~~  
 491 ~~distributions for entire measurement period will be discussed in details in Sec. 3.3. The diurnal~~  
 492 ~~variations of  $N_T$  (Fig. S7), on the other hand were very distinct from those of  $N_T$ . The size~~  
 493 ~~resolved  $dN_T/d\log D_a$  for each individual months exhibited a consistent and flat concentration~~  
 494 ~~profile at  $<1 \mu\text{m}$ , except for the month of August where a pronounced afternoon peak ( $\sim 12:00$ ) at~~  
 495  ~~$\sim 1 \mu\text{m}$  was observed. Reduced rainfall and substantial changes in meteorological parameters~~  
 496 ~~including the change in prevailing wind speed and shift in direction during later half of August~~  
 497 ~~might have caused the appearance of afternoon peak due to particles resulting from local sources.~~  
 498 ~~As like  $N_T$ ,  $N_T$  showed the strong quantitative variability amongst each individual month (Fig.~~

499 ~~S7). Previous studies where similar instrument was used have reported that pronounced diurnal~~  
 500 ~~variations in  $N_T$  are strongly coupled with diurnal variations in meteorological variables~~  
 501 ~~especially mixing layer depth (Garland et al., 2009; Raatikainen et al., 2014; Du et al., 2013).~~  
 502 ~~The absence of pronounced diurnal variations in  $N_T$  at this particular site may be a result of weak~~  
 503 ~~dependence of coarse mode TAP concentrations on meteorological parameters combined with~~  
 504 ~~persistent rainfall causing the washout of these particles (Radke et al., 1980; Raatikainen et al.,~~  
 505 ~~2014; Kanawade et al., 2014; Shika et al., 2016). This also indicates the absence of any strong~~  
 506 ~~and localized source of anthropogenic emissions during most of the campaign period. Diurnal~~  
 507 ~~patterns of  $N_T/N_T$  more or less followed the same pattern as that of  $N_T$  during all the measurement~~  
 508 ~~months owing to complete absence of diurnal variability in  $N_T$ . Averaged over the entire~~  
 509 ~~campaign the  $N_T/N_T$  was found to be highest during early morning hour at ~06:00 hr (~3.2%)~~  
 510 ~~consistent with the time of high  $N_T$  concentration (Fig. 4). The distinct diurnal pattern in  $N_T$  and~~  
 511  ~~$N_T$  supports the fact that the sources of TAP and FBAP were different over this region.~~

### 512 **3.2.2 Statistical distribution of mass concentration**

513 ~~Basically UV-APS measures the particle number; numbers, the average mass of size-resolved~~  
 514 ~~particles particle mass can be derived as first approximation also be estimated~~ by assuming the  
 515 particle density equal to  $1 \text{ g cm}^{-3}$  (unit density). ~~Accordingly Huffman et al., 2010, 2012). Based~~  
 516 ~~on this, the overview of mass concentration concentrations of FBAP over the course of~~  
 517 ~~measurement period is ( $M_F$ ) and TAP ( $M_T$ ) are presented here. The statistical distribution of five~~  
 518 ~~minutes mass concentration derived from number concentration measurements over the course of~~  
 519 ~~campaign is shown in Fig. 5 and tabulated in Tab. 2. in Fig. 3. The monthly mean values of  $M_T$~~   
 520 ~~exhibited the similar trend and temporal variability as that of shown by  $N_T$  with overall decrease~~  
 521 ~~in  $M_T$  through the course of measurement months as campaign progressed. The highest monthly~~

Formatted: Justified

522 ~~average concentration of  $M_T$  ( $\sim 10.6 \mu\text{g m}^{-3}$ ) was observed in the month of June whereas the~~  
 523 ~~lowest  $M_T$  of  $4.2 \mu\text{g m}^{-3}$  was observed in the month of August. Averaged over the entire~~  
 524 ~~measurement period the~~ as campaign progressed (Fig. 3d). The campaign mean  $M_T$  at Munnar  
 525 was  $\sim 7 \mu\text{g m}^{-3}$ , which was comparable to the values reported from a central European city ( $M_T$   
 526  $\sim 7.3 \mu\text{g m}^{-3}$ ) and higher than concentration of  $M_T$  ( $\sim 2.5 \mu\text{g m}^{-3}$ ) reported from a pristine  
 527 Amazonian rainforest region measured during wet season (Huffman et al., 2010; 2012). The  
 528 monthly mean values of  $M_F$ , on the other hand, did not exhibit a similar pattern ~~like to that shown~~  
 529 by  $M_T$ , but followed a temporal pattern ~~like similar to that shown by  $N_F$~~  (Fig. 3e). The highest  
 530 mean mass concentration of  $M_F$  ( $\sim 0.4 \mu\text{g m}^{-3}$ ) observed during June ~~and~~ was  $\sim 3$  and 2 times  
 531 lower than the concentrations observed at a central European city ( $\sim 1.26 \mu\text{g m}^{-3}$ ) and pristine  
 532 Amazonian rainforest ( $\sim 0.85 \mu\text{g m}^{-3}$ ), respectively. The higher difference between mean and  
 533 median values of the box plots indicates the higher temporal variability. ~~The relative difference~~  
 534 ~~between mean and median of  $N_F$  was found be higher than that of  $M_F$  indicating higher temporal~~  
 535 ~~variability of  $N_F$  during all measurement months. Averaged over the course of entire~~  
 536 ~~measurement period this trend was found to be consistent.~~ The median and mean for  $M_F/M_T$  over  
 537 the course of entire measurement period were 6 and 3% respectively, which is relatively low  
 538 compared to previously reported studies for various other environments (Huffman et al., 2010;  
 539 2012; Artaxo and Hansson, 1995; Schumacher et al., 2013; Fig. 3f). On the average, the relative  
 540 contribution of FBAP to TAP coarse mode particle mass was  $\sim 3$  times higher ( $\sim 6\%$ ) than its  
 541 contribution to coarse mode particle number concentration ( $\sim 2\%$ ). This is consistent with the  
 542 observations that FBAPs show enhanced prevalence among the larger aerosol particles (Huffman  
 543 et al., 2010).

### 544 3.1.2 Diurnal Patterns

Formatted: Font: Bold, Not Italic, German (Germany)



545 The average diurnal trends for three individual months and the entire measurement campaign  
 546 were analyzed. ~~patterns~~ Figure 4 shows the mean FBAP values for each hour of the day for three  
 547 individual months in the campaign, and Fig. S6 shows the corresponding TAP plots. Overall  $N_F$   
 548 exhibited a moderate diurnal pattern with a consistent early morning (06:00 hr.) peak at  $\sim 3 \mu\text{m}$   
 549 (Fig. ~~mass~~ 4a) except for the month of July, where this early morning peak was absent. A very  
 550 weak peak during late evening (20:00 hr.) in FBAP concentration at  $\sim 3 \mu\text{m}$  was observed in the  
 551 month of July. In the month of June, the average diurnal  $N_F$  concentration started increasing early  
 552 in the evening ( $\sim 18:00$  hr.), which gradually increased through the night reaching maximum at  
 553  $\sim 06:00$  hr. and started decreasing thereafter as the day progressed. A similar diurnal pattern was  
 554 also observed in August but without high FBAP concentrations in the evening hours. In general,  
 555 the weak diurnal pattern observed in  $N_F$  during the month of July seemed to follow the weak  
 556 diurnal patterns in RH and temperature, in the presence of persistent rainfall observed during  
 557 July. The early morning peak at  $\sim 3 \mu\text{m}$  on the diurnal scale was also reported from pristine  
 558 Amazonian rainforest environment (Huffman et al., 2012). Corresponding average size  
 559 distributions for entire measurement period will be discussed in details in Sec. 3.3. The diurnal  
 560 variations of  $N_T$  (Fig. S6), on the other hand were very distinct from those of  $N_F$ . The size  
 561 resolved  $dN_T/d\log D_a$  for each individual months exhibited a consistent and flat concentration  
 562 profile at  $<1 \mu\text{m}$ . Previous studies where similar instrument was used have reported that  
 563 pronounced diurnal variations in  $N_T$  are strongly coupled with diurnal variations in  
 564 meteorological variables especially mixing layer depth (Garland et al., 2009; Raatikainen et al.,  
 565 2014; Du et al., 2013). The absence of pronounced diurnal variations in  $N_T$  at this particular site  
 566 may be a result of weak dependence of coarse mode TAP concentrations on meteorological  
 567 parameters combined with persistent rainfall causing the washout of these particles (Radke et al.,

Formatted: Justified

Formatted: Font: Not Italic

Formatted: Font: Not Italic

1980; Raatikainen et al., 2014; Kanawade et al., 2014; Shika et al., 2016). This also indicates the absence of any strong and localized source of anthropogenic emissions during most of the campaign period. Diurnal patterns of  $N_F/N_T$  more or less followed the same pattern as that of  $N_F$  during all the measurement months. The distinct diurnal pattern in  $N_F$  and  $N_T$  supports the fact that the sources of TAP and FBAP were different over this region.

Formatted: Font: Not Italic

The diurnal trends in  $M_F$  and  $M_T$  for individual months and campaign average were also analyzed and are shown in Fig. 6. The corresponding diurnal trends in  $M_T$  are shown in Fig. Figures S7 and S8. The monthly averaged diurnal trends in  $M_F$  for individual months and entire campaign exhibited similar trend similar to that shown by corresponding to  $N_F$ . However, the prominent peak in  $dM_F/d\log D_a$  was observed at higher diameter ( $\sim 3 - 4 \mu m$ ), which is due to the fact that  $dM_F/d\log D_a$  has been derived from  $dN_F/d\log D_a$  assuming unit density. As observed for  $N_F$  during the month of June, the consistent morning peak was present in  $M_F$  with only difference of prominent second peak in  $M_F$ , which starts late in the evening at  $\sim 19:00$  hr and further extends up to morning hours ( $\sim 08:00$  hr). Thereafter  $M_F$  concentration steadily decreased as the day progressed reaching minimum at around mid day. The early morning peak in  $M_F$  concentration was consistently observed in the size range of  $3 - 4 \mu m$  for the all the measurement months. The characteristic distribution of  $M_T$  (Fig. S8), however, exhibited distinct behavior as compared to both  $M_F$  and  $N_T$ . The concentration peak of  $<1 \mu m$  observed in  $N_T$  shifted to the higher diameter range of  $\sim 2 - 3 \mu m$  as increase in mass is more associated with presence of coarse mode particles. For example in June  $M_T$  exhibited similar diurnal feature as that of  $N_T$ . The flatter trend observed in average  $M_T$  during the month of June disappeared during the month of July and August with appearance of less prominent peak in  $M_T$  at around  $12:00$  hr resulting in relatively pronounced diurnal pattern (Fig. S8). The concentration peak of  $<1 \mu m$  observed in  $N_T$  shifted

to the higher diameter range of  $\sim 3 - 4 \mu\text{m}$  as increase in mass is more associated with presence of coarse mode particles. The distribution of  $M_T$  (Fig. S8), however, exhibited a distinctly different trend compared to both  $M_F$  and  $N_T$ . The distinct diurnal patterns of  $M_F$  and  $M_T$  showed very less relative contribution of FBAP to TAP mass as compared to other observational sites (Huffman et al., 2010, 2012; Matthias-Maser and Jaenicke, 1995).

Formatted: Font: Bold

### 3.1.3 Size distribution of particle number and mass

Figure 75 shows the number and mass size distributions for TAPs and FBAPs averaged over the entire measurement period. The TAP number size distribution,  $dN_T/d\log D_a$ , was generally broad and dominated by a peak at the lower end of the measured size range of number size distribution ( $D_a \approx 0.9 \mu\text{m}$ ; Fig. 7a5a). In  $dN_T/d\log D_a$ , the concentrations exhibited a significant decrease above diameter  $\sim 3 \mu\text{m}$  with a long tail extending on the right hand side of the distribution. This peak may be comprised of mineral dust and sea salt particles, as also evident from SEM images (please refer to section 3.3) and as also reported by the previous studies investigating aerosol composition over India during monsoon season (Vinoj et al., 2014; Moorthy et al., 1991; Vinoj and Satheesh, 2003; Satheesh and Srinivasan, 2002; Li and Ramanathan, 2002). The corresponding monthly  $dN_T/d\log D_a$  are shown in Fig. S9. Overall the individual monthly  $dN_T/d\log D_a$  A similar peak in  $dN_T/d\log D_a$  at  $D_a \approx 0.9 \mu\text{m}$  was observed in pristine Amazonian rainforest during wet season and was attributed to mineral dust (Huffman et al., 2012; Fig. 5b). The corresponding monthly plots of  $dN_T/d\log D_a$  are shown in Fig. S9 and exhibited the similar qualitative number size distribution pattern as that of campaign averaged TAP number size distribution. Averaged over the entire measurement period, the mass size distribution,  $dM_T/d\log D_a$  (Fig. 7e5c), exhibited a broad peak at  $\sim 2.6 \mu\text{m}$  with an extended tail to the left side of the mass size distribution, whereas on the right side a second peak started appearing at  $D_a \approx 12$

Formatted: Justified

614 ~~μm.~~ The corresponding monthly averaged  $dM_T/d\log D_a$  are shown in Fig. ~~S10. As evident from~~  
615 ~~the figure S10 and appeared similar to~~ the campaign average TAP mass size distribution  
616 ~~appeared generally similar to each of the individual months.~~ For accurate representation of mass  
617 size distribution the unit-normalized mass distribution ~~in~~  $D_a$  plotted in Fig. ~~75~~ (c and d) is  
618 expected to shift to larger particle size with increased area under the curve, ~~as  $D_a$  is directly~~  
619 ~~proportional to square root of density of the particle under consideration~~ (Huffman et al., 2010;  
620 DeCarlo et al., 2004).

621 The campaign average number size distribution of FBAP (Fig. ~~7b5b~~) exhibited monomodal  
622 shape with much narrower peak than the TAP number size distribution, with a dominant mode at  
623  $D_a \sim 2.8 \mu\text{m}$ , which was consistent throughout measurement period. The corresponding monthly  
624 mean FBAP number size distributions are shown in Fig. S11. ~~This peak was much prominent~~  
625 ~~and narrow in the month of June with highest FBAP concentration and became less pronounced~~  
626 ~~in July, with the lowest FBAP concentration.~~ As reported by Huffman et al., (2010) multiple and  
627 broader peaks in  $dN_F/d\log D_a$  are most likely to originate from different sources and biological  
628 species. In the present study, however, we did not find multiple peaks in investigated FBAP  
629 number size distribution, suggesting that observed FBAPs comprised the particles from similar  
630 or same sources. The overall qualitative appearance of the average FBAP number size  
631 distribution is similar to that has been reported by previous measurements. For a semi-urban site  
632 in Central Europe Huffman et al., (2010) reported an average FBAP peak at  $3.2 \mu\text{m}$ . Gabey et al.,  
633 (2010) observed a ~~similar~~ peak at  $\sim 2.5 \mu\text{m}$  at a tropical rain forest site in Borneo. From a pristine  
634 Amazonian rainforest site during wet season Huffman et al., (2012) reported a ~~similar~~ peak at  
635  $\sim 2.3 \mu\text{m}$ . For another pristine observational site in boreal forest in Finland Schumacher et al.,  
636 (2013) reported a peak in FBAP number size distribution at  $\sim 3 \mu\text{m}$ . A ~~similar~~ peak at  $\sim 3 \mu\text{m}$  was

also observed by Healy et al., (2014) at a rural site in Killarney national park, Ireland. This dominant peak in the range of 2 – 3  $\mu\text{m}$  in FBAP number size distribution is strongly attributed to the fungal spores over the continent as reported by numerous previous researchers (Huffman et al., 2010, 2012; Schumacher et al., 2013; Li et al., 2011; Artaxo and Hansson, 1995; Healy et al., 2014; Gabey et al., 2010, 2013; Toprak and Schnaiter, 2013). Recently Valsan et al., (2015) investigated the morphological characteristics of PBAPs from the same site during non-monsoon season and found that fungal spores constituted the major fraction of PBAPs and nominally ranged in the size range of  $\sim 3 - 10 \mu\text{m}$ , which roughly translates into equivalent aerodynamic diameter of 2 – 5  $\mu\text{m}$ . (assuming particles to be a prolate spheroid). The scanning electron microscopy images obtained from the filter samples ~~occasionally~~ collected during this field campaign showed the strong presence of variety of fungal spore in the size range of ~~36~~ – 10  $\mu\text{m}$  (aerodynamic diameter ~~23~~ – 5  $\mu\text{m}$ ; discussed below; Fig. ~~1711~~). As an overview of the comparison, the FBAP concentration values observed at Munnar are compared to the FBAP concentration ranges obtained using similar online measurements techniques from diverse environmental conditions across the globe, and the details are tabulated in Tab. 3. The campaign averaged FBAP mass size distribution is shown in Fig. ~~745d~~, which nominally appeared bimodal with very sharp primary peak at  $D_a \approx 3.2 \mu\text{m}$  and very broad but ~~unappreciable~~ small second mode at  $D_a \approx 4 \mu\text{m}$ . ~~The distinct presence of particle mass in the higher diameter range ( $>10 \mu\text{m}$ ) in FBAP mass size distribution was not prominently noticed in Munnar as compared to previously reported studies (Huffman et al., 2010; 2012). In case of TAP mass size distribution the right side tail started showing positive slope at larger diameter whereas FBAP mass size distribution consistently showed the negative slope at larger diameters. Such a distinct shape of mass size distributions for TAP and FBAP reconfirms the fact that the larger particles observed in the TAP~~

660 ~~mass distribution originated from processes that did not produce particles of the biological origin~~  
 661 ~~as likewise reported by Huffman et al., (2010).~~ The corresponding monthly mean FBAP mass  
 662 size distributions are shown in Fig. S12. ~~The~~ The FBAP mass size distribution for individual  
 663 ~~month FBAP mass size distribution~~ months exhibited the similar qualitative shape to that of  
 664 average campaign. ~~As mentioned above highest FBAP mass concentration was observed in June,~~  
 665 ~~which coincided with a very sharp and narrow primary peak in FBAP mass size distribution,~~  
 666 ~~while the lowest FBAP mass concentration during July, on the other hand, coincided with a~~  
 667 ~~broad primary peak with lower slope.~~  
 668 The Figure 6 shows the size-resolved ratio of overall FBAP ~~to~~ /TAP ~~averaged over~~ for the course  
 669 of measurement ~~is shown in Fig. 8~~ and corresponding monthly ratios are shown in Fig. S13. The  
 670 relative contribution of FBAPs ( $dN_F$ ) to TAPs ( $dN_T$ ) in each size bin could be used to derive the  
 671 relative contribution of biological particles to total aerosol particles at each size. As reported by  
 672 Huffman et al., (2010) the assumption of unit density of each particle implies that the value of  
 673 the  $dN_F/dN_T$  ratio would invariably is equal to  $dM_F/dM_T$ . The integrated  $N_F/N_T$  and  $M_F/M_T$ ,  
 674 however, would have the distinct values. As can be seen from Fig. ~~86~~ 86 and ~~S13a~~ S13 considerable  
 675 quantitative and qualitative difference in mean (red) and median (green) curve was consistently  
 676 observed in all individual months, which likely is the result of poor counting statistics and very  
 677 high variability in ~~FBAP and~~ TAP number concentrations. Based on the results presented by  
 678 Huffman et al., (2010) the mean (red) curve, best represents the  $N_F/N_T$  ratios at the upper particle  
 679 sizes; ~~hence we will stick our further discussion about  $N_F/N_T$  ratios for the present study to the~~  
 680 ~~mean curve.~~ The mean  $N_F/N_T$  ratio curves for individual months and for entire campaign  
 681 exhibited two dominant peaks persistently in the particle size range  $\sim 3 - 4 \mu m$  and  $\sim 6 - 8 \mu m$ .  
 682 The first prominent peak in  $dN_F/dN_T$  distribution at  $3 - 4 \mu m$  comprised 15 – 16% while the

second peak at 6 – 8  $\mu\text{m}$  represented ~14 – 15% of the FBAP material in TAP over the entire measurement period (Fig. 8). ~~As can be observed from Fig. S13, the second peak in  $N_P/N_T$  ratios for July was higher (~12%) than the first peak (~10%) unlike other two observational months. The fact that  $N_P/N_T$  ratio is approximately zero for the particle sizes  $<1.7 \mu\text{m}$  indicated that FBAP mainly comprised of very small fraction of submicron aerosols at Munnar. The statistics for the individual months showed that the first peak in  $dN_P/dN_T$  was more or less consistent at ~22% during June and August except for the July when second peak in  $N_P/N_T$  ratios contributed more (~12%) than the first peak (~10%).~~6).

### 3.4.2 Focus periods

~~As described in Sec. 3.1 based on campaign overview the characteristics~~[The characteristic](#) properties of FBAP and specifically TAP number concentration exhibited strong temporal ~~variabilities~~[variability](#), which could be attributed to changes in prevailing meteorological conditions ~~especially wind direction~~ during monsoon season at Munnar. ~~To explore the potential impact of air mass origin on number and size distribution of FBAP and TAP, we highlight~~[The following](#) three distinct focus periods [during the campaign are highlighted as follows](#):

1. A [“dusty”](#) focus period ~~of “dusty episode”~~ was identified when prevailing wind was predominantly Westerly/Southwesterly and air masses mainly came from the Arabian Sea. ~~These air masses, although almost anthropogenically clean, are~~[These were](#) laden with sea salt and dust particles during the start of the monsoon, which dominate the coarse mode fraction of atmospheric aerosols (Vinoj et al., 2014; Li and Ramanathan, 2002). ~~These dust particles observed over this region mainly originate~~[originating](#) from West Asia, North Africa, and Arabian region (Vinoj et al., 2014). ~~During our measurement~~[\) and not from local anthropogenic](#)

Formatted: Justified

706 sources. In this campaign, such a dusty period ~~from 14-06-2014 00:00 hr to 25-06-2014 23:55 hr~~  
707 was observed ~~and is~~ between June 14-25, 2014, which was consistent with the description given  
708 above and also based on the SEM images, ~~which showed the presence of mineral~~ the dust,  
709 ~~obtained during dusty~~ collected in this period (see Sec. 3.5 below). This period was marked with  
710 an accumulated rainfall of ~1015 mm, average relative humidity of  $94.4 \pm 6.5\%$ , average  
711 temperature of  $17.7 \pm 1.5^\circ\text{C}$ , and average wind speed  $2.8 \pm 1.3 \text{ m s}^{-1}$  (maximum wind speed of  
712  $6.7 \text{ m s}^{-1}$ ).

713 2. A “clean” focus period ~~of “clean period”~~, was observed during latter half of the monsoon  
714 season when wind direction was still predominantly Westerly/Southwesterly and air masses  
715 originated over Arabian Sea. During this period, which was ~~chosen~~ observed from ~~09-07-July 9 –~~  
716 August 7, 2014 10:25 hr to 07-08-2014 23:55 hr, FBAP and TAP concentrations were extremely  
717 low with very ~~weak~~ low variability. This clean period was associated with persistent rainfall  
718 (accumulated rainfall of 2650 mm), average relative humidity of  $99.5 \pm 1.4\%$ , average  
719 temperature of  $16.4 \pm 0.5^\circ\text{C}$ , and average wind speed  $3.7 \pm 1 \text{ m s}^{-1}$  (maximum wind speed of  $8.3 \text{ m}$   
720  $\text{s}^{-1}$ ).

Formatted: Font: Italic

721 3. A “high bio” focus period ~~of “high bio”~~ comprised three discrete events of high FBAP  
722 concentration observed ~~from 01-06-between June 1-5, 2014-09:10 hr to 05-06-2014 18:20 hr,~~  
723 June 26-06-2014 00:05 hr to 30-06-2014 17:00 hr, and August 18-08-2014 00:00 hr to 22-08-  
724 2014 08:30 hr. Interestingly this, 2014. This period is marked with ~~the very~~ distinct metrological  
725 parameters compared to the clean period: accumulated rainfall 194 mm, average relative  
726 humidity  $93.4 \pm 8.4\%$ , average temperature  $18.0 \pm 2.4^\circ\text{C}$ , and average wind speed  $1.2 \pm 0.8 \text{ m s}^{-1}$   
727 (with maximum wind speed of  $4.6 \text{ m s}^{-1}$ ). ~~Briefly, during “It is suggested that these high-bio”~~  
728 period-stagnant- periods are due to high variability in relative humidity and temperature, and the

Formatted: Font: Italic



729 movement of air masses ~~came from~~with relatively low wind speed, over densely vegetated  
 730 region located north of observational site, ~~and relative humidity and temperature exhibited high~~  
 731 ~~variability.~~

### 732 3.42.1 Particle number and mass concentrations

733 The statistical distributions of  $N_T$ ,  $N_F$ ,  $M_T$ ,  $M_F$ , and  $M_F$  corresponding ratios for three different  
 734 focus periods (*dusty*, *clean*, and *high bio*) are shown in Fig. 97 and tabulated in Tab. 4. Each of  
 735 the focus periods discussed here ~~did were~~ not represent of equal duration ~~of the observations.~~

736 The average total particle number concentration,  $N_T$ , showed a decrease of ~70% from *dusty*  
 737 period to *clean* period (~4.2 cm<sup>-3</sup> and ~1.3 cm<sup>-3</sup> respectively), whereas the  $N_T$  concentration  
 738 during *high bio* period was ~1.8 cm<sup>-3</sup>. The high  $N_T$  concentration during the *dusty* period caused

739 the high variability between 5<sup>th</sup> and 95<sup>th</sup> percentile in  $N_T$  when averaged over entire campaign  
 740 period (Fig. 3a). The fraction of dust in coarse mode aerosol, which is observed to be very high  
 741 during pre-monsoon and first few days from the onset of monsoon rainfall, gradually decreased

742 as the monsoon progressed likely as a result of wash out and wet deposition due to persistent  
 743 rainfall in the path of air masses (Hirst 1953; Madden, 1997; Burge and Roger, 2000). The  $M_T$   
 744 exhibited similar pattern to that of  $N_T$  during three distinct focus periods with average mass

745 concentration of ~16.3 µg m<sup>-3</sup>, ~5.1 µg m<sup>-3</sup>, and ~7.7 µg m<sup>-3</sup> for *dusty*, *clean*, and *high bio*  
 746 periods, respectively. (Fig. 7d).

747 ~~As expected, the~~The mean  $N_F$  ~~was highest concentration~~ during the *high bio* period (Fig. 9b) ~~with~~  
 748 ~~an average concentration of 7b) was~~ 0.05±0.04 cm<sup>-3</sup> ~~and with~~ high variability in higher

749 concentration range (0.06 – 0.13 cm<sup>-3</sup>) as evident from the distance between 75<sup>th</sup> and 95<sup>th</sup>  
 750 percentile. The  $N_F$  was found to be relatively stable during the *dusty* period with an average

751 concentration of ~0.02±0.008 cm<sup>-3</sup>. The average mean  $N_F$  concentration was found to be an order

Formatted: Not Superscript/ Subscript

Formatted: Justified

Formatted: Font: Italic

Formatted: Font: Italic

Formatted: Font: Italic

Formatted: Font: Italic

Formatted: Font: Italic

Formatted: Font: Italic

Formatted: Font: Italic

Formatted: Font: Italic

Formatted: Font: Italic

Formatted: Font: Italic

Formatted: Font: Italic

Formatted: Font: Italic

752 of magnitude lower during the *clean* period ( $0.005 \pm 0.004 \text{ cm}^{-3}$ ) as compared to *high bio* period,  
 753 whereas corresponding decrease in  $N_T$  from *dusty* to *clean* period ( $\sim$  by factor of 3) was not of  
 754 similar magnitude. ~~We put forward~~ The following is the hypothesis proposed for such a  
 755 concentration difference in  $N_F$  and  $N_T$  during the three distinct periods: During the *clean* period  
 756 the predominant wind direction was Westerly/Southwesterly and air masses came from Arabian  
 757 Sea bringing clean marine influx marked by persistent rainfall. As a result, the coarse mode  
 758 aerosol fraction ( $N_F$  and  $N_T$ ) emitted locally were efficiently removed, however, the sea salt  
 759 particles present in the air masses, which came from Arabian Sea contributed to TAP number  
 760 concentration (see section 3.5.3). In addition to the efficient wet removal of FBAP due to  
 761 persistent rainfall, the high RH level (average 99.5%), ~~which~~ causes the dew formation that  
 762 further inhibit the spore release in turn ~~reduced~~ reducing the FBAP concentration (Schumacher et  
 763 al., 2013; Jones and Harrison, 2004). The mean values of  $M_F$  exhibited trends similar ~~temporal~~  
 764 ~~trends and qualitative pattern as~~ to those shown by  $N_F$ , with highest mass concentration of  $0.58$   
 765  $\mu\text{g m}^{-3}$  during *high bio* period, which reduced by  $\sim 86\%$  ( $0.08 \mu\text{g m}^{-3}$ ) during the *clean* period.  
 766 As anticipated the relative contribution of FBAP in TAP during *dusty* and *clean* periods was  
 767 almost negligible with  $N_F/N_T$  ratio of  $\sim 1\%$ . Whereas during the *high bio* period the relative  
 768 FBAP number and mass contribution to corresponding TAP was  $\sim 5\%$  and  $12\%$  respectively.

Formatted: Font: Italic

Formatted: Font: Italic

Formatted: Font: Italic

Formatted: Font: Italic

Formatted: Font: Italic

Formatted: Font: Italic

Formatted: Font: Italic

Formatted: Justified

Formatted: Font: Italic

Formatted: Font: Italic

Formatted: Font: Italic

### 769 **3.4.2.2 Size distribution of particle number and mass concentration**

770 Figure ~~108a~~ highlights the  $dN_F/d\log D_a$  during three distinct focus periods and corresponding  
 771  $dN_T/d\log D_a$  are shown in Fig. S14. ~~Overall~~ In general  $dN_F/d\log D_a$  during each focus period  
 772 exhibited pattern similar to that of campaign average.

Formatted: Justified

773 The  $dN_F/d\log D_a$  averaged over the ~~dusty-high bio~~ period ~~was dominated by~~ exhibited a ~~narrow~~  
 774 very prominent and sharp peak at  $\sim 2.5 - 3.4 \mu\text{m}$ . The corresponding  $dN_F/d\log D_a$  during *dusty*

775 ~~and clean period was overall broader also exhibited similar bell shaped distribution with less~~  
 776 ~~prominent peaks owing to the relatively lower FBAP concentrations as~~ compared to ~~dusty and~~  
 777 ~~high bio periods with gradual increase in FBAP number concentration from diameter range of ~1~~  
 778 ~~~2.3  $\mu\text{m}$ , with a sharp increase thereafter, whereas downward slope exhibited the consistent~~  
 779 ~~pattern.  $dN_F/d\log D_a$  during the high bio period exhibited relatively narrow peak at ~2.5  $\mu\text{m}$ .~~  
 780 Unlike previously reported studies (Huffman et al., 2010; 2012) the peak in  $dN_F/d\log D_a$  ( $D_a \approx 3$   
 781  $\mu\text{m}$ ) was not reflected in  $dN_T/d\log D_a$  mostly due to relatively less contribution of FBAP in  
 782 coarse mode TAP number concentration. As ~~can be~~ seen from Fig. ~~S14a~~S14 the total aerosol  
 783 particle number size distribution,  $dN_T/d\log D_a$ , during ~~dusty period~~all the three focus periods  
 784 ~~exhibited a peak at ~0.9  $\mu\text{m}$ , with a high negative slope on the left side of the distribution curve.~~  
 785 ~~This peak may be comprised of mineral dust and sea salt particles, as also evident from SEM~~  
 786 ~~images (please refer to section 3.5) and based on the previous studies investigated aerosol~~  
 787 ~~composition over India during monsoon season (Vinoj et al., almost similar pattern to that of~~  
 788 ~~campaign averaged 2014; Moorthy et al., 1991; Vinoj and Satheesh, 2003; Satheesh and~~  
 789 ~~Srinivasan, 2002; Li and Ramanathan, 2002). A similar peak in  $dN_T/d\log D_a$  at  $D_a \approx 0.9 \mu\text{m}$  was~~  
 790 ~~observed in pristine Amazonian rainforest and particles were mostly dominated by mineral dust~~  
 791 ~~during high dust period (Huffman et al., 2012, Fig. 5b). During clean period  $dN_T/d\log D_a$~~   
 792 ~~resembled the similar shape (with higher concentrations peaking at ~0.9  $\mu\text{m}$ ) to that of dusty~~  
 793 ~~period, however, with lower concentration. The corresponding  $dN_T/d\log D_a$  distribution (Fig.~~  
 794 ~~S14c), during high bio period, exhibited multiple peaks and appeared noisy for  $D_a < 1 \mu\text{m}$  with~~  
 795 ~~increasing trend in TAP number concentration for the lower diameter range of the distribution.~~  
 796 ~~The downward slope for  $D_a > 1 \mu\text{m}$  exhibited consistent shape (mean curve) compared to~~  
 797 ~~distributions observed during other two focus periods.~~

Formatted: Font: Italic

Formatted: Font: Italic

Formatted: Subscript

798 The FBAP mass size distribution (Fig. ~~44~~8b) during *dusty* period was dominated by bimodal  
 799 peaks with prominent peak at  $\sim 3 \mu\text{m}$  and a relatively less pronounced peak in the range of  $\sim 4 -$   
 800  $6 \mu\text{m}$  showing broader tail on the right side of the distribution curve. The  $dM_F/d\log D_a$  during  
 801 *clean* period, exhibited similar bimodal peaks with extended shoulder in the diameter range from  
 802  $\sim 4$  to  $7 \mu\text{m}$ . The  $dM_F/d\log D_a$  distribution during *high bio* period was ~~distinct~~distinctly different  
 803 compared to the two other focus periods discussed above with a prominent monomodal peak at  
 804  $\sim 3 \mu\text{m}$ . The primary peak observed in  $dM_F/d\log D_a$  in the range of  $\sim 3$  to  $4 \mu\text{m}$  was consistent  
 805 during individual months and different focus periods. TAP mass size distribution (Fig. S15)  
 806 exhibited similar qualitative pattern to that of campaign averaged  $dM_T/d\log D_a$  with peak  
 807 between  $\sim 2.5$  to  $3.5 \mu\text{m}$  with an extended tail on the right side, which gradually increased for  
 808  $D_a > 13 \mu\text{m}$ . The statistics representing 5th, 25th, 75th, and 95th percentile for  $dN_F/d\log D_a$  and  
 809  $dM_F/d\log D_a$  during individual focus periods are shown in Fig. S16 and S17.  
 810 The size resolved ratio of FBAP to TAP particles averaged for three distinct focus periods is  
 811 shown in Fig. ~~42~~9. As evident from the figure the largest fraction of FBAP particles during  
 812 *dusty* period occurred between  $\sim 6 - 9 \mu\text{m}$  ( $\sim 20\%$ ) with relatively small ( $\sim 7\%$ ) contribution in  
 813 the ~~size~~diameter range of  $\sim 3 - 4 \mu\text{m}$  ( ~~$\sim 7\%$~~ ). ~~The  $dN_F/dN_T$  exhibited the sloping tails on both the~~  
 814 ~~sides of the distribution with steep slope on the right side.~~ The fact that  $N_F/N_T$  is  
 815 ~~approximately~~near zero for ~~the~~ particle size ~~range~~ below  $\sim 1.5 \mu\text{m}$  is ~~consistent~~in line with  
 816 previous observations reported from a semi urban site in central Europe and during wet season of  
 817 pristine Amazonian rainforest (Huffman et al., 2010; 2012). During the *clean* period the  
 818 maximum contribution of FBAP to TAP number concentration reduced to  $\sim 10.5\%$  in the  
 819 diameter range of  $\sim 6$  to  $9 \mu\text{m}$  ~~with another prominent~~, but ~~relatively smaller contributing the~~  
 820 peak, appeared at  $\sim 3 - 4 \mu\text{m}$  and remained almost consistent with relative contribution of  $\sim 8\%$ .

Formatted: Font: Italic

Formatted: Font: Italic

Formatted: Font: Italic

Formatted: Font: Italic

Formatted: Font: Italic

821 ~~During~~ Whereas during *high bio* period the maximum contribution of FBAP to TAP occurred  
 822 between broader size range of  $\sim 3 - 8 \mu\text{m}$  with contribution range of  $\sim 28 - 19\%$  ~~and relatively~~  
 823 ~~broad  $dN_F/dN_T$  distribution %~~. Interestingly during the *high bio* period, the highest contribution  
 824 of FBAP to TAP number concentration occurred at  $D_a \approx \approx 3.5 \mu\text{m}$ , as opposed to the other two  
 825 focus periods when the highest contribution was observed in the larger diameter ranges of  $\sim 6 -$   
 826  $8 \mu\text{m}$ .  $N_F/N_T$  was consistently found to be ~~equal to~~ very low, with values approaching zero for the  
 827 diameter beyond  $13 \mu\text{m}$ , indicating ~~that~~ FBAP ~~comprised~~ constituted an extremely small fraction  
 828 of total aerosol particles (Huffman et al., 2010; 2012). The two prominent peaks observed during  
 829 the focus periods were clearly evident in campaign-averaged  $dN_F/dN_T$  (Fig. ~~86~~; peaks at  $\sim 3.5$  and  
 830  $6 \mu\text{m}$ ).

Formatted: Font: Italic

Formatted: Font: Italic

### 831 3.42.3 Diurnal patterns

832 A prominent early morning peak in  $N_F$  during the *high bio* period in the diameter range of  $1.5 - 3$   
 833  $\mu\text{m}$  was observed from 06:00 ~~hr~~ to 08:00 ~~hr~~ hrs., which clearly reflected in campaign averaged  
 834 diurnal patterns at the same hour of the day. The diurnal variations in  $N_F$  during the *dusty* and  
 835 *clean* periods were not so pronounced (Fig. ~~13~~ 10) as compared to the variations during the *high*  
 836 *bio* period. During the *dusty* period,  $N_F$  showed slightly high concentration starting from  
 837  ~~$\sim 20$~~  17:00 hrs. (lowest panel Fig. 10a) and persistently remained high until early morning without  
 838 any variations, whereas during the *clean* period,  $N_F$  concentration consistently remained flat  
 839 throughout 24 ~~hrs.~~ The evening peak observed during dusty period, however, was clearly absent  
 840 during high bio period. A moderately pronounced peak in  $N_F$  during evening hours at  $\sim 20:00$  hr  
 841 during dusty periods might indicate that releasing mechanism of bioaerosols was efficient as a  
 842 result of nocturnal sporulation. This can further imply that the morning and late evening peaks in  
 843  $dN_F/d\log D_a$  at  $D_a \approx 3 \mu\text{m}$  most likely resulted from different type of spores (Hirst, 1953). As

Formatted: Font: Italic

Formatted: Justified

Formatted: Font: Italic

Formatted: Font: Italic

Formatted: Font: Italic

Formatted: Font: Italic

Formatted: Font: Italic

844 ~~listed~~reported by Huffman et al., (2012) the emission and dispersal of bioaerosols is strongly  
 845 coupled with environmental variables such as solar radiation, temperature, and relative humidity  
 846 ~~and each.~~ Each of these variables ~~have strong~~exhibited relatively pronounced diurnal  
 847 ~~eyeles.~~variations during the high bio period (upper panel Fig. 10c). It has been well documented  
 848 that relative humidity, in particular, plays an important role in active wet discharge of fungal  
 849 spores (Adhikari et al., 2006; Burch and Levetin, 2002; Elbert et al., 2007; Jones and Harrison,  
 850 2004; Quintero et al., 2010; Zhang et al., 2010) , which constitutes major fraction of atmospheric  
 851 bioaerosols (Ansari et al., 2015; Bauer et al., 2008; Bowers et al., 2013; Fröhlich-Nowoisky et  
 852 al., 2009; Sesartic and Dallafior, 2011; Spracklen and Heald, 2014). The meteorological  
 853 parameters exhibited ~~pronounced~~significant diurnal variations during the high bio period, where  
 854 RH decreased to a level (~~←~~~60 – 80%)%, which is considered to be favorable for release of the  
 855 fungal spores (Jones and Harrison, 2004; Santarpia et al., 2013). During the dusty and clean  
 856 ~~period~~periods, the persistence of high RH values in the range of ~90 – 100%, ~~however,~~ might  
 857 have inhibited the active wet discharge of fungal spore (Schumacher et al., 2013;~~→~~) thus  
 858 resulting in the weak diurnal variation in  $N_F$ . Unlike  $N_F$ ,  $N_T$  remained nearly flat without any  
 859 pronounced diurnal variations during three distinct focus periods (Fig. ~~S16~~S18). The  
 860 corresponding diurnal cycle of FBAP mass concentration and 3D size distributions for three  
 861 focus periods are shown in Fig. ~~S17~~S19.  $M_F$  exhibited similar diurnal patterns to that of  $N_F$   
 862 during three distinct focus periods.  $M_T$  ~~as like and~~  $N_T$  remained flat during the dusty period,  
 863 ~~however~~but exhibited slightly pronounced diurnal pattern during the clean and the high bio  
 864 period between 09:00 hrs. and 16:00 hrs. (Fig. ~~S18~~S20).

Formatted: Font: Italic

Formatted: Font: Italic

Formatted: Font: Italic

Formatted: Font: Italic

Formatted: Font: Italic

Formatted: Font: Italic

Formatted: Space After: 0 pt

### 3.5.3 SEM images

Figure 14.11 shows ~~the exemplary~~representative SEM images of different biological particle types often observed during the SW monsoon season at Munnar. The details about the sampling techniques, instrument used, etc. for obtaining these bioaerosol images are discussed in details by Valsan et al., (2015). Note that these images are ~~not~~ being presented here ~~for any quantitative purpose and to draw any specific scientific conclusions but mainly~~ to showcase the particle types consistently observed throughout the measurement period. ~~As seen from the SEM images majority and not for quantitative purposes. The presence of the~~mineral dust and sea salt particles ~~are mostly likely fungal spores. Based on their distinct morphology the spores in Fig. 14a~~e confirms marine influence of the air mass sampled. Many particles observed by SEM were most likely ~~appeared to be of~~ Basidiospores. The appearance of small protuberances on ~~the surface~~their surfaces suggests that the ~~spore in~~spores (e.g. Fig. ~~14a~~11a and c) most likely belonged to the *Hydnaceae* family (Grand and Vandyke, 1976; Valsan et al., 2015). The Basidiospores shown in Fig. ~~14b~~11b and c were seen in abundance in all the samples collected during the campaign. Some of the spores observed appeared to be coated with salt particles (Fig. ~~14e~~11e) and might have been carried from a distant source by the SW monsoon winds. The spores shown in Fig. ~~14~~11 (d and f) most likely appeared to be spores of Ascomycota division. The particle shown in Fig. ~~14g~~11g was most likely a mineral dust particle sampled during high dusty episode. Similar particles of varying size during the *dusty* episode were consistently observed during SEM analysis. Fig. ~~14h~~11h and ~~11i~~11i shows the images of the typical sea salt particles observed during samples collected at Munnar during measurement campaign when wind predominantly came from Westerly/Southwesterly direction travelling over Indian Ocean and Arabian Sea.

Formatted: Justified, Space After: 0 pt

Formatted: Font: Italic

### 3.6.4 Meteorological Correlations

The results obtained with UV-APS data analysis during the campaign at Munnar were plotted correlated with ~~with respect to~~ meteorological parameters to investigate factors responsible for bioaerosol release and their variations in the atmosphere.

#### 3.4.1 Impact of wind direction

The wind rose diagrams scaled by  $N_F$ ,  $D_g$ , and  $D_{g,T}$  were also prepared for entire measurement period and three distinct focus periods. These plots are ~~in a way~~ similar to the traditional wind rose diagram (Fig. S19S21) except ~~that~~, instead of wind speed, they are scaled by characteristic FBAP and TAP parameters, which indicate the frequency of occurrence of respective parameter with respect to wind direction (Sherman et al., 2015). As ~~can be~~ seen from Fig. S19S21, predominant wind direction during entire campaign was Westerly/Southwesterly with frequency of occurrence of about ~90%. The wind speed broadly ranged between 2 – 5 m s<sup>-1</sup> with no prominent diurnal variations. The overall wind direction and back trajectory analysis (Fig. 1) shows that the sampled air masses may have ~~had their origin~~ originated over the Indian Ocean ~~thereafter and then~~ turning eastward after crossing the equator and travelling several hundred kilometers over Arabian Sea before reaching the observational site (Fig. 1). The predominant wind pattern during ~~the~~ *dusty* (>95% frequency of occurrence; 2 – 6 m s<sup>-1</sup>) and *clean* periods (~100 frequency of occurrence; 2 – 6 m s<sup>-1</sup>) was Westerly/Southwesterly. Whereas during ~~the~~ *high bio* period only ~50% of the time winds came from Westerly/Southwesterly direction and rest comprised ~~the stagnant and calm~~ of relatively slower (0 – 2 m s<sup>-1</sup>) winds from all other directions with highest contribution of northerly winds (Fig. S19). S21). Wind rose diagram scaled by FBAP number concentration is shown in Fig. 15.12. During the entire campaign the predominant wind showed that ~85% of the time FBAP concentration

Formatted: Space After: 0 pt

Formatted: Justified, Space After: 0 pt

Formatted: Font: Bold, Not Italic

Formatted: Space After: 0 pt

Formatted: Justified, Space After: 0 pt

Formatted: Font: Italic

Formatted: Font: Italic

Formatted: Font: Italic



913 occurred in the range of  $0 - 0.05 \text{ cm}^{-3}$  (Fig. ~~45a~~12a) occasionally exceeding  $0.05 \text{ cm}^{-3}$  and was  
 914 contributed by Westerly/Southwesterly winds. The occurrence of relatively low FBAP  
 915 concentration during entire campaign is ~~consistent~~coincidental with low concentration  
 916 occurrence during the *dusty* ( $0 - 0.05 \text{ cm}^{-3}$ ; >90% frequency of occurrence) and the *clean* ( $<0.01$   
 917  $\text{cm}^{-3}$ ; ~90% frequency of occurrence) periods. During the *high bio* period the FBAP  
 918 concentration,  $>0.05 \text{ cm}^{-3}$  exhibited ~40% frequency of occurrence of which ~50% was  
 919 contributed by predominant wind from the North and the Northwest.  
 920 Similarly the wind rose diagram scaled by geometric mean diameter ( $D_g$ ) of  $dN_F/d\log D_a$ , is  
 921 shown in Fig. ~~46~~13. The average size of the FBAP particles associated with  
 922 Westerly/Southwesterly winds when analyzed for the entire ~~the~~ campaign ranged between  $2 - 4$   
 923  $\mu\text{m}$  of which ~65% of the time  $D_g$  was observed to be  $\leq 3 \mu\text{m}$ . During the three ~~distinct~~ focus  
 924 periods the frequency of occurrence of FBAP particles in the higher size range ( $3 - 4 \mu\text{m}$ ) was  
 925 strongly associated with the Westerly/Southwesterly winds (Figs. ~~46b~~13b - d). The  
 926 corresponding wind rose diagram scaled by geometric mean diameter of  $dN_T/d\log D_a$  ( $D_{g,T}$ ) is  
 927 shown in Fig. ~~S20~~S22. During entire measurement campaign the frequency of occurrence of  
 928  $D_{g,T}$  in the size range of  $0.8 - 0.9 \mu\text{m}$  was ~70% and was mostly associated with  
 929 Westerly/Southwesterly winds. During the *dusty* period, particles in the size range of  $0.8 - 0.9$   
 930  $\mu\text{m}$  diameter contributed for >95% frequency of occurrence for the entire size range, whereas  
 931 during *clean* period ~20% occurrence of the particles in the size range other than  $0.8 - 0.9 \mu\text{m}$   
 932 were also observed. On the other hand during the *high bio* period total particles in the size range  
 933  $0.5 - 0.8 \mu\text{m}$  were observed with ~50% frequency of occurrence ~~constituted by varying wind~~  
 934 ~~patterns~~ mostly dominated by northerly winds.

Formatted: Font: Italic

Formatted: Font: Italic

Formatted: Font: Italic

Formatted: Font: Italic

Formatted: Font: Italic

Formatted: Font: Italic

935 The FBAP concentration exhibited strong dependence on the wind direction for this  
 936 observational site. During the *high bio* period the increase in frequency of occurrence of FBAP  
 937 number concentrations  $>0.1 \text{ cm}^{-3}$  coincided with ~~stagnant~~lower wind speed coming from the  
 938 North and Northwest (Fig. ~~17a~~14a). During the *high bio* period, as ~~like~~in the case of the *dusty*  
 939 and *clean* periods, the predominant wind pattern was Westerly/Southwesterly, ~~however~~but, with  
 940 relatively low frequency of occurrence as compared to the other two periods. To have ~~the a~~ better  
 941 understanding of the relative contribution of wind direction in high FBAP number concentration  
 942 during the *high bio* period, ~~we prepared the~~ separate wind rose diagrams for FBAP concentration  
 943  $>0.1 \text{ cm}^{-3}$  and  $<0.1 \text{ cm}^{-3}$  as shown in Fig. ~~17.14~~. The FBAP number concentration  $>0.1 \text{ cm}^{-3}$  was  
 944 associated with ~~calm~~lower wind speed ( $0 - 1 \text{ m s}^{-1}$ ; ~80% frequency of occurrence) and  
 945 predominant Northerly winds (Fig. ~~17a~~14a) as opposed to high wind speed ( $2 - 5 \text{ m s}^{-1}$ ) and  
 946 predominant Westerly/Southwesterly winds for the FBAP number concentration  $<0.1 \text{ cm}^{-3}$  (Fig.  
 947 ~~17b~~14b). The ~~calm-northerly~~Northerly winds with lower wind speed coming over from densely  
 948 vegetated regions in combination with local FBAP sources during the *high bio* period could be  
 949 the strong reason for the ~~built~~build up resulting in higher FBAP number concentration during this  
 950 episode, whereas, Westerly/Southwesterly winds were consistently marked by very low FBAP  
 951 number concentration mostly owing to higher wind speeds. Further, it might also due to the fact  
 952 that the air masses arriving at observational site ~~originated~~originating over cleaner marine region,  
 953 which may be potential but weak source of bioaerosols combined with possible wash out/wet  
 954 deposition due to persistent rainfall during the transport. ~~Nominally-the~~The frequency of  
 955 occurrence of larger particles ( $3 - 4 \text{ }\mu\text{m}$ ) during Westerly/Southwesterly winds was high  
 956 compared to the Northerly winds, where particles were mostly of smaller size ( $1 - 3 \text{ }\mu\text{m}$ ). We  
 957 hypothesize that during the Northerly wind the bioaerosols were mostly comprised of

Formatted: Font: Italic

Formatted: Font: Italic

Formatted: Font: Italic

Formatted: Font: Italic

Formatted: Font: Italic

Formatted: Font: Italic

Basidiospores, which is consistent with SEM images obtained during measurement period. Frohlich-Nowoisky et al., (2012) reported that, [a](#) region with dominant prevalence of marine air masses ~~have~~[has](#) larger proportions of Ascospores and in contrast, the continental air masses exhibit higher proportions of Basidiospores. However, due to technical difficulties associated with sampling we could not establish the ~~fact that~~[identity of the](#) spores observed at this observational site during Westerly/Southwesterly winds ~~were dominated by Ascospores~~ and these details will be addressed in follow up studies. The corresponding wind rose scaled by  $D_{g,T}$  obtained from  $dN_T/d\log D_a$  is shown in Fig. ~~S21~~[S23](#). As shown in Tab. 5 the wind speed was observed to ~~be~~[correlate](#) negatively ~~affecting the~~[with](#)  $N_F$  during entire measurement period and is consistent with previously reported studies (Hameed et al., 2012; Almaguer et al., 2013; Lyon et al., 1984; Quintero et al., 2010). The increased  $N_F$  concentration levels during ~~calm and stagnant~~[lower](#) wind [speed](#) might indicate that observed bioaerosols were dominated by the local source rather than transported from longer distances (Sadys et al., 2014; Hara and Zhang, 2012; Bovallius et al., 1978; Maki et al., 2013; Prospero et al., 2005; Creamean et al., 2013) as lower wind speed may actually increase emission of some specific type of spores (Huffman et al., 2012; Jones and Harrison, 2004; Troutt and Levetin, 2001; Kurkela, 1997).

### 3.6.14.2 Correlation with relative humidity and temperature

Correlation coefficient derived between  $N_F$  and relative humidity averaged over the entire campaign is shown in Fig. ~~18~~[15](#) and corresponding  $R^2$  values for three distinct focus periods are shown in Tab. 5. In general an increase in  $N_F$  concentration with increasing relative humidity was observed with moderate correlation coefficient ( $R^2=0.58$ ). Depending upon the type of bioaerosols, geographical location, and local climate,  $N_F$  has shown varied dependence on

Formatted: Space After: 0 pt

Formatted: Justified, Space After: 0 pt

981 relative humidity and [the](#) precise response of the spore concentration to relative humidity is  
 982 difficult to characterize. For example, [a](#) number of studies have shown that spores of genus like  
 983 *Cladosporium*, *Alternaria*, and *Epiccocum* are known to exhibit the negative correlation with  
 984 relative humidity (Oliveira et al., 2010; Herrero et al., 1996; Kurkela, 1997; Oh et al., 1998;  
 985 Healy et al., 2014); [while](#) on the other hand, [other](#) studies have also found these spores to be  
 986 positively correlated with relative humidity (Quintero et al., 2010; Hjelmroos, 1993; Ho et al.,  
 987 2005). ~~Whereas genus~~ [Genus](#) like *Ustilago* and some other Basidiospores may ~~as well~~ exhibit  
 988 strong positive correlation with relative humidity (Sabariego et al., 2000; Quintero et al., 2010;  
 989 Ho et al., 2005; Calderon et al., 1995). ~~Further~~, Ascospores concentrations are known to increase  
 990 during and after rainfall (Burch and Levetin, 2002; Elbert et al., 2007; Hasnain, 1993; Hirst,  
 991 1953; Toutt and Levetin, 2001; Lyon et al., 1984; Oh et al., 1998) whereas Basidiospores  
 992 exhibited a strong resemblance to the diurnal pattern of relative humidity (Li and Kendrick 1994;  
 993 Hasnain 1993; Tarlo et al., 1979; Trout and Levetin 2001). Almaguer et al., (2013) have reported  
 994 that in [a](#) tropical region, relative humidity has greater influence than temperature on the airborne  
 995 spore counts and may be a pre-requisite for release of spores (Hollins et al., 2004). Thus, the  
 996 combination of persistent threshold relative humidity (~60 – 95% as reported by Ho et al., 2005)  
 997 and rainfall can cause the increase in the spore concentration and the excessive and persistent  
 998 rain, however, tends to wash the spore out of the atmosphere further reducing their concentration  
 999 levels (Burge 1986; Horner et al., 1992; Troutt and Levetin, 2001). Based on these arguments  
 1000 combined with observed meteorological conditions we expect that the bioaerosols reported here  
 1001 from Munnar mainly consisted of Basidiospores during the SW monsoon season as also evident  
 1002 from SEM images (discussed above). This is consistent with results reported by Valsan et al.,  
 1003 (2015) where they found the dominant presence of dry air spora (*Cladosporium*) during

1004 relatively dry and warm weather from the same observational site. In general,  $N_F$  and  $N_F/N_T$   
 1005 decreased with increasing wind speed ( $R^2=0.6$  and  $R^2=0.78$ , respectively) indicating that wind  
 1006 speed may be one of the strong factors for observed high  $N_F$  concentrations at this site. As  
 1007 compared to previously reported correlation between  $N_F$  and meteorological parameters  
 1008 (Santarpia et al., 2013), the relations shown for this observational site appeared to be more robust  
 1009 and conclusive. ~~For example since the~~ The variability ~~derived~~ observed in  $N_T$  ( $N_T - N_{T,min}/N_{T,max} -$   
 1010  $N_{T,min}$ ; not shown here) was more consistent and high as compared to variability ~~derived~~ observed  
 1011 in  $N_F$  ( $N_F - N_{F,min}/N_{F,max} - N_{F,min}$ ), which was more episodic and hence one would expect the  
 1012 weak correlation between  $N_T$  and meteorological parameters (Tab. 5).  
 1013 ~~On the other hand several~~ Several studies have reported that in temperate regions, temperature is  
 1014 probably the most important meteorological parameter affecting the spore concentration (Levetin  
 1015 and Horner, 2002; Adhikari et al., 2006) with highest spore concentration during summer season  
 1016 (Emberlin et al., 1995; Hasnain, 1993; Herrero et al., 1996; Hjelmroos, 1993; Li et al., 2011;  
 1017 Schumacher et al., 2013). When the relation between temperature and spore concentration was  
 1018 investigated on ~~averaged~~ the basis of diurnal ~~basis, however~~ average, spore concentration have  
 1019 been observed to decrease with the increasing temperature (Burch and Levetin, 2002; Calderon  
 1020 et al., 1995; Sabariego et al., 2000; Schumacher et al., 2013; Trejo et al., 2013). Consistent with  
 1021 this trend, we have found significant negative correlation between  $N_F$  and temperature ( $R^2=0.65$ )  
 1022 averaged over the entire measurement period at Munnar. The correlation coefficient between  $N_F$   
 1023 and temperature for three distinct focus periods is given in Tab. 5. ~~The correlation coefficient~~  
 1024 ~~between  $N_F/N_T$  and meteorological parameters in general yielded higher  $R^2$  values. Note,~~  
 1025 ~~however, that the interpretation presented here based on the correlation analyses performed~~  
 1026 ~~between  $N_F$  are specific to this locality of sampling and meteorological parameters were~~

1027 ~~intended~~may not ~~to generalize and extrapolate conclusions~~be extrapolated to ~~various represent~~  
 1028 behavior in other ecosystems ~~(including in the~~ Indian region)~~) and different seasons of the year~~  
 1029 ~~(including non monsoon in India) but were~~. These results were, however, presented to ~~take an~~  
 1030 ~~opportunity to~~ formulate preliminary hypothesis about role of meteorological parameters in  
 1031 governing the ~~variabilites~~variability of ~~bioaerosls~~bioaerosols specific to this observational site  
 1032 for the monsoon season ~~only~~.

1033

#### 1034 4 Summary and Conclusions

1035 ~~During these maiden online measurements of biological aerosol particles we operated a~~ UV-  
 1036 APS was continuously operated during the SW monsoon season (~~1~~.June ~~–21.1~~ - August) ~~of 21,~~  
 1037 2014) at ~~a high altitude site of~~ Munnar in the Western Ghats in Southern tropical India. The  
 1038 number and mass size distributions and corresponding concentrations of biological aerosol were  
 1039 quantified for three distinct focus periods namely ~~dusty period, high-bio period, and clean period,~~  
 1040 identified based on the prominent wind direction. ~~We have analyzed the three month time series~~  
 1041 ~~of integrated coarse particle number and mass concentrations, as well as particle number and~~  
 1042 ~~mass size distributions of both, the total and fluorescence biological aerosol particles.~~ Over the  
 1043 course of the entire measurement period the coarse particle number concentration of FBAPs  
 1044 varied in the range of  $0.2 \times 10^{-3} \text{ cm}^{-3}$  to  $0.63 \text{ cm}^{-3}$  with an arithmetic mean value of  $0.02 \text{ cm}^{-3}$   
 1045 ( $\pm 0.02 \text{ cm}^{-3}$ ). This average concentration accounted for 0.04 – 53% (mean value  $2.1\% \pm 4.05\%$ ) of  
 1046 the total coarse particle number concentration. The coarse particle mass concentrations of FBAPs  
 1047 varied in the range of  $0.5 \times 10^{-3} - 4.93 \mu\text{g m}^{-3}$  with an arithmetic mean ( $\pm$ standard deviation)  
 1048 value of  $0.24 (\pm 0.28) \mu\text{g m}^{-3}$ .

Formatted: Space After: 0 pt

Formatted: Justified, Space After: 0 pt

Formatted: Font: Italic

Formatted: Font: Italic

Formatted: Font: Italic

1049 ~~The average FBAP concentration during the entire measurement period was found to be highest~~  
 1050 ~~in June ( $0.03 \text{ cm}^{-3}$ ) and lowest in July ( $0.007 \text{ cm}^{-3}$ ).~~ The FBAP concentrations observed at  
 1051 Munnar during SW monsoon season ~~are~~were within the range but slightly on the lower side of  
 1052 the ~~bioaerosol~~ concentrations reported by previous researchers using various online and offline  
 1053 techniques. ~~Numerous other studies from different part of the world have reported detailed~~  
 1054 ~~description about observed biological aerosol particle number concentrations using offline and~~  
 1055 ~~online techniques from various~~varying environments (Despres et al., 2007; Huffman et al., 2010,  
 1056 2012; Adhikari et al., 2004; Bovallius et al., 1978; Bowers, et al., 2009, 2013; Lee et al., 2010;  
 1057 Matthias-Maser and Jaenicke, 1995; Matthias-Maser et al., 2000; Shaffer and Lighthart, 1997;  
 1058 Tong and Lighthart, 1999; Wang et al., 2007; Li et al., 2011; Hameed et al., 2009; Bauer et al.,  
 1059 2008; Schumacher et al., 2013; Gabey et al., 2010, 2011, 2013; Saari et al., 2015; Toprak and  
 1060 Schnaiter, 2013; Healy et al., 2014). For brevity, here we compare the number concentrations  
 1061 observed at Munnar only with number concentrations from varying environments ~~reported by~~  
 1062 ~~previous researchers~~carried out using online measurements. Huffman et al., (2010) have reported  
 1063 coarse mode average FBAP number concentration from four months of measurement to be  $0.03$   
 1064  $\text{cm}^{-3}$ , which constituted ~4% of total coarse mode particles from a semi-urban site of Mainz in  
 1065 Central Europe. The median FBAP concentration during the wet season of pristine tropical  
 1066 Amazonian rainforest region was found be  $0.07 \text{ cm}^{-3}$ , which constituted ~24% of total coarse  
 1067 mode particle number concentration (Huffman et al., 2012). By analyzing the full one-year  
 1068 observations from Boreal forest in Hyytiala and pine forest in Colorado, Schumacher et al.,  
 1069 (2013) reported highest FBAP concentration in summer of  $0.046 \text{ cm}^{-3}$  (constituting ~13% of total  
 1070 coarse mode particles) and  $0.03 \text{ cm}^{-3}$  (constituting ~8.8% of total coarse mode particles),  
 1071 respectively. Healy et al., (2014) reported the average FBAP concentration of  $\sim 0.01 \text{ cm}^{-3}$

1072 using the UV-APS measurements carried out with in the Killarney national park, Kerry situated  
 1073 in Southwest of Ireland. Gabey et al., (2013) by performing the measurements at a high altitude  
 1074 ~~site~~ in central France reported averaged FBAP concentration of  $0.012 \text{ cm}^{-3}$  and  $0.095 \text{ cm}^{-3}$   
 1075 using two-wavelength (280 nm and 370 nm respectively) single-particle UV-induced  
 1076 fluorescence spectrometer. Gabey et al., (2010) from tropical rainforest in Borneo, Malaysia  
 1077 reported that mean FBAP number fraction in the size range of  $0.8 - 20 \text{ }\mu\text{m}$  was  $\sim 55\%$  and  $\sim 28\%$   
 1078 below and above the forest canopy, respectively. It is important to note, however, that the  
 1079 measurement results compared here were obtained from different instrumentation operating with  
 1080 different wavelength. ~~Nevertheless, the FBAP number concentrations observed under various~~  
 1081 ~~environmental conditions are largely comparable to the FBAP number concentration observed at~~  
 1082 ~~Munnar during SW monsoon season. Note that the relative contribution of FBAP number~~  
 1083 ~~concentration to total coarse mode particles may show a strong spatial variability.~~  
 1084 The average observed  $dN_F/d\log D_a$  exhibited a peak at  $\sim 3 \text{ }\mu\text{m}$ , which was consistent even during  
 1085 distinct focus periods with slight quantitative variation in the FBAP number concentration. Such  
 1086 a consistency in the peak of  $dN_F/d\log D_a$  during entire measurement period ~~is an indication of the~~  
 1087 ~~fact~~ indicates that sources and type of bioaerosols did not exhibit considerable variability and  
 1088 diversity at Munnar during SW monsoon season. The peak observed in  $dN_F/d\log D_a$  in this study  
 1089 is consistent with range of the peaks published by previous researchers. At a semi-urban site in  
 1090 Central Europe the peak in  $dN_F/d\log D_a$  was observed at  $\sim 3 \text{ }\mu\text{m}$  (Huffman et al., 2010). In  
 1091 pristine tropical rainforest region of Amazonia a peak in  $dN_F/d\log D_a$  was found at  $\sim 2.5 \text{ }\mu\text{m}$   
 1092 (Huffman et al., 2012). Whereas the peak in  $dN_F/d\log D_a$  at a boreal forest in Finland exhibited a  
 1093 strong seasonal dependence with different modes at  $\sim 1.5 \text{ }\mu\text{m}$ ,  $\sim 3 \text{ }\mu\text{m}$ , and  $\sim 5 \text{ }\mu\text{m}$  indicating  
 1094 differences in the bioaerosol sources (Schumacher et al., 2013). In the pine forest of Colorado the



1095 distinct peaks were observed at  $\sim 1.5 \mu\text{m}$  and  $\sim 5 \mu\text{m}$  (Schumacher et al., 2013). The mode at  $\sim 3$   
1096  $\mu\text{m}$  [reported for Colorado](#) is likely due to the fungal spore whose release mechanism is strongly  
1097 governed by the combination of relative humidity and temperature (Huffman et al., 2010 and  
1098 references therein).

1099 On the diurnal scale a pronounced diurnal cycle with  $\sim 3 \mu\text{m}$  peak with a maximum concentration  
1100 at  $\sim 06:00 \text{ hr}$  was observed when averaged over entire measurement period. This general pattern  
1101 is consistent with previous studies reporting the early morning peak in FBAP concentration for  
1102 various environmental conditions (Healy et al., 2014; Huffman et al., 2012; Schumacher et al.,  
1103 2013; Toprak and Schnaiter, 2013). The early morning peak, ~~which in the present case appears to~~  
1104 ~~be strongly governed by the diurnal variations in relative humidity, is most likely to be~~ [was](#)  
1105 contributed by Basidiospores as their release in the atmosphere is strongly coupled with relative  
1106 humidity (Adhikari et al., 2006; Burch and Levetin, 2002; Hasnain, 1993; Healy et al., 2014; Ho  
1107 et al., 2005; Huffman et al., 2012). This is also consistent with the SEM images shown and  
1108 discussed above.

1109 The meteorological parameters were observed to correlate significantly with FBAP concentration  
1110 at Munnar. ~~When investigated on a daily averaged basis (24 hr), however, no significant~~  
1111 ~~correlation between  $N_F$  and meteorological parameters except moderate negative correlation with~~  
1112 ~~precipitation was observed. During the entire measurement campaign, except on few occasions~~  
1113 ~~no significant variations in temperature and relative humidity was observed. This in combination~~  
1114 ~~with persistent rainfall resulting in the wash out/wet deposition of biological aerosol particles~~  
1115 ~~might have caused such a weak correlation for a daily averaged (24 hr) analysis. On a diurnal~~  
1116 ~~scale, however, a significant correlation between  $N_F$  and meteorological parameters was~~  
1117 ~~observed.~~ We observed that  $N_F$  followed the similar diurnal trend to that of relative humidity and

1118 was anti-correlated with temperature. As reported by previous studies from selected locations  
 1119 (Huffman et al., 2013; Schumacher et al., 2013; Prenni et al., 2013; Hirst 1953) we did not  
 1120 observe any sharp increase in  $N_F$  concentration immediately after or during rainfall. We  
 1121 hypothesize that the spore built-up and release of certain species can happen only at certain  
 1122 threshold relative humidity (Jones and Harrison, 2004). ~~Under~~Our results indicate that under the  
 1123 dry environmental conditions where relative humidity levels rarely attain such threshold required  
 1124 for fungal spore release can cause the strong built up of fungal spores inside fungal bodies.  
 1125 Under these conditions precipitation can cause the relative humidity levels to increase up to  
 1126 threshold required for fungal spore release in combination with mechanical splashing due to  
 1127 raindrops, and can cause the sudden and sharp increase in spore concentrations. On the contrary,  
 1128 like in present case, the ~~incessant persistence of~~persistent high humidity conditions can cause the  
 1129 continuous release of the spore without an opportunity for built-up of fungal spores in fungal  
 1130 body to be released during rainfall. It is also reported that persistent high levels of relative  
 1131 humidity can inhibit the sporulation (Schumacher et al., 2013) further considerably reducing the  
 1132 spore release. More detailed measurements are required from the regions where relative humidity  
 1133 persistently remains low (<60%) for extended amount of time and experiences sudden rainfall.  
 1134 The correlation between  $N_F$  and wind speed was found to be strongly negative. Since majority of  
 1135 the spore release was dominated by the local sources, the ~~stong~~strong winds coming over from  
 1136 West/Southwest direction, which were relatively clean, might have caused the dilution of air  
 1137 mass thus reducing the spore concentration.  
 1138 Overall, the long-term measurements reported in this manuscript showed the quantitative and  
 1139 qualitative agreement with previously reported studies. The emissions and abundance of  
 1140 biological aerosol particles in Western Ghats air during monsoon season appeared to be closely

Formatted: Justified

1141 linked to the ~~variabilties~~variability in the meteorological parameters. ~~As reported by Huffman et~~  
 1142 ~~al., (2012) and corroborated by the observations reported in this study, UV-APS is successfully~~  
 1143 ~~able to detect the aerosol particles of biological origin, however, may pose certain limitations in~~  
 1144 ~~scientific interpretation from the obtained data.~~ The scatter plot analysis carried out between  $N_F$   
 1145 and  $N_T$  for submicron and ~~supermicron~~super-micron particles indicated that submicron particles  
 1146 at this observational site were also dominated by aerosol particles of biological origin, thus  
 1147 indicating the lowest possible interference from particles of anthropogenic origin known to  
 1148 exhibit the fluorescence at the prescribed wavelength used in UV-APS. Hence, given  
 1149 observational site can be termed as relatively pristine while under the influence of SW monsoon  
 1150 season. This emphasizes the need to perform similar measurements under different land-use type  
 1151 during same season over Indian region. The contrasting characteristics of this observational site  
 1152 associated with pollution and interference of non-biological aerosol particles in fluorescence will  
 1153 be discussed in follow up studies. We propose ~~and intend to take forward these~~more studies by  
 1154 means of performing simultaneous online measurements of biological aerosol particle ~~number~~  
 1155 ~~concentrations in high time and size resolution~~ under contrasting environments during distinct  
 1156 meteorological seasons over Indian region. ~~This future work~~These measurements could be  
 1157 supplemented with advanced offline measurement techniques including SEM analysis, DNA  
 1158 analysis, and fluorescence microscopy of the samples collected in parallel with the  
 1159 measurements. We believe that such a comprehensive approach over Indian region would be  
 1160 helpful in understanding the possible tight coupling between aerosol and hydrological cycle  
 1161 especially during monsoon. This could also help to better understand the implication of  
 1162 biological aerosols on crops and human health where agricultural industry has the major share in  
 1163 GDP to cater the need of 18% of the world's total population.

1164 **Acknowledgement:**

1165 | SSG acknowledge the combined financial support from Max Planck Society and Department of Science and  
1166 Technology, Government of India under the Max Planck Partner Group Program. Authors are thankful to Akila M,  
1167 Hema P, Shika S, ~~Aleena~~[Aliena](#), Hasitha, Reshma, Sanu, and Tabish U. Ansari for their support in planning,  
1168 execution, and completion of the measurement campaign. Authors thankfully acknowledge the support from  
1169 Gerhard Lammel, Multiphase Chemistry Department, Max Planck Institute for Chemistry for his support during  
1170 campaign and providing the meteorological data for comparison. Authors are grateful to the Sophisticated Analytical  
1171 Instrument Facility (SAIF), IIT Madras for making SEM available for morphological analysis. Authors gratefully  
1172 acknowledge US Geological Survey for the topography data in DEM format and NOAA ARL for providing  
1173 HYSPLIT air mass back trajectory calculations.

1174 **References:**

- 1175 Adhikari, A., Sen, M. M., Gupta-Bhattacharya, S., and Chanda, S.: Air-borne viable, non-viable,  
1176 and allergenic fungi in a rural agricultural area of India: a 2-year study at five outdoor sampling  
1177 stations, *Science of the Total Environment*, 326, 123-141, 10.1016/j.scitotenv.2003.12.007,  
1178 2004.
- 1179 Adhikari, A., Reponen, T., Grinshpun, S. A., Martuzevicius, D., and LeMasters, G.: Correlation  
1180 of ambient inhalable bioaerosols with particulate matter and ozone: A two-year study,  
1181 *Environmental Pollution*, 140, 16-28, 10.1016/j.envpol.2005.07.004, 2006.
- 1182 Agranovski, V., Ristovski, Z., Hargreaves, M., Blackall, P. J., and Morawska, L.: Performance  
1183 evaluation of the UVAPS: influence of physiological age of airborne bacteria and bacterial  
1184 stress, *Journal of Aerosol Science*, 34, 1711-1727, 10.1016/s0021-8502(03)00191-5, 2003.
- 1185 Agranovski, V., Ristovski, Z. D., Ayoko, G. A., and Morawska, L.: Performance evaluation of  
1186 the UVAPS in measuring biological aerosols: Fluorescence spectra from NAD(P)H coenzymes  
1187 and riboflavin, *Aerosol Sci. Technol.*, 38, 354-364, 10.1080/02786820490437505, 2004.
- 1188 Agranovski, V., and Ristovski, Z. D.: Real-time monitoring of viable bioaerosols: capability of  
1189 the UVAPS to predict the amount of individual microorganisms in aerosol particles, *Journal of*  
1190 *Aerosol Science*, 36, 665-676, 10.1016/j.jaerosci.2004.12.005, 2005.
- 1191 Almaguer, M., Aira, M.-J., Rodríguez-Rajo, F. J., and Rojas, T. I.: Temporal dynamics of  
1192 airborne fungi in Havana (Cuba) during dry and rainy seasons: influence of meteorological  
1193 parameters, *International Journal of Biometeorology*, 58, 1459-1470, 10.1007/s00484-013-0748-  
1194 6, 2013.
- 1195 Andreae, M. O., and Rosenfeld, D.: Aerosol-cloud-precipitation interactions. Part I. The nature  
1196 and sources of cloud-active aerosols, *Earth Science Reviews*, 89, 13-41, 2008.
- 1197 Ansari, T. U., Valsan, A. E., Ojha, N., Ravikrishna, R., Narasimhan, B., and Gunthe, S. S.:  
1198 Model simulations of fungal spore distribution over the Indian region, *Atmospheric*  
1199 *Environment*, 122, 552-560, <http://dx.doi.org/10.1016/j.atmosenv.2015.10.020>, 2015.

Formatted: Justified

1200 Artaxo, P., and Hansson, H. C.: Size distribution of biogenic aerosol-particles from the Amazon  
1201 basin, *Atmospheric Environment*, 29, 393-402, 10.1016/1352-2310(94)00178-n, 1995.

1202 [Baron, P. A., and Willeke, K.: Aerosol Measurement – Principles, Techniques and Applications,  
1203 Second edition, John Wiley & Sons. 2005.](#)

1204 Bauer, H., Schueller, E., Weinke, G., Berger, A., Hitzenberger, R., Marr, I. L., and Puxbaum, H.:  
1205 Significant contributions of fungal spores to the organic carbon and to the aerosol mass balance  
1206 of the urban atmospheric aerosol, *Atmospheric Environment*, 42, 5542-5549,  
1207 10.1016/j.atmosenv.2008.03.019, 2008.

1208 Bhati, H. S., and Gaur, R. D.: Studies on Aerobiology - Atmospheric fungal spores, *New  
1209 Phytologist*, 82, 519-527, 10.1111/j.1469-8137.1979.tb02678.x, 1979.

1210 Bovallius, A., Bucht, B., Roffey, R., and Anas, P.: 3-Year investigation of natural airborne  
1211 bacterial-flora at 4 localities in Sweden, *Applied and Environmental Microbiology*, 35, 847-852,  
1212 1978.

1213 Bowers, R. M., Lauber, C. L., Wiedinmyer, C., Hamady, M., Hallar, A. G., Fall, R., Knight, R.,  
1214 and Fierer, N.: Characterization of Airborne Microbial Communities at a High-Elevation Site  
1215 and Their Potential To Act as Atmospheric Ice Nuclei, *Applied and Environmental  
1216 Microbiology*, 75, 5121-5130, 10.1128/aem.00447-09, 2009.

1217 Bowers, R. M., Clements, N., Emerson, J. B., Wiedinmyer, C., Hannigan, M. P., and Fierer, N.:  
1218 Seasonal Variability in Bacterial and Fungal Diversity of the Near-Surface Atmosphere,  
1219 *Environmental Science & Technology*, 47, 12097-12106, 10.1021/es402970s, 2013.

1220 Brosseau, L. M., Vesley, D., Rice, N., Goodell, K., Nellis, M., and Hairston, P.: Differences in  
1221 detected fluorescence among several bacterial species measured with a direct-reading particle  
1222 sizer and fluorescence detector, *Aerosol Sci. Technol.*, 32, 545-558, 10.1080/027868200303461,  
1223 2000.

1224 Burch, M., and Levetin, E.: Effects of meteorological conditions on spore plumes, *International  
1225 Journal of Biometeorology*, 46, 107-117, 10.1007/s00484-002-0127-1, 2002.

1226 Burge, H. A.: Some comments on the aerobiology of fungus spores, *Grana*, 25, 143-146, 1986.

1227 Burge, H. A., and Rogers, C. A.: Outdoor allergens, *Environmental Health Perspectives*, 108,  
1228 653-659, 10.2307/3454401, 2000.

1229 Burrows, S. M., Butler, T., Jöckel, P., Tost, H., Kerkweg, A., Pöschl, U., and Lawrence, M. G.:  
1230 Bacteria in the global atmosphere - Part 2: Modeling of emissions and transport between  
1231 different ecosystems, *Atmos. Chem. Phys.*, 9, 9281-9297, 2009.

1232 Calderon, C., Lacey, J., McCartney, H. A., and Rosas, I.: Seasonal and diurnal-variation of  
1233 airborne basidiomycete spore concentrations in Mexico-city, *Grana*, 34, 260-268, 1995.

1234 Chakraborty, P., Gupta-Bhattacharya, S., Chakraborty, C., Lacey, J., and Chanda, S.: Airborne  
1235 allergenic pollen grains on a farm in West Bengal, India, *Grana*, 37, 53-57, 1998.

1236 Coz, E., Artinano, B., Clark, L. M., Hernandez, M., Robinson, A. L., Casuccio, G. S., Lersch, T.  
1237 L., and Pandis, S. N.: Characterization of fine primary biogenic organic aerosol in an urban area  
1238 in the northeastern United States, *Atmospheric Environment*, 44, 3952-3962,  
1239 10.1016/j.atmosenv.2010.07.007, 2010.

1240 Creamean, J. M., Suski, K. J., Rosenfeld, D., Cazorla, A., DeMott, P. J., Sullivan, R. C., White,  
1241 A. B., Ralph, F. M., Minnis, P., Comstock, J. M., Tomlinson, J. M., and Prather, K. A.: Dust and  
1242 Biological Aerosols from the Sahara and Asia Influence Precipitation in the Western U.S.,  
1243 *Science*, 339, 1572-1578, 10.1126/science.1227279, 2013.

1244 DeCarlo, P. F., Slowik, J. G., Worsnop, D. R., Davidovits, P., and Jimenez, J. L.: Particle  
1245 morphology and density characterization by combined mobility and aerodynamic diameter  
1246 measurements. Part 1: Theory, *Aerosol Sci. Technol.*, 38, 1185-1205, 2004.

1247 DeLeon-Rodriguez, N., Lathem, T. L., Rodriguez-R, L. M., Barazesh, J. M., Anderson, B. E.,  
1248 Beyersdorf, A. J., Ziemba, L. D., Bergin, M., Nenes, A., and Konstantinidis, K. T.: Microbiome  
1249 of the upper troposphere: Species composition and prevalence, effects of tropical storms, and  
1250 atmospheric implications, *Proceedings of the National Academy of Sciences of the United States*  
1251 *of America*, 110, 2575-2580, 10.1073/pnas.1212089110, 2013.

1252 Despres, V. R., Nowoisky, J. F., Klose, M., Conrad, R., Andreae, M. O., and Pöschl, U.:  
1253 Characterization of primary biogenic aerosol particles in urban, rural, and high-alpine air by  
1254 DNA sequence and restriction fragment analysis of ribosomal RNA genes, *Biogeosciences*, 4,  
1255 1127-1141, 2007.

1256 Despres, V. R., Huffman, J. A., Burrows, S. M., Hoose, C., Safatov, A. S., Buryak, G., Frohlich-  
1257 Nowoisky, J., Elbert, W., Andreae, M. O., Pöschl, U., and Jaenicke, R.: Primary biological  
1258 aerosol particles in the atmosphere: a review, *Tellus Series B-Chemical and Physical*  
1259 *Meteorology*, 64, 10.3402/tellusb.v64i0.15598, 2012.

1260 Du, C., Liu, S., Yu, X., Li, X., Chen, C., Peng, Y., Dong, Y., Dong, Z., and Wang, F.: Urban  
1261 Boundary Layer Height Characteristics and Relationship with Particulate Matter Mass  
1262 Concentrations in Xi'an, Central China, *Aerosol and Air Quality Research*, 13, 1598-1607,  
1263 10.4209/aaqr.2012.10.0274, 2013.

1264 Elbert, W., Taylor, P. E., Andreae, M. O., and Pöschl, U.: Contribution of fungi to primary  
1265 biogenic aerosols in the atmosphere: wet and dry discharged spores, carbohydrates, and  
1266 inorganic ions, *Atmospheric Chemistry and Physics*, 7, 4569-4588, 2007.

1267 Emberlin, J., Newman, T., and Bryant, R.: The incidence of fungal spores in the ambient air and  
1268 inside homes: Evidence from London, *Aerobiologia*, 11, 253-258, 10.1007/bf02447205, 1995

1269 Fisher, M. C., Henk, D. A., Briggs, C. J., Brownstein, J. S., Madoff, L. C., McCraw, S. L., and  
1270 Gurr, S. J.: Emerging fungal threats to animal, plant and ecosystem health, *Nature*, 484, 186-194,  
1271 10.1038/nature10947, 2012.

1272 Fröhlich-Nowoisky, J., Pickersgill, D. A., Després, V. R., and Pöschl, U.: High diversity of fungi  
1273 in air particulate matter, *Proceedings of the National Academy of Sciences*, 106, 12814-12819,  
1274 10.1073/pnas.0811003106, 2009.

1275 Froehlich-Nowoisky, J., Burrows, S. M., Xie, Z., Engling, G., Solomon, P. A., Fraser, M. P.,  
1276 Mayol-Bracero, O. L., Artaxo, P., Begerow, D., Conrad, R., Andreae, M. O., Despres, V. R., and  
1277 Poeschl, U.: Biogeography in the air: fungal diversity over land and oceans, *Biogeosciences*, 9,  
1278 1125-1136, 10.5194/bg-9-1125-2012, 2012.

1279 Fuzzi, S., Mandrioli, P., and Peretto, A.: Fog droplets - An atmospheric source of secondary  
1280 biological aerosol particles, *Atmospheric Environment*, 31, 287-290, 10.1016/1352-  
1281 2310(96)00160-4, 1997.

1282 Gabey, A. M., Gallagher, M. W., Whitehead, J., Dorsey, J. R., Kaye, P. H., and Stanley, W. R.:  
1283 Measurements and comparison of primary biological aerosol above and below a tropical forest  
1284 canopy using a dual channel fluorescence spectrometer, *Atmospheric Chemistry and Physics*, 10,  
1285 4453-4466, 10.5194/acp-10-4453-2010, 2010.

1286 Gabey, A. M., Stanley, W. R., Gallagher, M. W., and Kaye, P. H.: The fluorescence properties of  
1287 aerosol larger than 0.8  $\mu\text{m}$  in urban and tropical rainforest locations, *Atmospheric Chemistry*  
1288 *and Physics*, 11, 5491-5504, 10.5194/acp-11-5491-2011, 2011.

1289 Gabey, A. M., Vaitilingom, M., Freney, E., Boulon, J., Sellegri, K., Gallagher, M. W., Crawford,  
1290 I. P., Robinson, N. H., Stanley, W. R., and Kaye, P. H.: Observations of fluorescent and  
1291 biological aerosol at a high-altitude site in central France, *Atmospheric Chemistry and Physics*,  
1292 13, 7415-7428, 10.5194/acp-13-7415-2013, 2013.

1293 Gangamma, S.: Characteristics of airborne bacteria in Mumbai urban environment, *Science of*  
1294 *the Total Environment*, 488, 70-74, 10.1016/j.scitotenv.2014.04.065, 2014.

1295 Garland, R. M., Schmid, O., Nowak, A., Achtert, P., Wiedensohler, A., Gunthe, S. S., Takegawa,  
1296 N., Kita, K., Kondo, Y., Hu, M., Shao, M., Zeng, L. M., Zhu, T., Andreae, M. O., and Pöschl, U.:  
1297 Aerosol optical properties observed during Campaign of Air Quality Research in Beijing 2006  
1298 (CAREBeijing-2006): Characteristic differences between the inflow and outflow of Beijing city  
1299 air, *Journal of Geophysical Research-Atmospheres*, 114, 2009.

1300 Grand, L. F., and Vandyke, C. G.: Scanning electron microscopy of basidiospores of species of  
1301 *hydnum*, *hydnum*, *phellodon*, and *bankera* (*hydnum*), *Journal of the Elisha Mitchell*  
1302 *Scientific Society*, 92, 114-123, 1976.

1303 Hairston, P. P., Ho, J., and Quant, F. R.: Design of an instrument for real-time detection of  
1304 bioaerosols using simultaneous measurement of particle aerodynamic size and intrinsic  
1305 fluorescence, *Journal of Aerosol Science*, 28, 471-482, 10.1016/s0021-8502(96)00448-x, 1997.

1306 Hallar, A. G., Chirokova, G., McCubbin, I., Painter, T. H., Wiedinmyer, C., and Dodson, C.:  
1307 Atmospheric bioaerosols transported via dust storms in the western United States, *Geophysical*  
1308 *Research Letters*, 38, 10.1029/2011gl048166, 2011.

1309 Hameed, A. A. A., Khoder, M. I., Ibrahim, Y. H., Saeed, Y., Osman, M. E., and Ghanem, S.:  
 1310 Study on some factors affecting survivability of airborne fungi, *Science of the Total*  
 1311 *Environment*, 414, 696-700, 10.1016/j.scitotenv.2011.10.042, 2012.

1312 Hameed, A. A. A., Khoder, M. I., Yuosra, S., Osman, A. M., and Ghanem, S.: Diurnal  
 1313 distribution of airborne bacteria and fungi in the atmosphere of Helwan area, Egypt, *Science of*  
 1314 *the Total Environment*, 407, 6217-6222, 10.1016/j.scitotenv.2009.08.028, 2009.

1315 Hara, K., and Zhang, D.: Bacterial abundance and viability in long-range transported dust,  
 1316 *Atmospheric Environment*, 47, 20-25, 10.1016/j.atmosenv.2011.11.050, 2012.

1317 Hasnain, S. M.: Influence of meteorological factors on the air spora, *Grana*, 32, 184-188, 1993.

1318 Healy, D. A., Huffman, J. A., O'Connor, D. J., Poehlker, C., Poeschl, U., and Sodeau, J. R.:  
 1319 Ambient measurements of biological aerosol particles near Killarney, Ireland: a comparison  
 1320 between real-time fluorescence and microscopy techniques, *Atmospheric Chemistry and Physics*,  
 1321 14, 8055-8069, 10.5194/acp-14-8055-2014, 2014.

1322 Herrero, B., FombellaBlanco, M. A., FernandezGonzalez, D., and ValenciaBarrera, R. M.: The  
 1323 role of meteorological factors in determining the annual variation of *Alternaria* and  
 1324 *Cladosporium* spores in the atmosphere of Palencia, 1990-1992, *International Journal of*  
 1325 *Biometeorology*, 39, 139-142, 10.1007/bf01211226, 1996.

1326 Hirst, J. M.: Changes in atmospheric spore content: Diurnal periodicity and the effects of  
 1327 weather, *Transactions of the British Mycological Society*, 36, 375-IN378,  
 1328 [http://dx.doi.org/10.1016/S0007-1536\(53\)80034-3](http://dx.doi.org/10.1016/S0007-1536(53)80034-3), 1953.

1329 Hjelmroos, M.: Relationship between airborne fungal spore presence and weather variables -  
 1330 *cladosporium and alternaria*, *Grana*, 32, 40-47, 1993.

1331 Ho, H. M., Rao, C. Y., Hsu, H. H., Chiu, Y. H., Liu, C. M., and Chao, H. J.: Characteristics and  
 1332 determinants of ambient fungal spores in Hualien, Taiwan, *Atmospheric Environment*, 39, 5839-  
 1333 5850, 10.1016/j.atmosenv.2005.06.034, 2005.

1334 Hollins, P. D., Kettlewell, P. S., Atkinson, M. D., Stephenson, D. B., Corden, J. M., Millington,  
 1335 W. M., and Mullins, J.: Relationships between airborne fungal spore concentration of  
 1336 *Cladosporium* and the summer climate at two sites in Britain, *International Journal of*  
 1337 *Biometeorology*, 48, 137-141, 10.1007/s00484-003-0188-9, 2004.

1338 Horner, W. E., Oneil, C. E., and Lehrer, S. B.: Basidiospore aeroallergens, *Clinical Reviews in*  
 1339 *Allergy*, 10, 191-211, 1992.

1340 Huffman, J. A., Treutlein, B., and Pöschl, U.: Fluorescent biological aerosol particle  
 1341 concentrations and size distributions measured with an Ultraviolet Aerodynamic Particle Sizer  
 1342 (UV-APS) in Central Europe, *Atmos. Chem. Phys.*, 10, 3215-3233, 2010.

1343 Huffman, J. A., Sinha, B., Garland, R. M., Snee-Pollmann, A., Gunthe, S. S., Artaxo, P., Martin,  
 1344 S. T., Andreae, M. O., and Pöschl, U.: Size distributions and temporal variations of biological



1345 aerosol particles in the Amazon rainforest characterized by microscopy and real-time UV-APS  
1346 fluorescence techniques during AMAZE-08, *Atmospheric Chemistry and Physics*, 12, 11997-  
1347 12019, 10.5194/acp-12-11997-2012, 2012.

1348 Huffman, J. A., Prenni, A. J., DeMott, P. J., Poehlker, C., Mason, R. H., Robinson, N. H.,  
1349 Froehlich-Nowoisky, J., Tobo, Y., Despres, V. R., Garcia, E., Gochis, D. J., Harris, E., Mueller-  
1350 Germann, I., Ruzene, C., Schmer, B., Sinha, B., Day, D. A., Andreae, M. O., Jimenez, J. L.,  
1351 Gallagher, M., Kreidenweis, S. M., Bertram, A. K., and Poeschl, U.: High concentrations of  
1352 biological aerosol particles and ice nuclei during and after rain, *Atmospheric Chemistry and*  
1353 *Physics*, 13, 6151-6164, 10.5194/acp-13-6151-2013, 2013.

1354 Jones, A. M., and Harrison, R. M.: The effects of meteorological factors on atmospheric  
1355 bioaerosol concentrations - a review, *Science of the Total Environment*, 326, 151-180,  
1356 10.1016/j.scitotenv.2003.11.021, 2004.

1357 Kanaani, H., Hargreaves, M., Ristovski, Z., and Morawska, L.: Performance assessment of  
1358 UVAPS: Influence of fungal spore age and air exposure, *Journal of Aerosol Science*, 38, 83-96,  
1359 10.1016/j.jaerosci.2006.10.003, 2007.

1360 Kanaani, H., Hargreaves, M., Smith, J., Ristovski, Z., Agranovski, V., and Morawska, L.:  
1361 Performance of UVAPS with respect to detection of airborne fungi, *Journal of Aerosol Science*,  
1362 39, 175-189, 10.1016/j.jaerosci.2007.10.007, 2008.

1363 Kanawade, V. P., Shika, S., Poehlker, C., Rose, D., Suman, M. N. S., Gadhavi, H., Kumar, A.,  
1364 Nagendra, S. M. S., Ravikrishna, R., Yu, H., Sahu, L. K., Jayaraman, A., Andreae, M. O.,  
1365 Poeschl, U., and Gunthe, S. S.: Infrequent occurrence of new particle formation at a semi-rural  
1366 location, Gadanki, in tropical Southern India, *Atmospheric Environment*, 94, 264-273,  
1367 10.1016/j.atmosenv.2014.05.046, 2014.

1368 Kurkela, T.: The number of *Cladosporium* conidia in the air in different weather conditions,  
1369 *Grana*, 36, 54-61, 1997.

1370 Lee, S.-H., Lee, H.-J., Kim, S.-J., Lee, H. M., Kang, H., and Kim, Y. P.: Identification of  
1371 airborne bacterial and fungal community structures in an urban area by T-RFLP analysis and  
1372 quantitative real-time PCR, *Science of the Total Environment*, 408, 1349-1357,  
1373 10.1016/j.scitotenv.2009.10.061, 2010.

1374 Levetin, E., and Horner, W. E.: Fungal aerobiology: Exposure and measurement, *Fungal Allergy*  
1375 *and Pathogenicity*, 81, 10-27, 2002.

1376 Li, D. W., and Kendrick, B.: Functional-relationships between airborne fungal spores and  
1377 environmental-factors in Kitchener-Waterloo, Ontario, as detected by canonical correspondence-  
1378 analysis, *Grana*, 33, 166-176, 1994.

1379 Li, F., and Ramanathan, V.: Winter to summer monsoon variation of aerosol optical depth over  
1380 the tropical Indian Ocean, *Journal of Geophysical Research-Atmospheres*, 107,  
1381 10.1029/2001jd000949, 2002.

1382 Li, M., Qi, J., Zhang, H., Huang, S., Li, L., and Gao, D.: Concentration and size distribution of  
1383 bioaerosols in an outdoor environment in the Qingdao coastal region, *Science of the Total*  
1384 *Environment*, 409, 3812-3819, 10.1016/j.scitotenv.2011.06.001, 2011.

1385 Lyon, F. L., Kramer, C. L., and Eversmeyer, M. G.: Variation of airspora in the atmosphere due  
1386 to weather conditions, *Grana*, 23, 177-181, 1984.

1387 Madden, L. V.: Effects of rain on splash dispersal of fungal pathogens, *Canadian Journal of Plant*  
1388 *Pathology*, 19, 225-230, 1997.

1389 Maki, T., Kakikawa, M., Kobayashi, F., Yamada, M., Matsuki, A., Hasegawa, H., and Iwasaka,  
1390 Y.: Assessment of composition and origin of airborne bacteria in the free troposphere over Japan,  
1391 *Atmospheric Environment*, 74, 73-82, 10.1016/j.atmosenv.2013.03.029, 2013.

1392 Matthias-Maser, S., Obolkin, V., Khodzer, T., and Jaenicke, R.: Seasonal variation of primary  
1393 biological aerosol particles in the remote continental region of Lake Baikal/Siberia, *Atmospheric*  
1394 *Environment*, 34, 3805-3811, 10.1016/s1352-2310(00)00139-4, 2000.

1395 Matthiasmaser, S., and Jaenicke, R.: A method to identify biological aerosol-particles with radius  
1396 greater-than 0.3  $\mu\text{m}$  for the determination of their size distribution, *Journal of Aerosol Science*,  
1397 22, S849-S852, 10.1016/s0021-8502(05)80232-0, 1991.

1398 Matthiasmaser, S., and Jaenicke, R.: Examination of atmospheric bioaerosol particles with radii  
1399 greater-than-0.2  $\mu\text{m}$ , *Journal of Aerosol Science*, 25, 1605-1613, 10.1016/0021-8502(94)90228-  
1400 3, 1994.

1401 MatthiasMaser, S., and Jaenicke, R.: The size distribution of primary biological aerosol particles  
1402 with radii  $>0.2 \mu\text{m}$  in an urban rural influenced region, *Atmospheric Research*, 39, 279-286,  
1403 10.1016/0169-8095(95)00017-8, 1995.

1404 Moehler, O., DeMott, P. J., Vali, G., and Levin, Z.: Microbiology and atmospheric processes: the  
1405 role of biological particles in cloud physics, *Biogeosciences*, 4, 1059-1071, 2007.

1406 Moorthy, K. K., Nair, P. R., and Murthy, B. V. K.: Size distribution of coastal aerosols - effects  
1407 of local-sources and sinks, *Journal of Applied Meteorology*, 30, 844-852, 10.1175/1520-  
1408 0450(1991)030<0844:sdocae>2.0.co;2, 1991.

1409 Morris, C. E., Georgakopoulos, D. G., and Sands, D. C.: Ice nucleation active bacteria and their  
1410 potential role in precipitation, *Journal De Physique Iv*, 121, 87-103, 10.1051/jp4:2004121004,  
1411 2004.

1412 Morris, C. E., Conen, F., Huffman, J. A., Phillips, V., Poeschl, U., and Sands, D. C.:  
1413 Bioprecipitation: a feedback cycle linking Earth history, ecosystem dynamics and land use  
1414 through biological ice nucleators in the atmosphere, *Global Change Biology*, 20, 341-351,  
1415 10.1111/gcb.12447, 2014.

1416 Myers, N., Mittermeier, R. A., Mittermeier, C. G., da Fonseca, G. A. B., and Kent, J.:  
1417 Biodiversity hotspots for conservation priorities, *Nature*, 403, 853-858, 10.1038/35002501, 2000.

1418 Naja, M., and Lal, S.: Surface ozone and precursor gases at Gadanki (13.5 degrees N, 79.2  
1419 degrees E), a tropical rural site in India, *Journal of Geophysical Research-Atmospheres*, 107,  
1420 10.1029/2001jd000357, 2002.

1421 Oh, J.-W., Lee, H.-B., Lee, H.-R., Pyun, B.-Y., Ahn, Y.-M., Kim, K.-E., Lee, S.-Y., and Lee, S.-  
1422 I.: Aerobiological study of pollen and mold in Seoul, Korea, *Allergology International*, 47, 263-  
1423 270, <http://dx.doi.org/10.2332/allergolint.47.263>, 1998.

1424 Oliveira, M., Amorim, M. I., Ferreira, E., Delgado, L., and Abreu, I.: Main airborne Ascomycota  
1425 spores: characterization by culture, spore morphology, ribosomal DNA sequences and enzymatic  
1426 analysis, *Applied Microbiology and Biotechnology*, 86, 1171-1181, 10.1007/s00253-010-2448-z,  
1427 2010.

1428 Pachauri, T., Singla, V., Satsangi, A., Lakhani, A., and Kumari, K. M.: Characterization of major  
1429 pollution events (dust, haze, and two festival events) at Agra, India, *Environmental Science and  
1430 Pollution Research*, 20, 5737-5752, 10.1007/s11356-013-1584-2, 2013.

1431 Pan, Y. L., Holler, S., Chang, R. K., Hill, S. C., Pinnick, R. G., Niles, S., and Bottiger, J. R.:  
1432 Single-shot fluorescence spectra of individual micrometer-sized bioaerosols illuminated by a  
1433 351- or a 266-nm ultraviolet laser, *Optics Letters*, 24, 116-118, 10.1364/ol.24.000116, 1999a.

1434 Pan, Y. L., Holler, S., Chang, R. K., Hill, S. C., Pinnick, R. G., Niles, S., Bottiger, J. R., and  
1435 Bronk, B. V.: Real-time detection and characterization of individual flowing airborne biological  
1436 particles: fluorescence spectra and elastic scattering measurements, in: *Air Monitoring and  
1437 Detection of Chemical and Biological Agents II*, edited by: Leonelli, J., and Althouse, M. L.,  
1438 *Proceedings of the Society of Photo-Optical Instrumentation Engineers (Spie)*, 117-125, 1999b.

1439 | Poehlker, C., Huffman, J. A., and Poeschl, U.: ~~Auto~~fluorescenceAuto fluorescence of  
1440 atmospheric bioaerosols - fluorescent biomolecules and potential interferences, *Atmospheric  
1441 Measurement Techniques*, 5, 37-71, 10.5194/amt-5-37-2012, 2012.

1442 | Poehlker, C., Huffman, J. A., Foerster, J. D., and Poeschl, U.: ~~Auto~~fluorescenceAuto  
1443 fluorescence of atmospheric bioaerosols: spectral fingerprints and taxonomic trends of pollen,  
1444 *Atmospheric Measurement Techniques*, 6, 3369-3392, 10.5194/amt-6-3369-2013, 2013.

1445 Pöschl, U.: Atmospheric aerosols: Composition, transformation, climate and health effects,  
1446 *Angewandte Chemie-International Edition*, 44, 7520-7540, 10.1002/anie.200501122, 2005.

1447 Pöschl, U., Martin, S. T., Sinha, B., Chen, Q., Gunthe, S. S., Huffman, J. A., Borrmann, S.,  
1448 Farmer, D. K., Garland, R. M., Helas, G., Jimenez, J. L., King, S. M., Manzi, A., Mikhailov, E.,  
1449 Pauliquevis, T., Petters, M. D., Prenni, A. J., Roldin, P., Rose, D., Schneider, J., Su, H., Zorn, S.  
1450 R., Artaxo, P., and Andreae, M. O.: Rainforest Aerosols as Biogenic Nuclei of Clouds and  
1451 Precipitation in the Amazon, *Science*, 329, 1513-1516, 10.1126/science.1191056, 2010.

1452 Pranisha, T. S., and Kamra, A. K.: Scavenging of aerosol particles by large water drops .2. The  
1453 effect of electrical forces, *Journal of Geophysical Research-Atmospheres*, 102, 23937-23946,  
1454 10.1029/97jd01834, 1997a.

1455 Pranesha, T. S., and Kamra, A. K.: Scavenging of aerosol particles by large water drops .3.  
 1456 Washout coefficients, half-lives, and rainfall depths, *Journal of Geophysical Research-*  
 1457 *Atmospheres*, 102, 23947-23953, 10.1029/97jd01835, 1997b.

1458 Prenni, A. J., Petters, M. D., Kreidenweis, S. M., Heald, C. L., Martin, S. T., Artaxo, P., Garland,  
 1459 R. M., Wollny, A. G., and Poeschl, U.: Relative roles of biogenic emissions and Saharan dust as  
 1460 ice nuclei in the Amazon basin, *Nature Geoscience*, 2, 401-404, 2009.

1461 Prenni, A. J., Tobo, Y., Garcia, E., DeMott, P. J., Huffman, J. A., McCluskey, C. S.,  
 1462 Kreidenweis, S. M., Prenni, J. E., Poehlker, C., and Poeschl, U.: The impact of rain on ice nuclei  
 1463 populations at a forested site in Colorado, *Geophysical Research Letters*, 40, 227-231,  
 1464 10.1029/2012gl053953, 2013.

1465 Prospero, J. M.: Mineral and sea salt aerosol concentrations in various ocean regions, *Journal of*  
 1466 *Geophysical Research-Oceans and Atmospheres*, 84, 725-731, 10.1029/JC084iC02p00725,  
 1467 1979.

1468 Prospero, J. M., Blades, E., Mathison, G., and Naidu, R.: ~~Interhemispheric~~[Inter-hemispheric](#)  
 1469 transport of viable fungi and bacteria from Africa to the Caribbean with soil dust, *Aerobiologia*,  
 1470 21, 1-19, 10.1007/s10453-004-5872-7, 2005.

1471 Quintero, E., Rivera-Mariani, F., and Bolanos-Rosero, B.: Analysis of environmental factors and  
 1472 their effects on fungal spores in the atmosphere of a tropical urban area (San Juan, Puerto Rico),  
 1473 *Aerobiologia*, 26, 113-124, 10.1007/s10453-009-9148-0, 2010.

1474 Raatikainen, T., Hyvarinen, A. P., Hatakka, J., Panwar, T. S., Hooda, R. K., Sharma, V. P., and  
 1475 Lihavainen, H.: The effect of boundary layer dynamics on aerosol properties at the Indo-  
 1476 Gangetic plains and at the foothills of the Himalayas, *Atmospheric Environment*, 89, 548-555,  
 1477 10.1016/j.atmosenv.2014.02.058, 2014.

1478 Radke, L. F., Hobbs, P. V., and Eltgroth, M. W.: Scavenging of aerosol-particles by  
 1479 precipitation, *Journal of Applied Meteorology*, 19, 715-722, 10.1175/1520-  
 1480 0450(1980)019<0715:soapbp>2.0.co;2, 1980.

1481 Saari, S., Niemi, J. V., Ronkko, T., Kuuluvainen, H., Jarvinen, A., Pirjola, L., Aurela, M.,  
 1482 Hillamo, R., and Keskinen, J.: Seasonal and Diurnal Variations of Fluorescent Bioaerosol  
 1483 Concentration and Size Distribution in the Urban Environment, *Aerosol and Air Quality*  
 1484 *Research*, 15, 572-581, 10.4209/aaqr.2014.10.0258, 2015.

1485 [Saari, S., Reponen, T., and Keskinen, J.: Performance of Two Fluorescence - Based Real-Time](#)  
 1486 [Bioaerosol Detectors: Bioscout vs. UVAPS, \*Aerosol Sci. Technol\*, 48, 371-378,](#)  
 1487 [10.1080/02786826.2013.877579, 2014.](#)

1488 Sabariego, S., de la Guardia, C. D., and Alba, F.: The effect of meteorological factors on the  
 1489 daily variation of airborne fungal spores in Granada (southern Spain), *International Journal of*  
 1490 *Biometeorology*, 44, 1-5, 10.1007/s004840050131, 2000.

1491 Sadys, M., Skjoth, C. A., and Kennedy, R.: Back-trajectories show export of airborne fungal  
 1492 spores (*Ganoderma* sp.) from forests to agricultural and urban areas in England, *Atmospheric*  
 1493 *Environment*, 84, 88-99, 10.1016/j.atmosenv.2013.11.015, 2014.

1494 Santarpia, J. L., Ratnesar-Shumate, S., Gilberry, J. U., and Quizon, J. J.: Relationship Between  
 1495 Biologically Fluorescent Aerosol and Local Meteorological Conditions, *Aerosol Sci. Technol.*,  
 1496 47, 655-661, 10.1080/02786826.2013.781263, 2013.

1497 Satheesh, S. K., and Srinivasan, J.: Enhanced aerosol loading over Arabian Sea during the pre-  
 1498 monsoon season: Natural or anthropogenic?, *Geophysical Research Letters*, 29,  
 1499 10.1029/2002gl015687, 2002.

1500 Schumacher, C. J., Poehlker, C., Aalto, P., Hiltunen, V., Petaja, T., Kulmala, M., Poeschl, U.,  
 1501 and Huffman, J. A.: Seasonal cycles of fluorescent biological aerosol particles in boreal and  
 1502 semi-arid forests of Finland and Colorado, *Atmospheric Chemistry and Physics*, 13, 11987-  
 1503 12001, 10.5194/acp-13-11987-2013, 2013.

1504 Sesartic, A., and Dallafior, T. N.: Global fungal spore emissions, review and synthesis of  
 1505 literature data, *Biogeosciences*, 8, 1181-1192, 10.5194/bg-8-1181-2011, 2011.

1506 Shaffer, B. T., and Lighthart, B.: Survey of culturable airborne bacteria at four diverse locations  
 1507 in Oregon: Urban, rural, forest, and coastal, *Microbial Ecology*, 34, 167-177,  
 1508 10.1007/s002489900046, 1997.

1509 Sharma, N. K., and Rai, A. K.: Allergenicity of airborne cyanobacteria *Phormidium fragile* and  
 1510 *Nostoc muscorum*, *Ecotoxicology and Environmental Safety*, 69, 158-162,  
 1511 10.1016/j.ecoenv.2006.08.006, 2008.

1512 Sherman, J. P., Sheridan, P. J., Ogren, J. A., Andrews, E., Hageman, D., Schmeisser, L.,  
 1513 Jefferson, A., and Sharma, S.: A multi-year study of lower tropospheric aerosol variability and  
 1514 systematic relationships from four North American regions, *Atmospheric Chemistry and Physics*,  
 1515 15, 12487-12517, 10.5194/acp-15-12487-2015, 2015.

1516 Shika, S., et al.: Atmospheric aerosol properties at a semi-rural location in South India: particle  
 1517 size distributions and implications for cloud formation, to be submitted.

1518 Sivaprakasam, V., Huston, A. L., Scotto, C., and Eversole, J. D.: Multiple UV wavelength  
 1519 excitation and fluorescence of bioaerosols, *Optics Express*, 12, 4457-4466,  
 1520 10.1364/opex.12.004457, 2004.

1521 Spracklen, D. V., and Heald, C. L.: The contribution of fungal spores and bacteria to regional  
 1522 and global aerosol number and ice nucleation immersion freezing rates, *Atmospheric Chemistry*  
 1523 *and Physics*, 14, 9051-9059, 10.5194/acp-14-9051-2014, 2014.

1524 Srivastava, A., Singh, M., and Jain, V. K.: Identification and characterization of size-segregated  
 1525 bioaerosols at Jawaharlal Nehru University, New Delhi, *Natural Hazards*, 60, 485-499,  
 1526 10.1007/s11069-011-0022-3, 2012.

1527 Tarlo, S. M., Bell, B., Srinivasan, J., Dolovich, J., and Hargreave, F. E.: Human sensitization to  
 1528 ganoderma antigen, *Journal of Allergy and Clinical Immunology*, 64, 43-49, 10.1016/0091-  
 1529 6749(79)90082-4, 1979.

1530 Tong, Y and Lighthart, B.: Diurnal Distribution of Total and Culturable Atmospheric Bacteria at  
 1531 a Rural Site, *Aerosol Sci. Technol.*, 30, 246-254, 10.1080/027868299304822, 1999.

1532 Toprak, E., and Schnaiter, M.: Fluorescent biological aerosol particles measured with the  
 1533 Waveband Integrated Bioaerosol Sensor WIBS-4: laboratory tests combined with a one year  
 1534 field study, *Atmospheric Chemistry and Physics*, 13, 225-243, 10.5194/acp-13-225-2013, 2013.

1535 Trejo, M., Douarche, C., Bailleux, V., Poulard, C., Mariot, S., Regeard, C., and Raspaud, E.:  
 1536 Elasticity and wrinkled morphology of *Bacillus subtilis* pellicles, *Proceedings of the National*  
 1537 *Academy of Sciences of the United States of America*, 110, 2011-2016,  
 1538 10.1073/pnas.1217178110, 2013.

1539 Troutt, C., and Levetin, E.: Correlation of spring spore concentrations and meteorological  
 1540 conditions in Tulsa, Oklahoma, *International Journal of Biometeorology*, 45, 64-74,  
 1541 10.1007/s004840100087, 2001.

1542 Valsan, A. E., Priyamvada, H., Ravikrishna, R., Després, V. R., Biju, C. V., Sahu, L. K., Kumar,  
 1543 A., Verma, R. S., Philip, L., and Gunthe, S. S.: Morphological characteristics of bioaerosols from  
 1544 contrasting locations in southern tropical India – A case study, *Atmospheric Environment*, 122,  
 1545 321-331, <http://dx.doi.org/10.1016/j.atmosenv.2015.09.071>, 2015.

1546 Vinoj, V., and Satheesh, S. K.: Measurements of aerosol optical depth over Arabian Sea during  
 1547 summer monsoon season, *Geophysical Research Letters*, 30, 10.1029/2002gl016664, 2003.

1548 Vinoj, V., Satheesh, S. K., and Moorthy, K. K.: Optical, radiative, and source characteristics of  
 1549 aerosols at Minicoy, a remote island in the southern Arabian Sea, *Journal of Geophysical*  
 1550 *Research-Atmospheres*, 115, 10.1029/2009jd011810, 2010.

1551 Vinoj, V., Rasch, P. J., Wang, H., Yoon, J.-H., Ma, P.-L., Landu, K., and Singh, B.: Short-term  
 1552 modulation of Indian summer monsoon rainfall by West Asian dust, *Nature Geoscience*, 7, 308-  
 1553 313, 10.1038/ngeo2107, 2014.

1554 Wang, C.-C., Fang, G.-C., and Lee, L.: Bioaerosols study in central Taiwan during summer  
 1555 season, *Toxicology and Industrial Health*, 23, 133-139, 10.1177/0748233707078741, 2007.

1556 Yu, X., Wang, Z., Zhang, M., Kuhn, U., Xie, Z., Cheng, Y., Pöschl, U., and Su, H.: Ambient  
 1557 measurement of fluorescent aerosol particles with a WIBS in the Yangtze River Delta of China:  
 1558 potential impacts of combustion-generated aerosol particles, *Atmos. Chem. Phys. Discuss.*,  
 1559 doi:10.5194/acp-2016-228, in review, 2016.

1560 Zhang, T., Engling, G., Chan, C.-Y., Zhang, Y.-N., Zhang, Z.-S., Lin, M., Sang, X.-F., Li, Y. D.,  
 1561 and Li, Y.-S.: Contribution of fungal spores to particulate matter in a tropical rainforest,  
 1562 *Environmental Research Letters*, 5, 10.1088/1748-9326/5/2/024010, 2010.

1563

1564

1565 Table 1: List of frequently used acronyms and symbols with units.

1566

1567

Symbol	Quantity, Unit	
$D_a$	Aerodynamic diameter, $\mu\text{m}$	1568
$D_g$	Geometric midpoint diameter of fluorescent particles	1569
$D_{g,T}$	Geometric midpoint diameter of total particles	1570
DNA	Deoxyribonucleic acid	
FBAP	Fluorescent biological aerosol particle	1571
He-Ne	Helium-Neon	1572
ITCZ	Inter Tropical Convergence Zone	
<a href="#">Lpm</a>	<a href="#">Liters per minute</a>	1573
$M_F$	Integrated mass concentration of fluorescent particles, $\mu\text{g m}^{-3}$	1574
$M_T$	Integrated mass concentration of total particles, $\mu\text{g m}^{-3}$	1575
Nd:YAG	Neodymium-doped yttrium Aluminum garnet	1576
NE	Northeast	
$N_F$	Integrated number concentration of fluorescent particles, $\text{cm}^{-3}$	1577
$N_T$	Integrated number concentration of total particles, $\text{cm}^{-3}$	1578
PAH	Polycyclic aromatic hydrocarbon	1579
PBAPs	Primary Biological Aerosol Particles	1580
RH	Relative Humidity	1581
SEM	Scanning Electron Microscopy	1582
SW	Southwest	1583
TAP	Total Aerosol Particle	
TSP	Total Suspended Particle	
UV-APS	Ultraviolet Aerodynamic Particle Sizer	
$\lambda$	Wavelength, nm	

1583

1584

1585

1586

1587

1588

1589

1590



1591

1592

Number		June	July	August	Campaign
$N_T$ (cm <sup>-3</sup> )	Mean	2.66	1.54	0.96	1.77
	Median	2.45	1.48	0.73	1.44
$N_F$ (cm <sup>-3</sup> )	Mean	0.03	0.007	0.015	0.017
	Median	0.02	0.006	0.007	0.01
$N_F/N_T$ (%)	Mean	0.03	0.01	0.03	0.02
	Median	0.01		0.01	0.01
Mass		June	July	August	Campaign
$M_T$ (μg m <sup>-3</sup> )	Mean	10.61	6.15	4.15	7.17
	Median	9.58	5.55	2.8	5.57
$M_F$ (μg m <sup>-3</sup> )	Mean	0.42	0.11	0.18	0.24
	Median	0.33	0.09	0.1	0.15
$M_F/M_T$ (%)	Mean	0.09	0.03	0.08	0.06
	Median	0.04	0.02	0.03	0.03

1593

1594 Table 2: Integrated number concentrations and mass concentrations of coarse TAP and FBAP (~1–20 μm):  
1595 arithmetic mean and median for each month and for the entire measurement campaign  
1596

1597

1598

1599

1600

1601

1602

1603

1604

1605

Sl No:	Location	Land Use	Measurement Measurement Period	Season	Instrument	FBAP Number Concentration	Total Number Concentration	Number Ratio (%)	Reference
1	Mainz, Central Europe	Semi-urban	Aug-Dec, 2006		UVAPS	$3 \times 10^{-2} \text{ cm}^{-3}$	$1.05 \text{ cm}^{-3}$	4	Huffman et al., 2010
2	Central Amazonia rainforest	Tropical rainforest	Feb-Mar, 2008		UVAPS	$7.3 \times 10^{-2} \text{ cm}^{-3}$	$0.33 \text{ cm}^{-3}$	24	Huffman et al., 2012
3	Manchester, UK	Urban	December, 2009		WIBS-3	$2.9 \times 10^{-4} \text{ cm}^{-3}$ (FL1)	$1.38 \times 10^{-2} \text{ cm}^{-3}$	2.1	Gabey et al., 2011
						$5.2 \times 10^{-4} \text{ cm}^{-3}$ (FL2)		3.7	
						$1.1 \times 10^{-5} \text{ cm}^{-3}$ (FL3)		7.8	
4	Central France	Rural	22 Jun-3 July, 2010		WIBS-3	$1.2 \times 10^{-2} \text{ cm}^{-3}$ (280 nm)			Gabey et al., 2013
						$9.5 \times 10^{-2} \text{ cm}^{-3}$ (370 nm)			
5	Helinski, Finland	Urban	Feb, 2012 (Winter)	Winter	BioScout	$1 \times 10^{-2} \text{ cm}^{-3}$		23	Saari et al., 2015
			June-Aug, 2012 (Summer)	Summer		$2.8 \times 10^{-2} \text{ cm}^{-3}$		6	
				Summer	UVAPS	$1.3 \times 10^{-2} \text{ cm}^{-3}$		8	
6	Colorado, USA	Pine forest	June-July, 2011	Dry period	WIBS-3			5.8	Crawford et al., 2014
				Wet Period	WIBS-4			15.2	
7	Finland	Rural forest	August, 2009 - April, 2011	Spring	UVAPS	$1.5 \times 10^{-2} \text{ cm}^{-3}$	$0.43 \text{ cm}^{-3}$	4.4	Schumacher et al., 2013
				Summer		$4.6 \times 10^{-2} \text{ cm}^{-3}$	$0.45 \text{ cm}^{-3}$	13	
				Fall		$2.7 \times 10^{-2} \text{ cm}^{-3}$	$0.41 \text{ cm}^{-3}$	9.8	
				Winter		$0.4 \times 10^{-2} \text{ cm}^{-3}$	$0.47 \text{ cm}^{-3}$	1.1	

	Colorado , USA	Rural, semi-arid	2011-2012	Spring	UVAPS	$1.5 \times 10^{-2} \text{ cm}^{-3}$	$0.73 \text{ cm}^{-3}$	2.5	
				Summer		$3 \times 10^{-2} \text{ cm}^{-3}$	$0.44 \text{ cm}^{-3}$	8.8	
				Fall		$1.7 \times 10^{-2} \text{ cm}^{-3}$	$0.28 \text{ cm}^{-3}$	5.7	
				Winter		$0.53 \times 10^{-2} \text{ cm}^{-3}$	$0.2 \text{ cm}^{-3}$	3	
8	Karlsruhe, Germany	Semi-rural	April 2010 - April 2011		WIBS - 4	$3.1 \times 10^{-2} \text{ cm}^{-3}$	$0.583 \text{ cm}^{-3}$	7.34	Toprak and Schnaiter., 2013 Yu et al., 2016
9	Nanjing, China	Sub-urban	Oct-Nov, 2013	Autumn	WIBS-4		$13.1 \text{ cm}^{-3}$		
						$0.6 \text{ cm}^{-3}$ (FL1)		4.6	
						$3.4 \text{ cm}^{-3}$ (FL2)		25.3	
						$2.1 \text{ cm}^{-3}$ (FL3)		15.6	

1606

1607 Table 3: Comparison with other online measurements carried out under various environmental conditions across the globe.

Number		Dusty	Clean	<del>HighBio</del> High Bio
$N_T$ (cm <sup>-3</sup> )	Mean	4.2	1.27	1.78
	Median	4.36	1.15	1.4
$N_F$ (cm <sup>-3</sup> )	Mean	0.02	0.005	0.05
	Median	0.019	0.004	0.038
$N_F/N_T$	Mean	0.01	0.01	0.05
	Median			0.03
Mass		Dusty	Clean	<del>HighBio</del> High Bio
$M_T$ (μg m <sup>-3</sup> )	Mean	16.34	5.12	7.7
	Median	16.84	4.28	5.85
$M_F$ (μg m <sup>-3</sup> )	Mean	0.36	0.08	0.58
	Median	0.33	0.05	0.47
$M_F/M_T$	Mean	0.02	0.03	0.12
	Median	0.02	0.01	0.08

1608

1609 Table 4: Integrated number concentrations and mass concentrations of coarse TAP and FBAP (~1–20 μm):  
1610 | arithmetic mean and median for each focus period (Dusty, Clean and ~~HighBio~~High Bio).  
1611

1612

1613

1614

1615

1616

1617

1618

1619

1620

1621

1622

1623

	Campaign			Dusty			Clean			High Bio		
	$N_T$	$N_F$	$N_F/N_T$	$N_T$	$N_F$	$N_F/N_T$	$N_T$	$N_F$	$N_F/N_T$	$N_T$	$N_F$	$N_F/N_T$
RH	-0.64	0.58	0.85	-0.25		0.18	-0.66	-0.01	0.13	-0.64	0.5	0.68
Temperature	0.45	-0.65	-0.82	0.34	-0.04	-0.25	0.78	0.02	-0.2	0.43	-0.68	-0.83
Wind Speed	0.4	-0.6	-0.78	0.09	-0.18	-0.31	-0.18	-0.27	0	0.3	-0.61	-0.74

Table 5:  $R^2$  values for correlation between meteorological parameters (RH, Temperature and Wind Speed) and  $N_T$ ,  $N_F$  and  $N_F/N_T$  during the entire campaign and each focus periods.

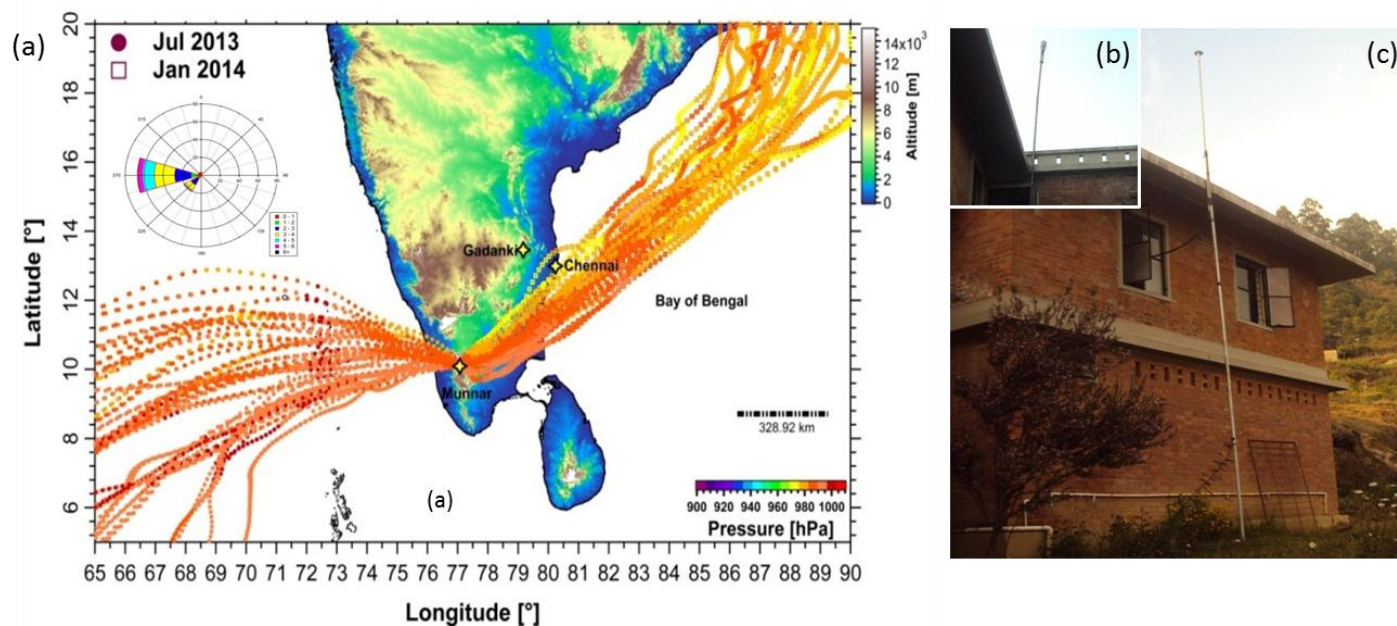
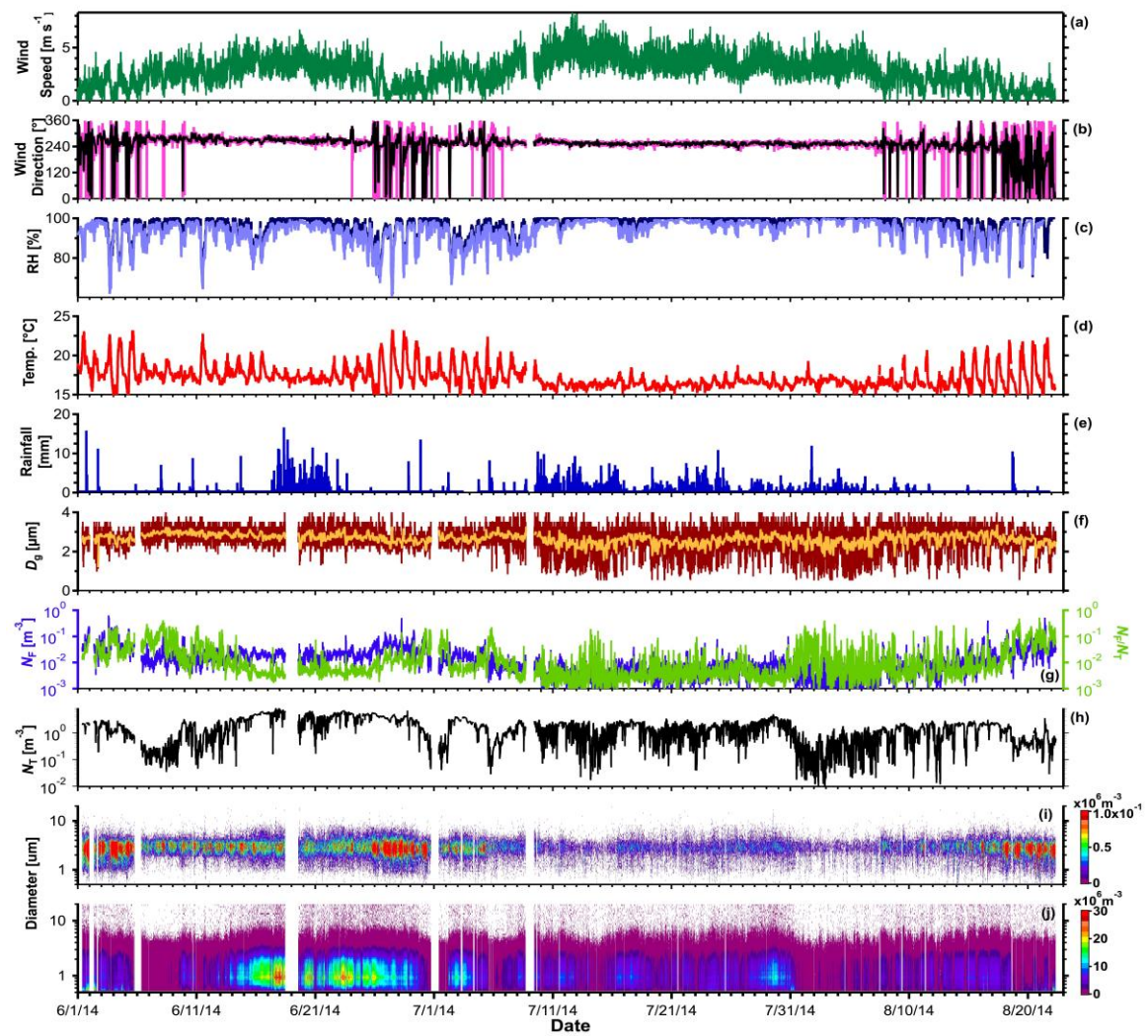


Figure 1: Location of measurement site Munnar (10.09°N, 77.06°E; 1605 m amsl – above mean sea level) located in the Western Ghats mountain range in Southern tropical India with 10 days back trajectories (HYSPLIT, NOAA-ARL GDAS1 model; start height 50 m above ground level; starting time 23:30 local time) illustrating the distinct and contrasting wind patterns during two contrasting seasons; Southwest monsoon season (representative month Jul) and Northeast monsoon/Winter season (representative month Jan) when field measurement campaign was carried out. It is evident that predominant wind pattern during Southwest monsoon season was Westerly/Southwesterly bringing the clean marine influx. Also shown in inset is as also evident from the wind rose diagram prepared using the data obtained shown in inset(a). The meteorological parameters were recorded using the ultrasonic weather station (a) installed close to the inlet system (b). The inlet system prepared for sampling the air using Ultraviolet Aerodynamic Particle Sizer (UV-APS) for bioaerosol number size distribution measurement. Inset shows the arrangement made for installing the ultrasonic weather station (b), (c). The map shown is color-coded by topography (meters).

|





) and trajectories are color-coded by atmospheric pressure level (hPa)

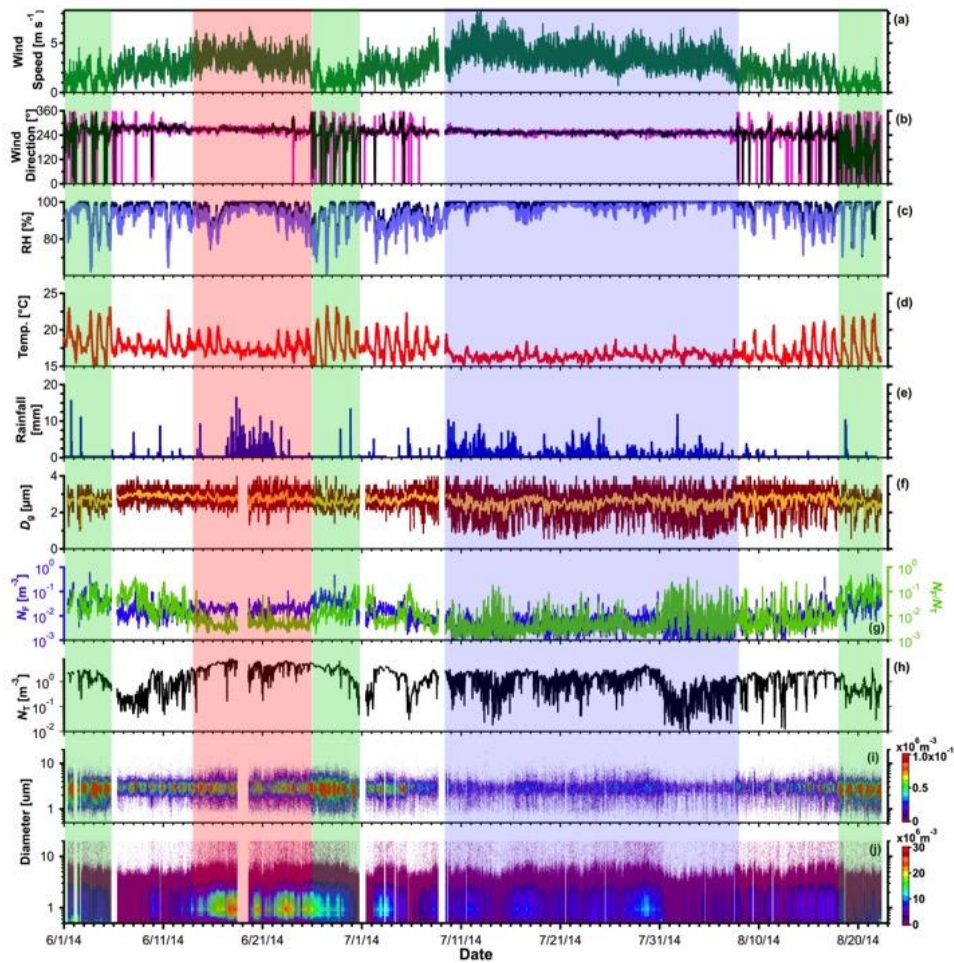


Figure 2: Time series of measured meteorological parameters, parameters derived from FBAP and total particle number size distribution measurements using UV-APS: (a) wind speed, (b) wind direction: five minutes average (magenta) and one hour average (black), (c) relative humidity, (d) temperature, (e) rainfall, (f) geometric mean diameter ( $D_g$ ) five minutes average (dark red) and one hour average (yellow), (g) FBAP number concentration ( $N_F$ ; blue) and relative contribution of FBAP to TAP ( $N_F/N_T$ ; green), (h) TAP number concentration ( $N_T$ ), (i) a contour plot of FBAP number size distribution ( $dN/d\log D_F$ ), and (j) a contour plot of TAP number size distribution ( $dN/d\log D_T$ ). The shadowed block represents the different focus periods ([red for dusty](#); [green for high bio](#); [blue for clean](#); please refer to text for more details).

Formatted: Justified

Formatted: Font: 10 pt

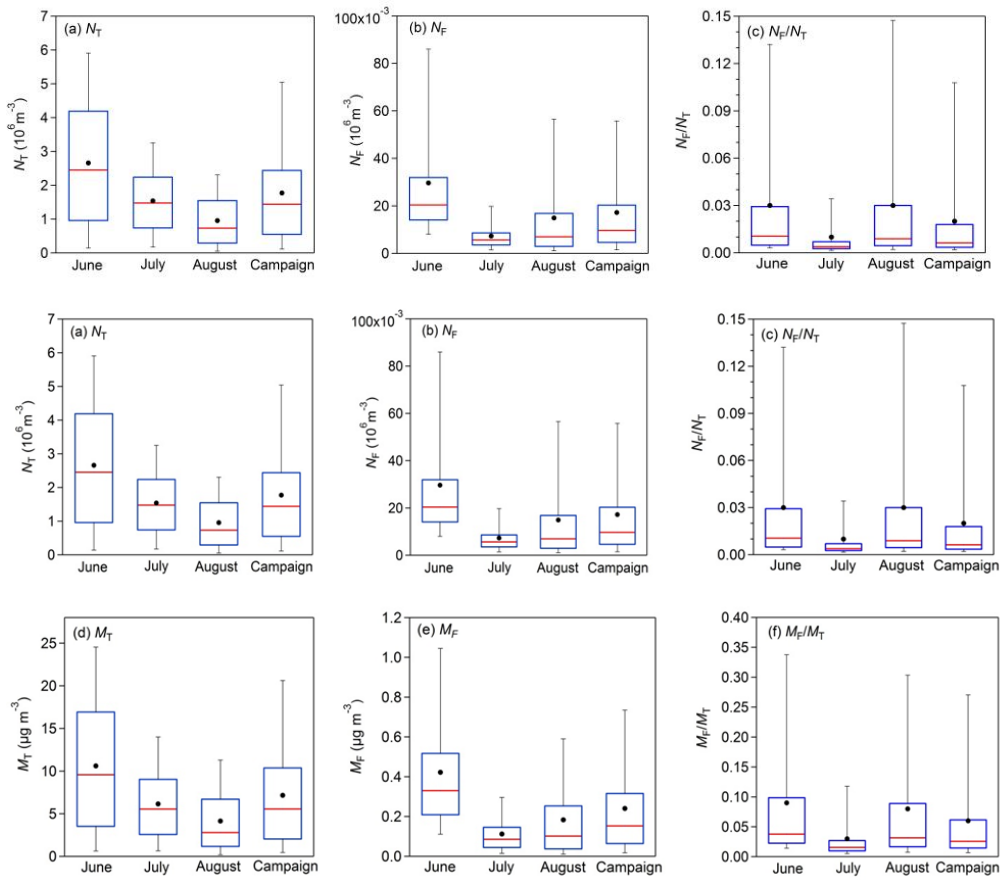
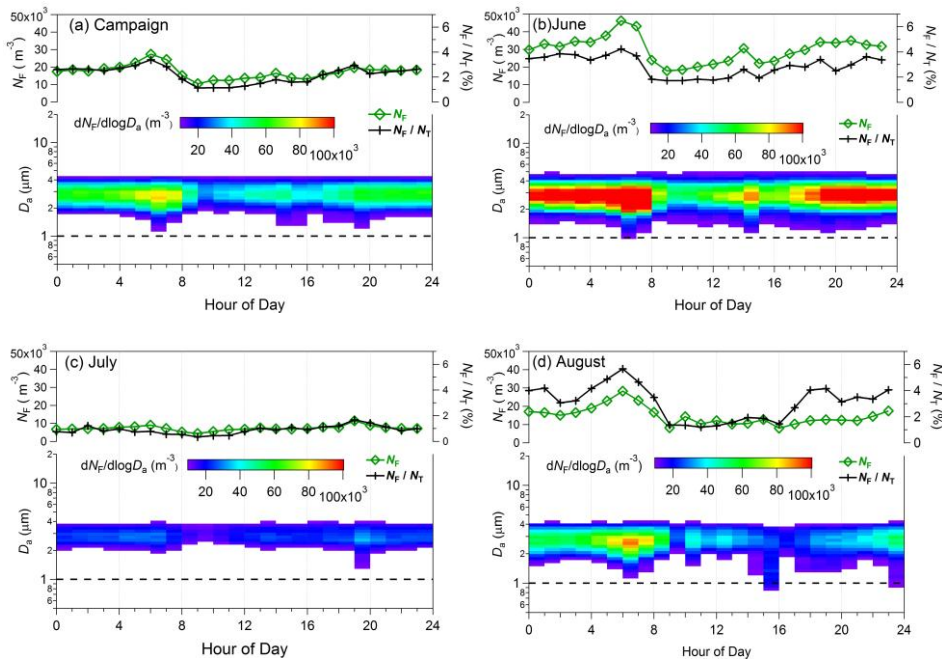


Figure 3: Statistical distribution of integrated (~1 – 20 μm) FBAP and TAP number and ~~contribution of  $N_F$  to  $N_T$  mass and their ratios~~ measured during each month (Jun – Aug) of SW monsoon season and averaged over the entire measurement campaign carried out at Munnar as box whisker plots: (a) TAP number concentration ( $N_T$ ), (b) FBAP number concentration ( $N_F$ ), ~~and~~ (c) contribution of FBAP number concentration to TAP number concentration ( $N_F/N_T$ ), ~~and~~ (d) TAP mass concentration ( $M_T$ ), (e) FBAP mass concentration ( $M_F$ ) and (f) contribution of FBAP to TAP mass concentration ( $M_F/M_T$ ).

Formatted: Justified

Formatted: Font: Times New Roman, 0 pt, Not Bold, Font color: Black, Character scale: 0%, Border: : (No border), Pattern: Clear (Black)



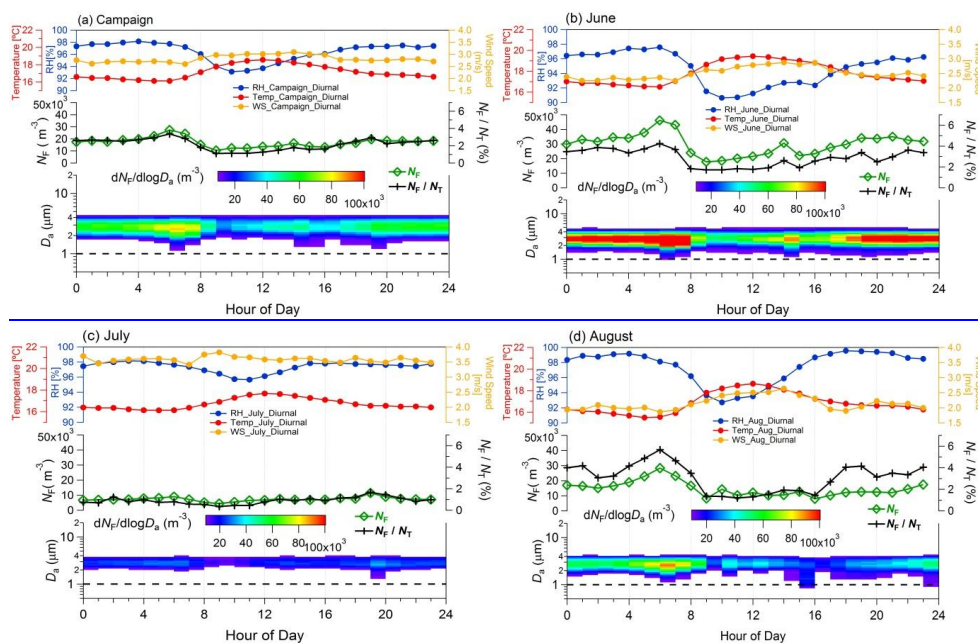


Figure 4: Diurnal cycles of observed meteorological parameters, FBAP number concentrations ( $N_F$ ) and size distributions averaged over individual month of measurement and entire campaign (hourly median mean values plotted against the local time of the day). Upper portion of each panel shows the observed meteorological parameters: relative humidity (%; blue), temperature ( $^{\circ}\text{C}$ ; red), and wind speed ( $\text{m s}^{-1}$ ; orange on right axis). Middle panel shows integrated FBAP number concentration ( $\sim 1 - 20 \mu\text{m}$ ;  $N_F$ ) on the left axis (green color) and FBAP fraction of TAP number ( $N_F/N_T$ ) on the right axis (black color). Lower portion of each panel FBAP number size distribution (3-D plot) plotted against hour of the day on x-axis, aerodynamic diameter on y-axis and color is scaled for  $dN_F/d\log D_a$  indicates the concentration. Dashed black lines in lower portion of the each panel at  $1.0 \mu\text{m}$  shows the particle size cut-off diameter below which fluorescent particles were not considered as FBAP due to potential interference with non-biological aerosol particles. (a) averaged over entire campaign, (b) Jun, (c) Jul, and (d) Aug. Please refer to supplementary Figs. for corresponding TAP plots. ▲

Formatted: Font: +Body (Calibri), Bold

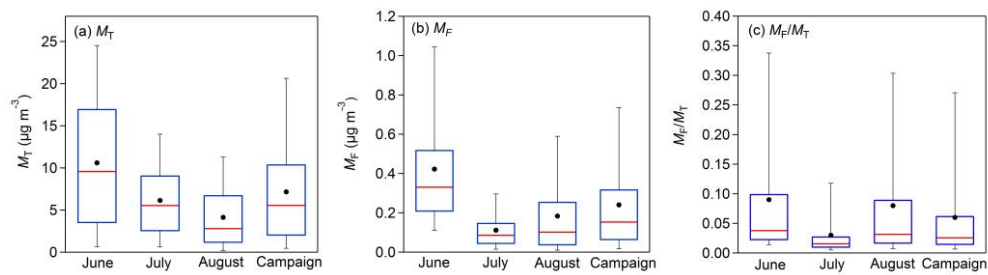


Figure 5: Same as Fig. 3 but for integrated ( $< 1 - 20 \mu\text{m}$ ) FBAP ( $M_F$ ) and TAP ( $M_T$ ) mass concentrations derived from number measurements by assuming unit density and shape factor.

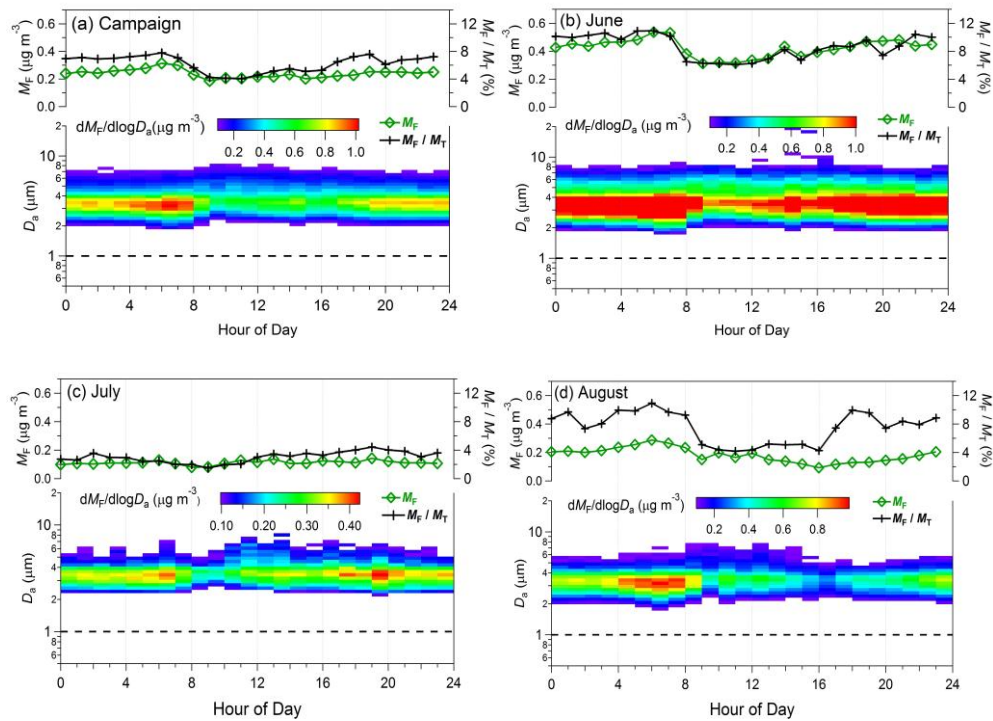


Figure 6: Same as Fig. 4 but representing the FBAP ( $M_F$ ) mass concentrations.

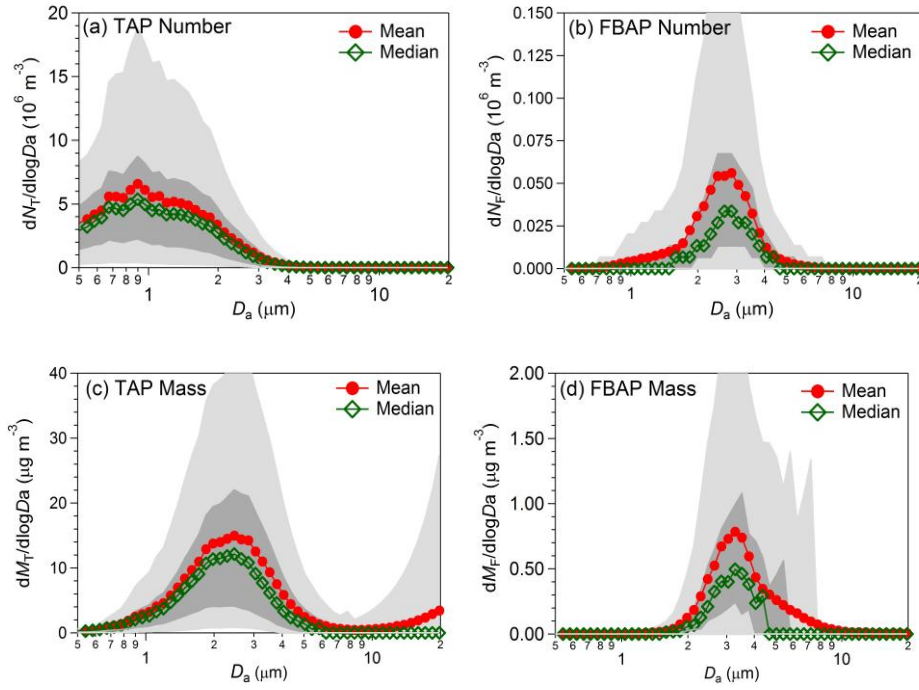


Figure 7.5: Particle number size and unit-normalized number size and mass size distributions averaged over the entire measurement campaign carried out at Munnar. Lower and upper parts of dark and light shaded area represents the 5<sup>th</sup>, 25<sup>th</sup>, 75<sup>th</sup>, and 95<sup>th</sup> percentile respectively. (a) TAP number ( $dN_T/d\log D_a$ ), (b) FBAP number ( $dN_F/d\log D_a$ ), (c) total mass ( $dM_T/d\log D_a$ ), and (d) FBAP mass ( $dM_F/d\log D_a$ ).



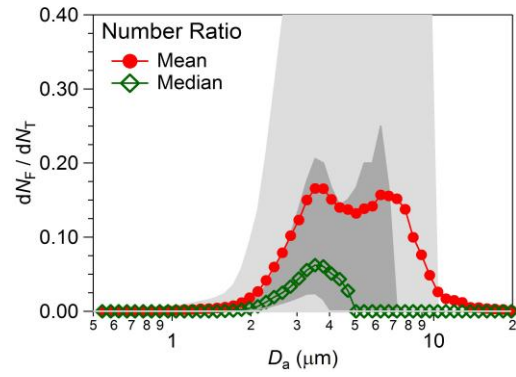


Figure 86: Size distribution of FBAP to TAP ratio averaged over the entire measurement period carried out at Munnar ( $dN_F/d\log D_a = dM_F/d\log D_a$ ). Lower and upper parts of dark and light shaded area represents the 5<sup>th</sup>, 25<sup>th</sup>, 75<sup>th</sup>, and 95<sup>th</sup> percentile respectively.

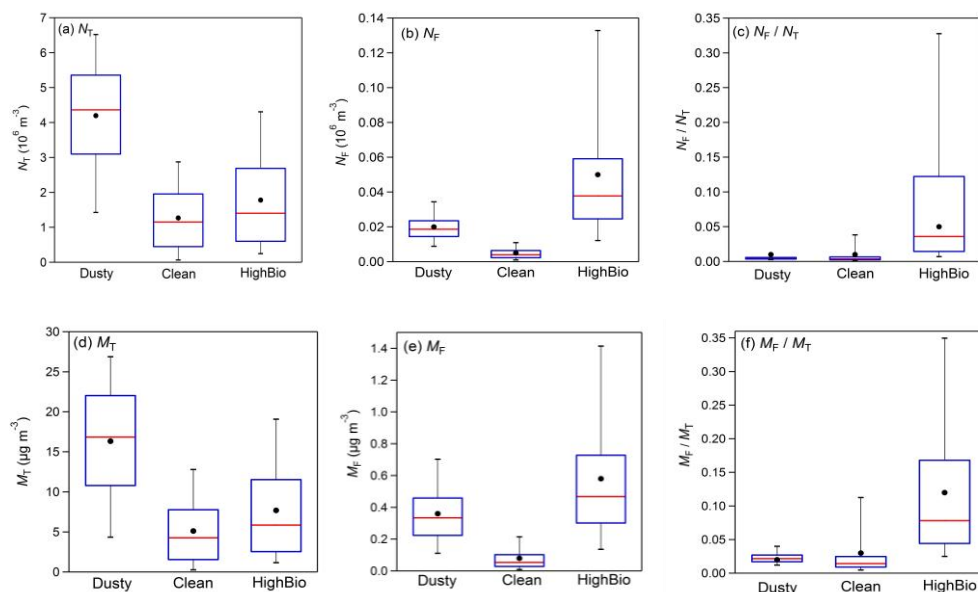


Figure 97: Statistical distribution of integrated ( $\sim 1 - 20 \mu\text{m}$ ) FBAP and TAP number and mass contribution of  $N_F$  to  $N_T$ , and  $M_F$  to  $M_T$  averaged over each distinct focus periods (dusty, clean, and high bio; please refer to the text for definitions related to each focus period) measurements carried out at Munnar as box whisker plots: (a) TAP number concentration ( $N_T$ ), (b) FBAP number concentration ( $N_F$ ), (c) contribution of FBAP number concentration to TAP number concentration ( $N_F/N_T$ ), (d) TAP mass concentration ( $M_T$ ), (e) FBAP mass concentration ( $M_F$ ), and (f) contribution of FBAP mass concentration to TAP mass concentration ( $M_F/M_T$ ).

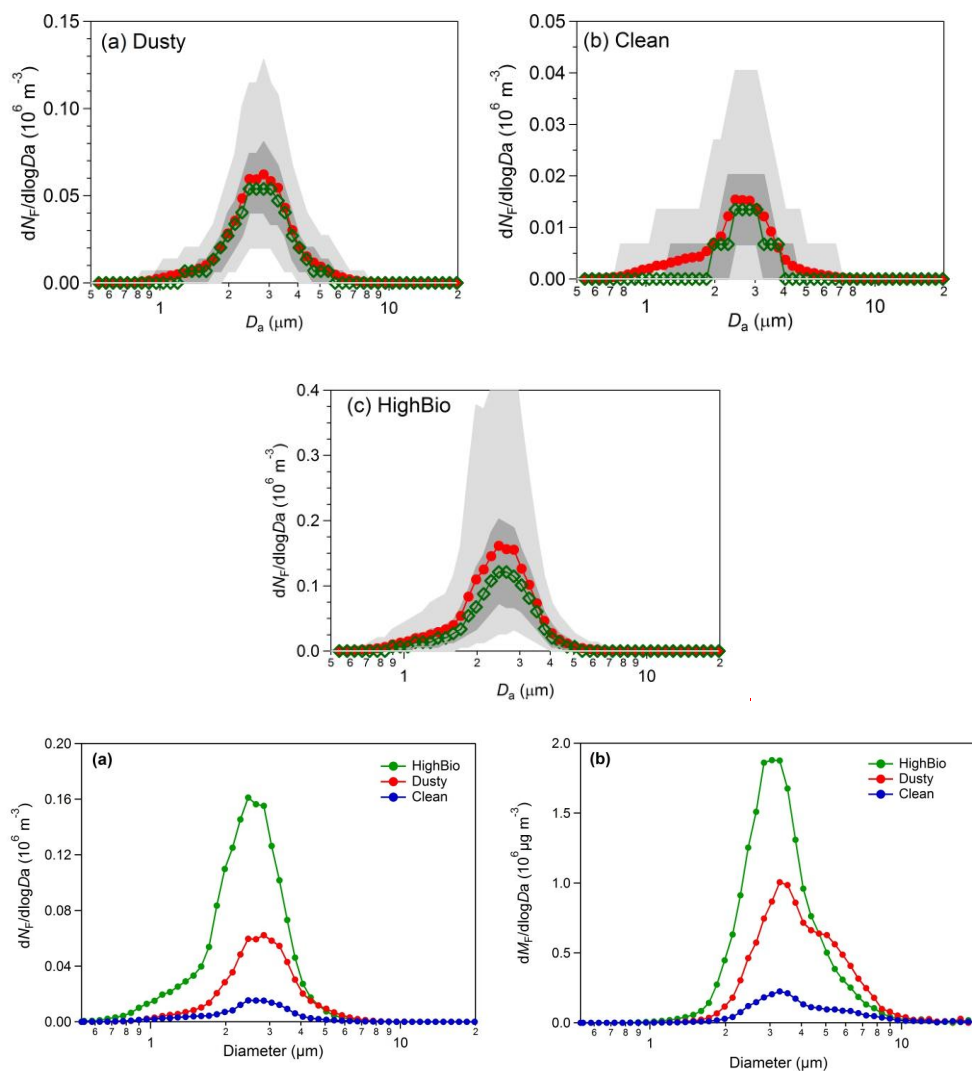


Figure 108: FBAP number size distributions ( $dN_F/d\log D_a$ ) and mass ( $dM_F/d\log D_a$ ) size distribution averaged over each distinct focus periods during the measurement campaign carried out at Munnar. Lower and upper parts of dark (a) number size distribution, and light shaded area represents the 5<sup>th</sup>, 25<sup>th</sup>, 75<sup>th</sup>, and 95<sup>th</sup> percentile respectively. (a) dusty period, (b) clean period, and (c) high bio period mass size distribution.

Formatted: Font: +Body (Calibri), Bold

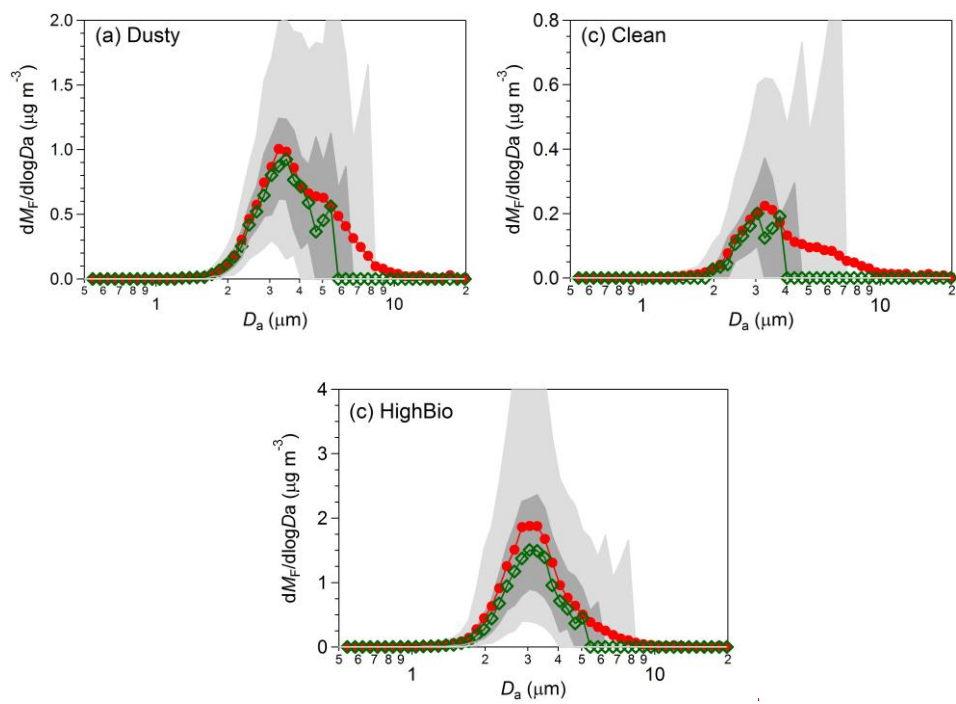


Figure 11: Same as Fig. 10 but representing PBAP mass size distribution ( $dM_F/d\log D_a$ ).

|

|

← Formatted: Centered

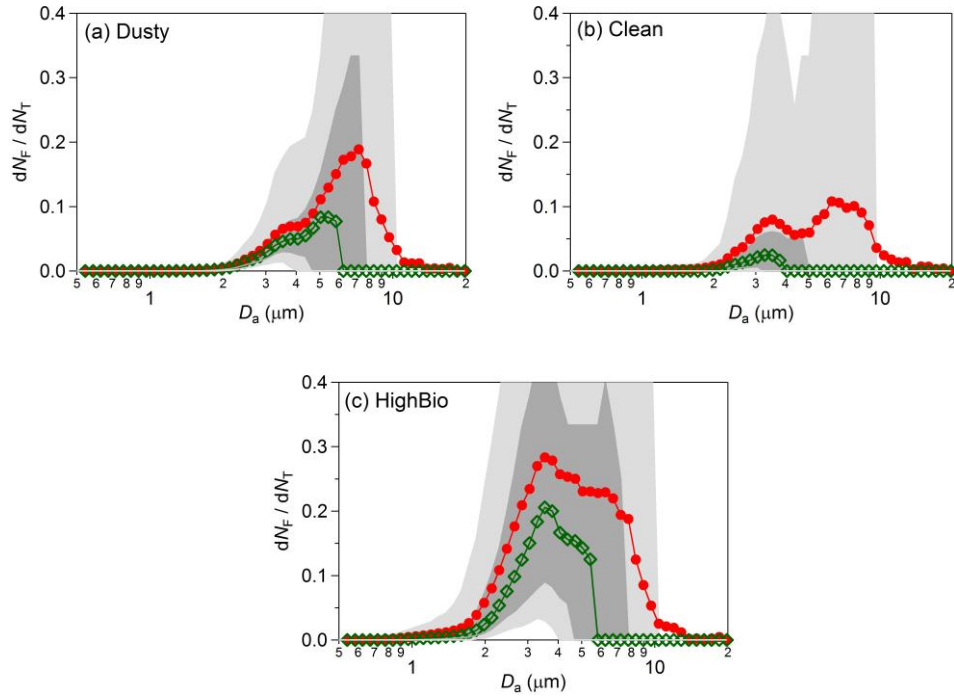


Figure 429: Size distribution of FBAP to TAP ratio averaged over the each distinct focus periods during the measurements carried out at Munnar ( $dN_F/d\log D_a = dM_F/d\log D_a$ ). Lower and upper parts of dark and light shaded area represents the 5<sup>th</sup>, 25<sup>th</sup>, 75<sup>th</sup>, and 95<sup>th</sup> percentile respectively: (a) dusty, (b) clean, and (c) high bio.

**Formatted:** Font: Times New Roman, Not Bold

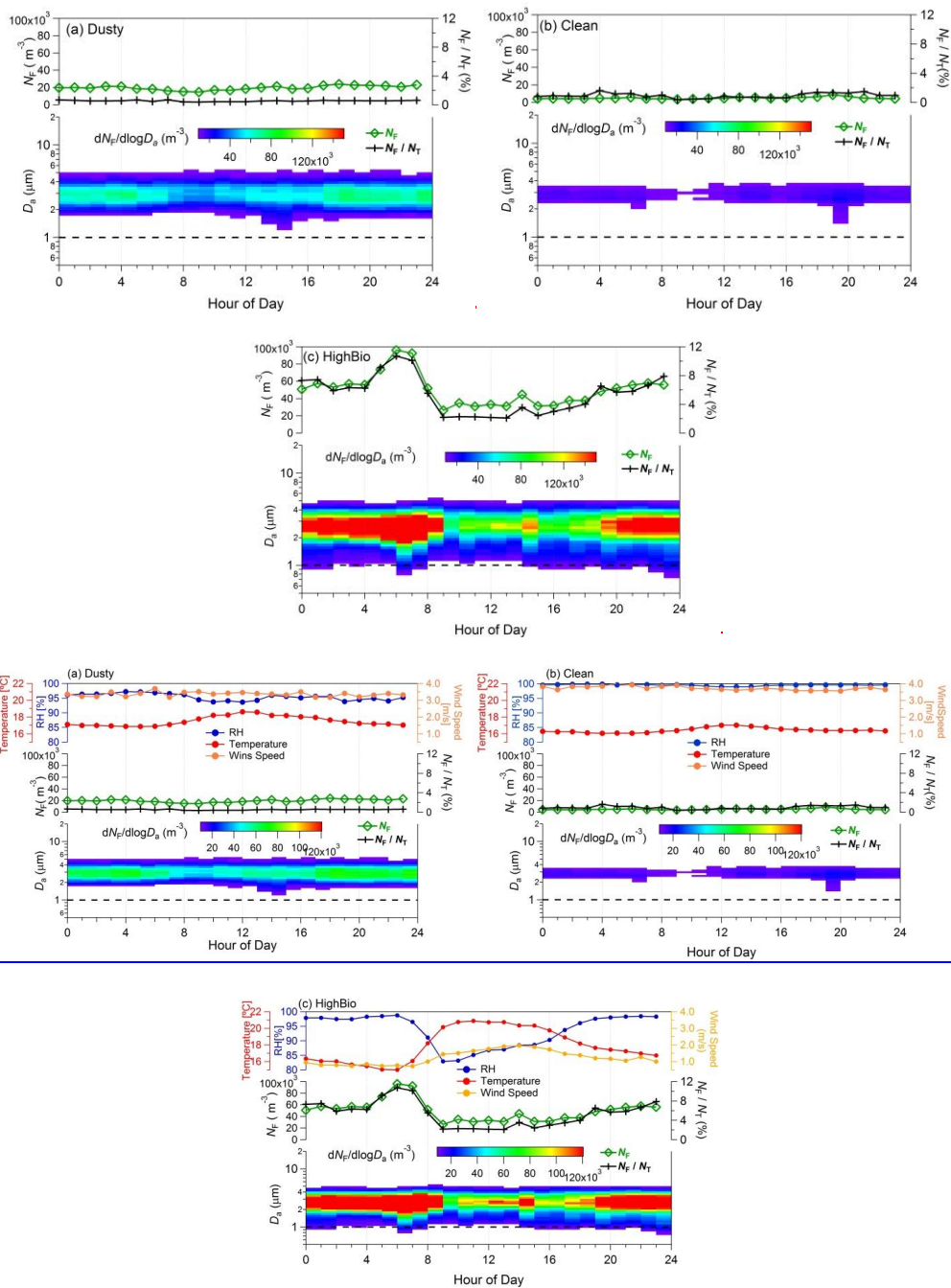


Figure 4.10: Diurnal cycles of observed meteorological parameters, FBAP number concentrations ( $N_F$ ) and size distributions averaged over each distinct focus period identified during measurements carried out at Munnar (hourly ~~median~~ mean values plotted against the local time of the day). Upper portion of each panel shows the observed meteorological parameters: relative humidity (%) blue), temperature (°C; red), and wind speed (m s<sup>-1</sup>; orange on right axis). Middle panel shows integrated FBAP number concentration (~1 – 20 µm;  $N_F$ ) on the left axis (green color) and FBAP fraction of TAP number ( $N_F/N_T$ ) on the right axis (black color). Lower portion of each panel FBAP number size distribution (3-D plot) plotted against hour of the day on x-axis, aerodynamic diameter on y-axis and color is scaled for  $DN_F/d\log D_a$  indicates the concentration. Dashed black lines in lower portion of the each panel at 1.0 µm shows the particle size cut-off diameter below which fluorescent particles were not considered as FBAP due to potential interference with non-biological aerosol particles. (a) dusty (b) clean, and (c) high bio. Please refer to supplementary Figs. for corresponding TAP plots.

**Formatted:** Font: Times New Roman, 0 pt, Not Bold, Font color: Black, Character scale: 0%, Border: : (No border), Pattern: Clear (Black)

**Formatted:** Centered



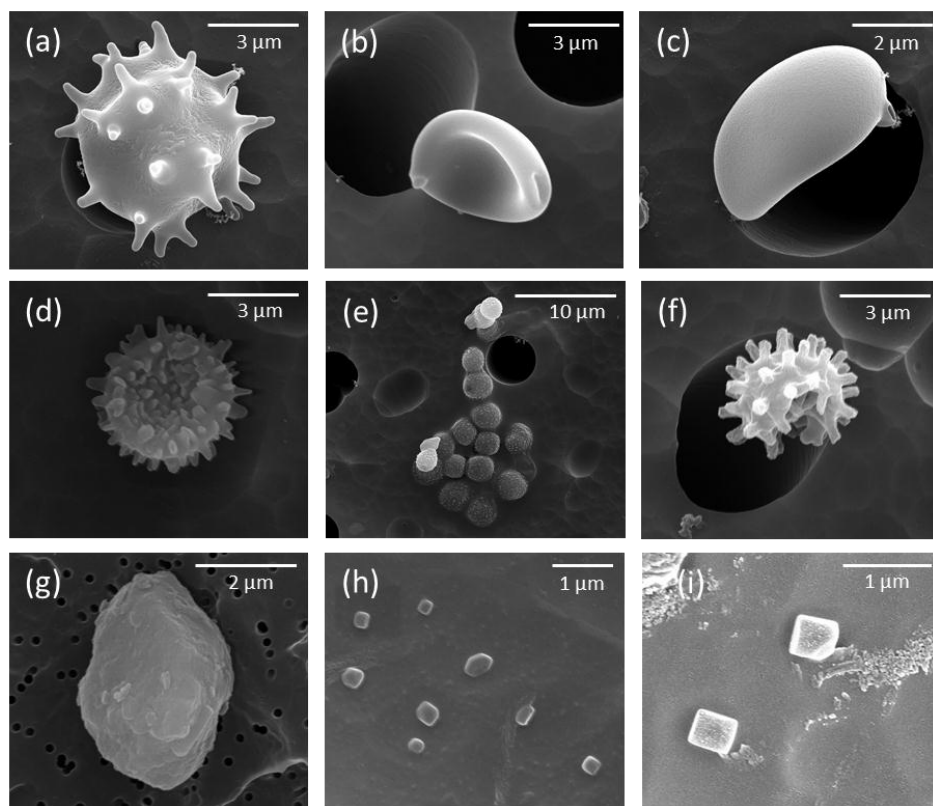
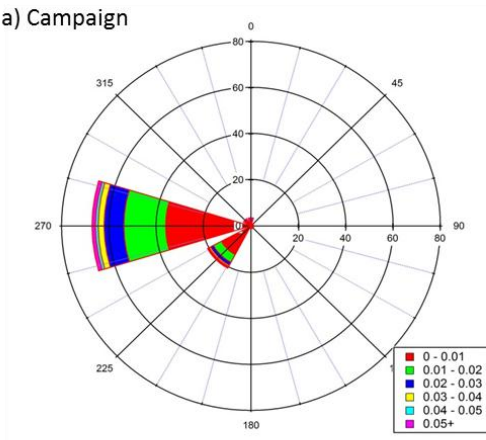


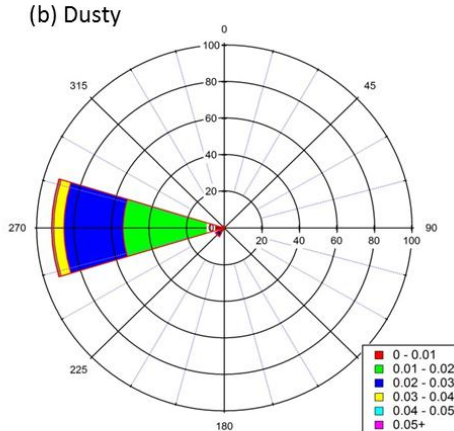
Figure 4.11: Scanning electron microscope images of the exemplary aerosol particles (FBAP and TAP) observed during the campaign at Munnar. The scale bar is shown at the top right corner of each image.

**Formatted:** Font: Times New Roman, Not Bold

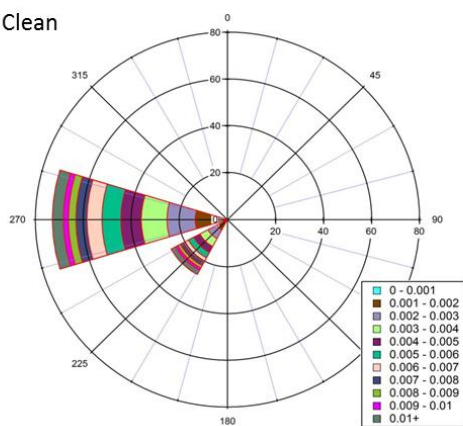
(a) Campaign



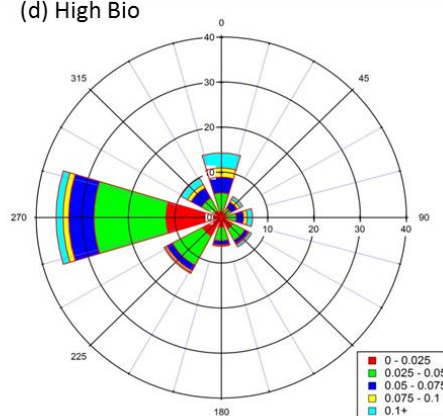
(b) Dusty



(c) Clean



(d) High Bio



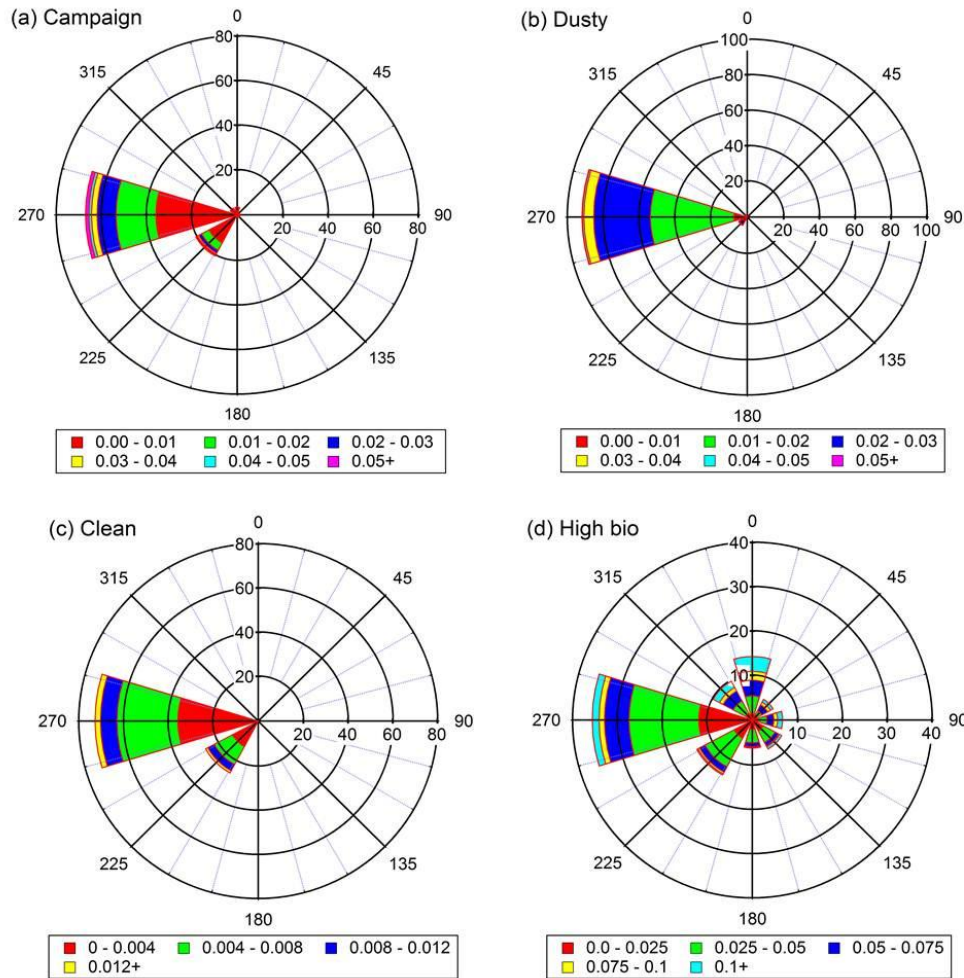
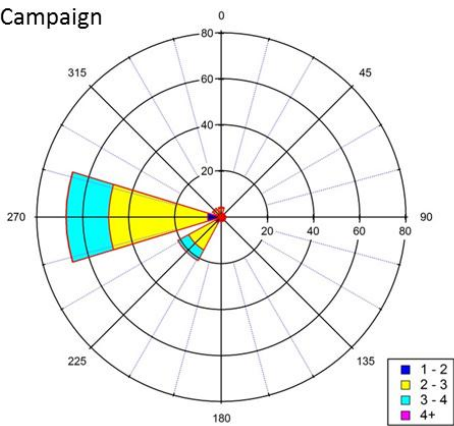


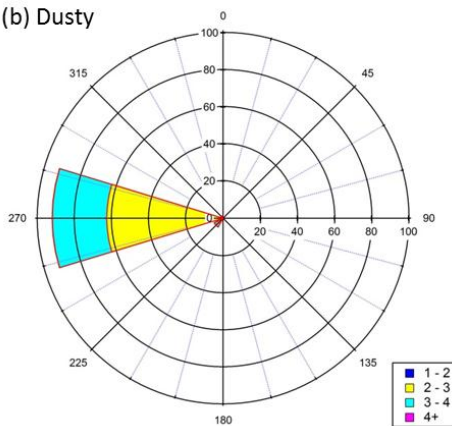
Figure 4-12: Wind rose diagram scaled over FBAP number concentration ( $N_F$ ). These diagrams in a way are similar to the traditional wind rose diagram except representing the  $N_F$  in this case instead of wind speed. These diagram can be nominally interpreted as followed: For example (a) shows that ~52% of frequency of occurrence of  $N_F$  concentration in the range of  $0 - 0.00401 \text{ cm}^{-3}$  was associated with Westerly/Southwesterly winds and on the contrary (d) indicates that out ~18% of frequency of occurrence of high concentration ( $N_F > 0.1 \text{ cm}^{-3}$ ) ~16% was associated with Northerly/Northwesterly winds. (a) entire campaign, (b) dusty period, (c) clean period, and (d) high bio period. Note that non-uniform scale of each panel has unit of  $\text{cm}^{-3}$ .

Formatted: Font: Times New Roman, Not Bold

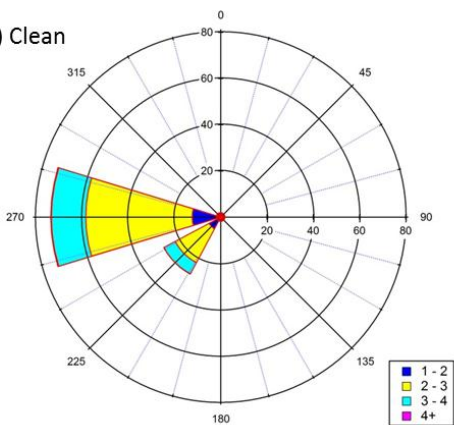
(a) Campaign



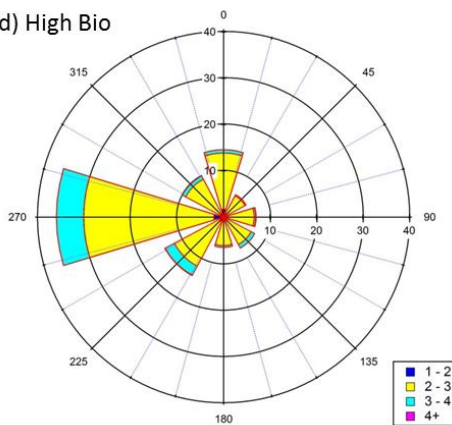
(b) Dusty



(c) Clean



(d) High Bio



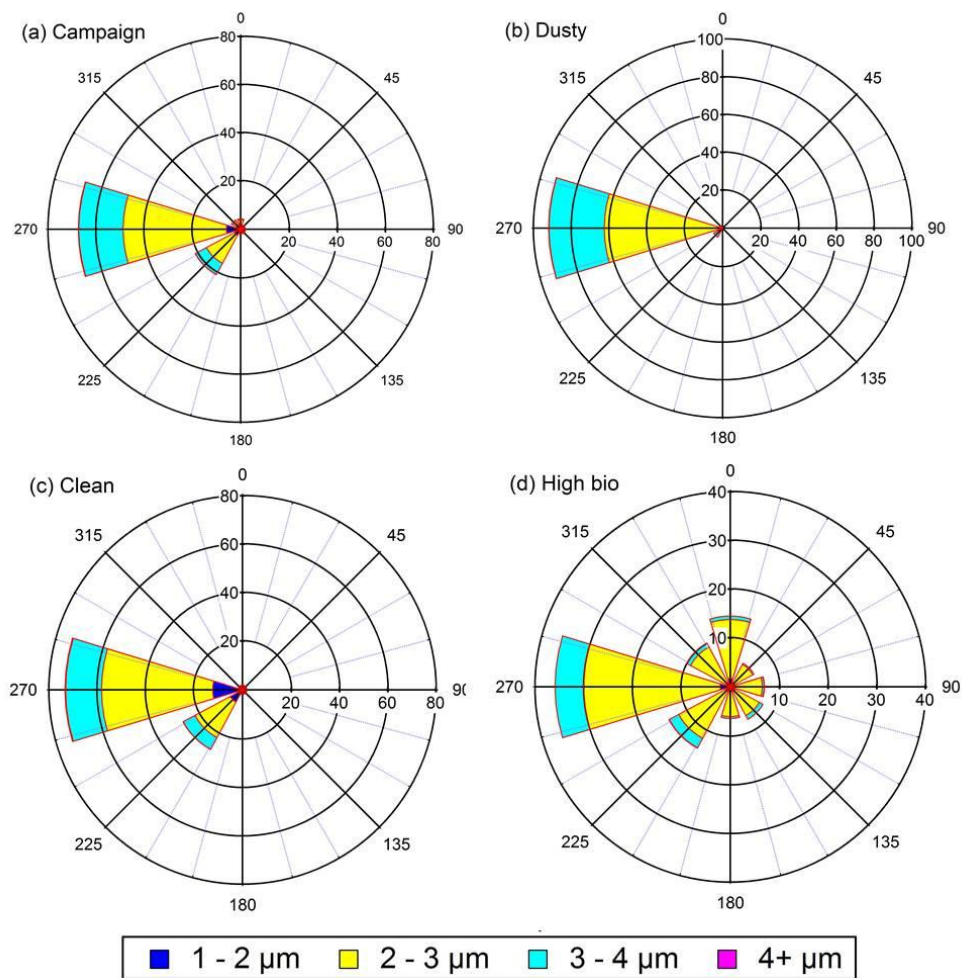
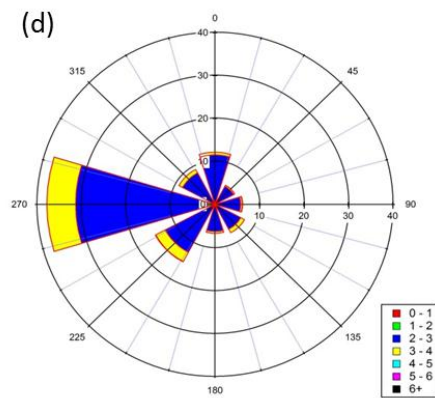
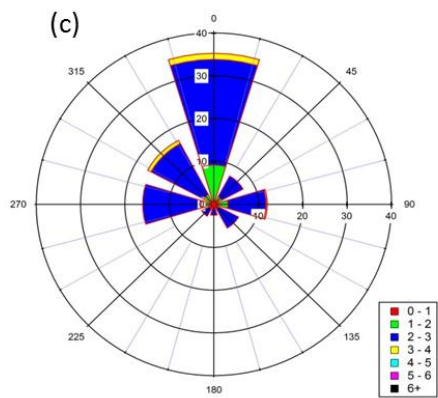
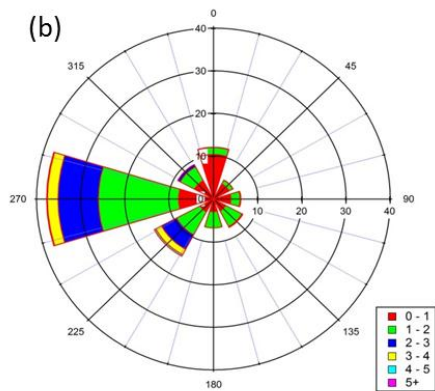
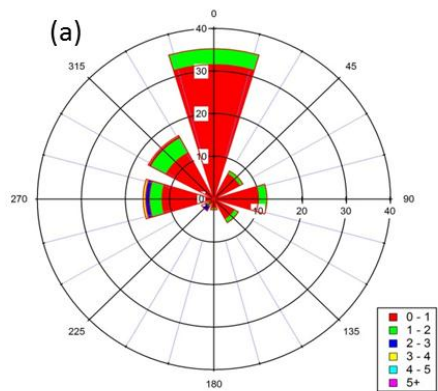


Figure 4.6.13: Same as Fig. 4.8.13 but scaled by geometric mean diameter ( $D_g$ ) of  $dN_F/d\log D_a$ . (a) entire campaign, (b) dusty period, (c) clean period, and (d) high bio period.





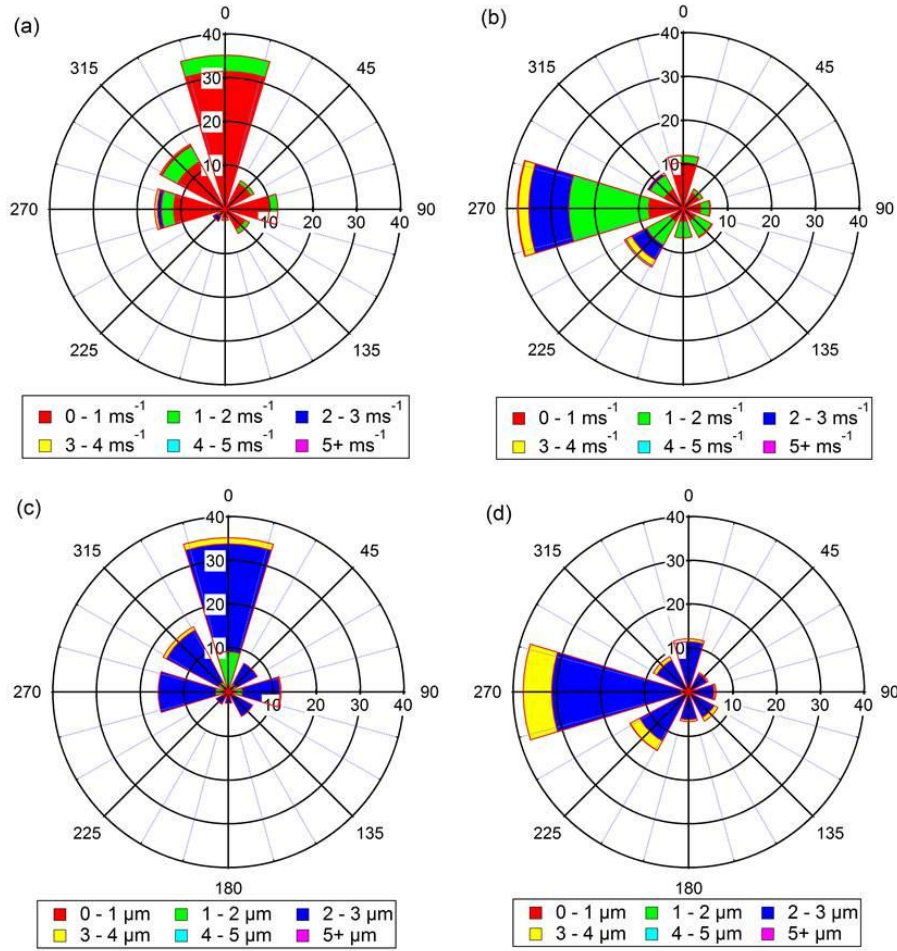


Figure 4-14: Wind rose diagram scaled by wind speed and geometric mean diameter ( $D_g$ ) of  $dN_p/d\log D_a$ . The figures have been separated for FBAP number concentration ( $N_F$ ) range,  $N_F > 0.1 \text{ cm}^{-3}$  and  $N_F < 0.1 \text{ cm}^{-3}$  observed during high bio period. For example: when,  $N_F > 0.1 \text{ cm}^{-3}$  ~60% of the time wind was observed to be in the range of 0 - 1  $\text{m s}^{-1}$  (a) and ~94% of the time the geometric mean diameter ( $D_g$ ) of  $dN_p/d\log D_a$  was in the range of 2 - 3  $\mu\text{m}$  (c). On the other hand for  $N_F < 0.1 \text{ cm}^{-3}$  ~60% of the time wind was greater than 1  $\text{m s}^{-1}$  (b), and ~80% of the time geometric mean diameter ( $D_g$ ) of  $dN_p/d\log D_a$  was in the range of 2 - 3  $\mu\text{m}$  (d).

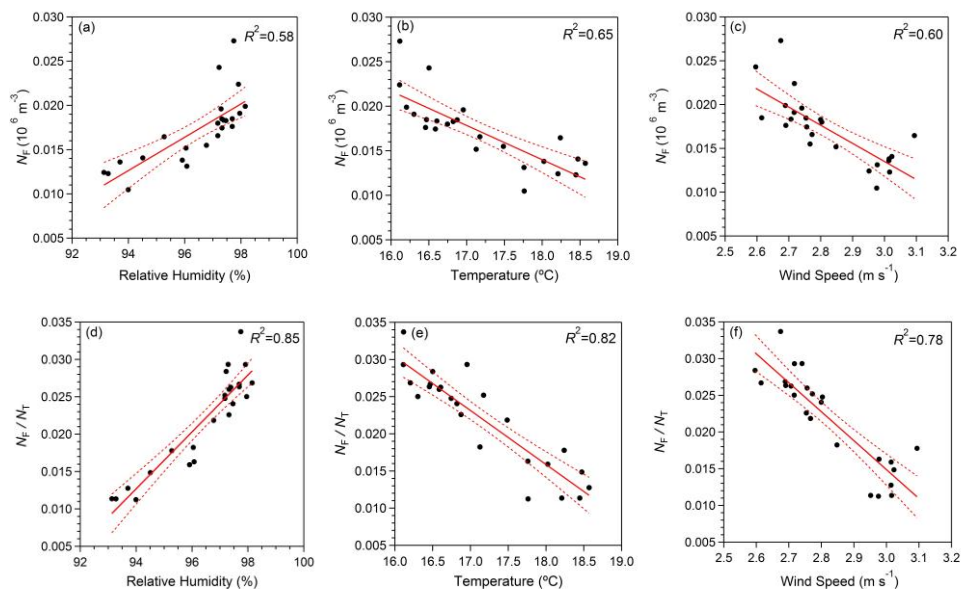


Figure 8.15: Correlation between aerosol particle number concentrations ( $N_F$ ,  $N_T$ , and  $N_F/N_T$ ) and meteorological parameters (relative humidity, temperature, and wind speed). Red line indicates the best fit to the scattered points and dashed black line indicates the 95% confidence level obtained for the best fit.